PHYSICO-CHEMICAL STUDIES ON THE DIMERISATION OF SOME METALLOPORPHYRINS

SYNOPSIS

BY

CORNELIA MARY LYNGDOH

DEPARTMENT OF CHEMISTRY
SCHOOL OF PHYSICAL SCIENCES

SUBMITTED

IN PARTIAL FULFILMENT OF THE REQUIREMENT OF THE DEGREE OF DOCTOR OF PHILOSOPHY

IN

CHEMISTRY

TO

NORTH EASTERN HILL UNIVERSITY
SHILLONG -793 022
INDIA

MARCH 2006

SYNOPSIS

This thesis entitled "**Physico-Chemical studies on the dimerisation of some Metalloporphyrins**" incorporates the information, results and discussion of our investigation on the dimerisation of some metalloporphyrins. It comprises of six chapters. We emphasize our investigation mainly to the visible absorption spectra and cyclic voltammetry. Our investigation is mainly on (metal = VO, Mn, Co, Ni, Cu, Zn and Sn) derivatives of protoporphyrin IX –dimethyl ester, mesoporphyrin IX-dimethyl ester and hematoporphyrin IX- dimethyl ester.

In the introduction, we have highlighted the reasons for carrying out this investigation.

Chapter-1 comprises a brief review on the dimerization of porphyrin, mainly H_2O soluble porphyrin. Different types of dimerization are also briefly reviewed.

Chapter-2 discusses the experimental details such as the synthesis of metalloprotoporphyrin IX-dimethyl ester, metallomesoporphyrin IX- dimethyl ester, vanadyl mesoporphyrin IX-dihydrochloride and metallohematoporphyrin IX-dimethyl ester; purification of solvents and reagents. Besides the experimental parameters such as Cyclic Voltammetry, UV-Visible Spectroscopy and Conductance measurements also described briefly.

Chapter-3 discusses the dimerization of metalloprotoporphyrin IX-dimethyl ester by means of UV-Visible absorption spectroscopy. Visible absorption spectra of unoxidised species obtain at different concentrations; changes of the different visible band are studied. Dimerization is observed at the concentration range 10^{-4}M and above while monomers are observed at concentration range 10^{-5}M and below. Deviation from the Beer's Law is also indicative of the dimerization. Different plots of Beer's Law have shown the deviation for all the system we have studied.

Further, we carried out the oxidation of the metalloporphyrin with $SbCl_5$ and studied the effect on dimerization. In most cases we observed a blue shift of the soret band accompanied by splitting indicating dimerization. The presence of isosbestic points in the Q bands also indicates the presence of two species i.e. monomer and dimer. From the visible absorption studies we conclude the following.

(i) Un-oxidized MPPIXDME systems exist as dimers above the concentration range 10^{-5}M in the neutral solvents such as Dichloromethane.

(ii) Below 10^{-6}M it exists as monomer and

(iii) On oxidation with $SbCl_5$, dimerization occurs even below 10^{-5}M.

Chapter-4 discusses the dimerisation of some metallomesoporphyrin IX-dimethyl ester and vanadyl mesoporphyrin IX- dihydrochloride at different concentration range (10^{-4}M and 10^{-5}M) by using UV-visible Spectroscopy at room temperature. The dimerisation is observed within the concentration range of 10^{-4}M and 10^{-5}M. The dimer dissociate into monomer below 10^{-5}M solution. The soret bands shift towards the shorter wavelength and the Q bands shift towards the longer wavelength

when the dimer dissociate into monomer. The oxidation of the metallomesoporphyrin IX-dimethyl ester with $SbCl_5$ was carried out and observed the changes in the soret and Q bands on dimerisation. The isosbestic points and splitting of the soret bands also indicate that the system is dimer or oligomer. From these studies we conclude the following points

i) For unoxidised metallomesoporphyrin IX-dimethyl ester, the blue shift of the soret band on dilution cannot be explained by the exciton theory. Therefore, we qualitatively attribute it to the dissociation of the dimer to monomer at around 10^{-5}M concentration and

(ii) Even at concentration 10^{-5}M due to the presence of $SbCl_5$, metallomesoporphyrins IX- dimethyl ester and Vanadyl mesoporphyrin IX-dihydrochloride dimerises and show shifts as predicted by exciton theory.

Chapter-5 discusses the dimerisation of some metallohematoporphyrin IX-dimethyl ester as above and concluded the following points

(i) Most of the MHPIXDME exists as dimer at the concentration around 10^{-5}M. Below this concentration the dimer dissociate to monomers and

(ii) On oxidation almost all MHPIXDME, we have studied show dimerization.

Chapter-6 discusses the cyclic voltammetric and conductance measurements of some metalloprotoporphyrin-IX-dimethyl ester, metallomesoporphyrin IX-dimethyl ester, vanadyl mesoporphyrin IX-dihydrochloride and metallohematoporphyrin IX-dimethyl ester. Almost all metalloporphyrin studied at different concentrations (10^{-2} M,10^{-3}M, 10^{-4}M and 10^{-5}M) exhibits broad redox peaks. The broad peaks indicate to be an overlap of two waves. Their ΔE and i_a/i_c values deviate from one-electron transfer processes because ΔE values are not equal to 59mV and i_a/i_c are also not equal to one. Almost all

the voltammograms on repeated scan show reduce peak heights and shifted their peak positions. This may be due to the thin film formation on the electrode surface.

From the cyclic voltammetric study we conclude the following:

(i) All metalloporphyrins we have studied show dimerization between 10^{-2}M and 10^{-5}M. In case of metallomesoporphyrin in neutral solvent such as CH_2Cl_2 dimer dissociates to monomer from 10^{-5}M concentration and below

(ii) Strong aggregation is observed even in the neutral organic solvent such as CH_2Cl_2

(iii) All metalloporphyrins we have studied show rapid film formation on the electrode surface. It shows that metalloporphyrins of proto, meso and hemato have strong tendency to aggregate even at low concentrations on oxidation and

(iv). From the conductance measurements we observed that VOMPIXDME exhibit dimer at higher concentration range while it exists as monomer below 10^{-5}M solutions

PHYSICO-CHEMICAL STUDIES ON THE DIMERISATION OF SOME METALLOPORPHYRINS

THESIS

BY

CORNELIA MARY LYNGDOH

DEPARTMENT OF CHEMISTRY
SCHOOL OF PHYSICAL SCIENCES

SUBMITTED

IN PARTIAL FULFILMENT OF THE REQUIREMENT
OF THE DEGREE OF
DOCTOR OF PHILOSOPHY
IN
CHEMISTRY
TO

NORTH EASTERN HILL UNIVERSITY
SHILLONG -793 022
INDIA

MARCH 2006

DECLARATION

NORTH – EASTERN HILL UNIVERSITY

FEBRUARY 2006

I, **Mrs. Cornelia Mary Lyngdoh**, hereby declare that the subject matter of this is the record of work done by me, that the content of this thesis did not form basis of the award of any previous degree to me or to the best of my knowledge to anybody else, and that the thesis has not been submitted by me for research degree in any other University/Institute.

This is being submitted to the North-Eastern Hill University for the **Ph. D.** Degree in **Chemistry.**

CORNELIA MARY LYNGDOH
(CANDIDATE)

Prof. R. H. Duncan Lyngdoh
(HEAD)
DEPARTMENT OF CHEMISTRY
NEHU

Dr. A. Lemtur
(SUPERVISOR)

ACKNOWLEDGEMENT

I sincerely express my profound gratitude to Dr A. Lemtur for his guidance and help extended to me in carrying out the course of this investigation. Inspite of his busy schedule, he was always available for discussions. The discussions I had with him gave me a keen insight and this contributed greatly in giving me a better understanding of the underlying concepts.

I would like to thank the Head, Department of Chemistry, Prof. R. H. Duncan, NEHU, Shillong for all the help rendered to me. My thanks go to the Department of Chemistry NEHU, for the facilities available and to all the faculty members for their gracious encouragement. My thanks also go to my lab mates Murugan, Icy, Don for their cooperation and all the research scholars for their company and moral support.

I would like to express my thanks to Mrs. Florence for recording the UV spectra. My sincere gratitude goes to Kong Wanda, Kong Siew, Kong Maria, Kong Myrthong, Bah Dkhar and other office staff for their help rendered to me during the course.

It gives me great pleasure to thank Kong Rit, Binu and all library staff for their help in assisting me with library facilities.

I also would like to express my gratitude to my beloved Parents, brothers and Kong Deborah for their enduring patience, constant prayers and encouragement till I completed the course. A special thanks and indebted gratitude to my beloved husband Dr. A. Tomba Singh for his constant loving guidance, encouragement, prayers and full support he had rendered in all round including typing this thesis.

My thanks also go to Dr. Ashish Malhotra, Head of Department of Chemistry, Union Christian College, Barapani for allowing me to use the Conductometric Instrument and also for the support rendered to me during the course. I would also like to thank my colleagues Mrs. H. Shangpliang, Mr. Rudolf Manih, Mr. Pliningstar and specially the Principal Union Christian College for the support, help and inspiration.

Last but the greatest gratitude goes to God Almighty for without Him, I would not be able to complete this research work and I dedicated this work to Him.

CONTENTS

Page No.

LIST OF TABLES
LIST OF FIGURES

PREFACE I-II

INTRODUCTION 1

CHAPTER 1. BRIEF REVIEW ON DIMERISATION AND AGGREGATION OF PORPHYRINS 2-8
REFERENCES

CHAPTER 2. EXPERIMENTAL SECTION 9-15
- 2.1 Introduction
- 2.2 Purification of reagents and solvents
- 2.3 Preparation of supporting electrolyte (TBAP)
- 2.4 Synthesis of Metalloporphyrins
- 2.5 Instrumentation

REFERENCES

CHAPTER 3. VISIBLE ABSORPTION STUDY ON THE DIMERISATION OF METALLOPROTOPORPHYRIN –IX DIMETHYL ESTER (MPP-IXDME), M=VO,Mn,Co,Ni,,Cu,Zn and Sn 16-39
- 3.1 Introduction
- 3.2 Experimental details
- 3.3 Results
- 3.4 Oxidation of MPPIXDME
- 3.5 Beer's law experiment
- 3.6 Discussion
- 3.7 Conclusion

REFERENCES

CHAPTER 4. VISIBLE ABSORPTION STUDY ON THE DIMERISATION OF METALLOMESOPORPHYRIN –IX DIMETHYL ESTER (M'MP-IXDME), M'=VO,Mn,Co,Ni, and Cu 40-55

4.1 Introduction
4.2 Experimental details
4.3 Results
4.4 Discussion
4.5 Conclusion

REFERENCES

CHAPTER 5. VISIBLE ABSORPTION STUDIES ON THE DIMERISATION OF METALLOHEMATOPORPHYRIN IX- DIMETHYL ESTER (MHPIX-DME), M=VO,Mn,Co,Ni,and Cu 56-68

5.1 Introduction
5.2 Experimental details
5.3 Results
5.4 Discussion
5.5 Conclusion

REFERENCES

CHAPTER 6. CYCLIC VOLTAMMETRIC AND CONDUCTANCE STUDIES OF SOME METALLOPORPHYRINS 69-131

6.1 Introduction
6.2 Cyclic voltammetry in brief
6.3 Cyclic voltammetry of Metalloporphyrins
6.4 Results
6.5 Discussion
6.6 Measurement of conductance
6.7 Results
6.8 *Discussion*
6.9 Conclusion

REFERENCES

SUMMARY 132-135

LIST OF TABLES

..... Page 25-27

Table 3.1 UV-Visible absorption data of Unoxidised, Oxidised and Reduced products of metalloprotoporphyrin IX-dimethyl ester, metal = VO, Mn, Co, Ni, Cu, Zn, and Sn in CH_2Cl_2 containing 0.1M $SbCl_5$ (at room temperature)

Table 3.2 UV- Visible absorption data of metalloprotoporphyrin IX-dimethyl ester, metal = VO, Co and Cu indicating isosbestic points in CH_2Cl_2 containing 0.1M $SbCl_5$ (at room temperature)

Table 3.3 UV- Visible data of Absorbance and concentration of metalloprotoporphyrin IX-dimethyl ester, metal=VO, Mn, Co, Ni Cu, Zn and Sn (at room temperature).

..... 44-46

Table 4.1 UV- Visible absorption data of Unoxidised, Oxidised and Reduced products of metallomesoporphyrin IX -dimethyl ester, metal = VO, Mn, Co, Ni and Vanadyl mesoporphyrin IX-dihydrochloride in CH_2Cl_2 containing 0.1M $SbCl_5$ (at room temperature)

Table 4.2 UV- Visible absorption data of metallomesoporphyrin IX- dimethyl ester, metal= VO, and Co and Vanadyl mesoporphyrin IX-dihydrochloride indicating isosbestic points in CH_2Cl_2 containing 0.1M $SbCl_5$ (at room temperature)

Table 4.3 UV- Visible data of Absorbance and concentration of metallomesoporphyrin IX-dimethyl ester, metal=VO, Mn, Co, Ni, Cu and Vanadyl mesoporphyrin IX – dihydrochloride (at room temperature)

..... 60-61

Table 5.1 UV-Visible absorption data of Unoxidised, Oxidised and Reduced products of metallohematoporphyrin IX- dimethyl ester, metal = VO, Mn, Co, Ni and Cu in CH_2Cl_2 containing 0.1M $SbCl_5$ (at room temperature)

Table 5.2 UV-Visible absorption data of Nickel hematoporphyrin IX-dimethyl ester indicating isosbestic points in CH_2Cl_2 containing 0.1M $SbCl_5$ (at room temperature).

..... 88-91

Table 6.1 Redox potentials (in volt) for MPPIXDME, M=VO, Mn, Co, Ni, Cu, Zn and Sn using TBAP as supporting electrolyte at room temperature.

Table 6.2 Redox potentials (in volt) for metallomesoporphyrin IX dimethyl ester using TBAP as supporting electrolyte at room temperature.

Table 6.3 Redox potentials (in volt) for metallohematoporphyrin IX dimethyl ester using TBAP as supporting electrolyte at room temperature.

Table 6.4 Conductance measurements of Metalloporphyrins. Cell constant= 0.9. Range=20Ms 129

LIST OF FIGURES

..... Page no.17-19

Figure 3.1a Structure of free base protoporphyrin IX-dimethyl ester

Figure 3.1b Structure of metalloprotoporphyrin IX-dimethyl ester

Figure 3.2 Energy Level diagram of free base porphyrin and metalloporphyrin

Figure 3.3 UV-Visible absorption spectra of Etio-type porphyrin (characteristic bands) 28-37

Figure 3.4a UV-Visible absorption spectra of CoPPIXDME (10^{-4}M) solution in CH_2Cl_2 unoxidised (—), oxidised(with 0.1M $SbCl_5$) ····, ----, — ·, — x , — · · and reduced (with diethyl amine) — · · ·

Figure 3.4b UV-Visible absorption spectra of CoPPIXDME (10^{-5}M) solution in CH_2Cl_2 unoxidised (—), oxidised(with 0.1M $SbCl_5$) — ·, ····, ---, — x and reduced (with diethyl amine) — Δ

Figure 3.4c UV-Visible absorption spectra of NiPPIXDME (10^{-4}M) solution in CH_2Cl_2 unoxidised (—), oxidised(with 0.1M $SbCl_5$) —·, ----, ····, — · · , and reduced (with diethyl amine) — x

Figure 3.4d UV-Visible absorption spectra of NiPPIXDME (10^{-5}M) solution in CH_2Cl_2 unoxidised (—), oxidised(with 0.1M $SbCl_5$) —x, —·, ····, ---- and reduced (with diethyl amine) — ·

Figure 3.5 UV-Visible absorption spectra of MnPPIXDME (10^{-5}M) solution in CH_2Cl_2 unoxidised (—), oxidised(with 0.1M $SbCl_5$)· · · ·, —·, ---- and reduced (with diethyl amine) — ···

Figure 3.6 UV-Visible absorption spectra of CoPPIXDME (10^{-6}M) solution

Figure 3.7a UV-Visible absorption spectra of VOPPIXDME (10^{-4}M) solution in CH_2Cl_2 indicating isosbestic point

Figure 3.7b UV-Visible absorption spectra of VOPPIXDME (10^{-5}M) solution in CH_2Cl_2 indicating isosbestic point, unoxidised (—), oxidised (with 0.1M $SbCl_5$) —·, ---, —x, ···· and reduced (with diethyl amine) — ···

Figure 3.8 UV-Visible absorption spectra of CuPPIXDME (10^{-4}M) solution in CH_2Cl_2 indicating isosbestic point, unoxidised (—), oxidised (with 0.1M $SbCl_5$ ····, — ·, —x, --- and reduced (with diethyl amine) — ··

Figure 3.9 Plot of Absorbance vs. Concentration of MPPIXDME

..... Page No.41

Figure 4.1a Structure of free base mesoporphyrin IX-dimethyl ester

Figure 4.1b Structure of metallomesoporphyrin IX-dimethyl ester

..... 47-54

Figure 4.2a UV-Visible absorption spectra of VOMPIXDME (10^{-5}M) solution in CH_2Cl_2 unoxidised (—), oxidised(with 0.1M $SbCl_5$) ····, ----, — ·, — x , and reduced (with diethyl amine) — ··

Figure 4.2b UV-Visible absorption spectra of CoMPIXDME (10^{-5}M) solution in CH_2Cl_2 unoxidised (—Δ), oxidised(with 0.1M $SbCl_5$) — ·, ····, —, — ··, ···· Δ ···· and and reduced (with diethyl amine) — x

Figure 4.2c UV-Visible absorption spectra of NiMPIXDME (10^{-4}M) solution in CH_2Cl_2 unoxidised (—), oxidised(with 0.1M $SbCl_5$) ----, ····, —·, — x and reduced (with diethyl amine) —Δ

Figure 4.2d UV-Visible absorption spectra of NiMPIXDME (10^{-5}M) solution in CH_2Cl_2 unoxidised (—), oxidised(with 0.1M $SbCl_5$) ----, —·,· ···· and reduced (with diethyl amine) — x

Figure 4.2e UV-Visible absorption spectra of CuMPIXDME (10^{-5}M) solution in CH_2Cl_2 unoxidised (—), oxidised(with 0.1M $SbCl_5$) ----, —·,— ·· and reduced (with diethyl amine) — x

Figure 4.2f UV-Visible absorption spectra of VOMPIXDME (10^{-4}M) solution in CH_2Cl_2 unoxidised (—), oxidised(with 0.1M $SbCl_5$) —x, —·—·, ----, and reduced (with diethyl amine) — x

Figure 4.2g UV-Visible absorption spectra of CuMPIXDME (10^{-5}M) solution in CH_2Cl_2 unoxidised (—), oxidised(with 0.1M $SbCl_5$) ----, —·,—Δ,—x and reduced (with diethyl amine) — x x

Figure 4.3(a-f) Plot of Absorbance vs. Concentration of M'MPIXDME and VOMPIXdiHCl

..... Page 57

Figure 5.1a Structure of free base hematoporphyrin IX-dimethyl ester

Figure 5.1b Structure of metallohematoporphyrin IX-dimethyl ester

..... 62-67

Figure 5.2a UV-Visible absorption spectra of MnHPIXDME (10^{-4}M) solution in CH_2Cl_2 unoxidised (—) oxidised(with 0.1M $SbCl_5$) ----, ····, — ·, — ··, and reduced (with diethyl amine) —Δ

Figure 5.2b UV-Visible absorption spectra of MnHPIXDME (10^{-5}M) solution in CH_2Cl_2 unoxidised (····x) oxidised(with 0.1M $SbCl_5$) —Δ, -x-x-x-, · x· x·, — ·, — , ·····,----, —x and reduced (with diethyl amine) — · ·

Figure 5.2c UV-Visible absorption spectra of CoHPIXDME (10^{-5}M) solution in CH_2Cl_2 unoxidised (—) oxidised(with 0.1M $SbCl_5$) ----, ···· , —·and reduced (with diethyl amine) —Δ

Figure 5.2d UV-Visible absorption spectra of NiHPIXDME (10^{-4}M) solution in CH_2Cl_2 unoxidised (···· Δ) oxidised(with 0.1M $SbCl_5$) —, — ·, — ··, — x , ----, ···· and reduced (with diethyl amine) — Δ

Figure 5.2e UV-Visible absorption spectra of NiHPIXDME (10^{-5}M) solution in CH_2Cl_2 unoxidised (—) oxidised(with 0.1M $SbCl_5$) ----, ···· , —· and reduced (with diethyl amine) — ··

Figure 5.3 (a-e) Plot of Absorbance vs Concentration of MHPIXDME

..... Page 73-74

Figure 6.1 HOMO representation for Metalloporphyrins.

Figure 6.2(a) Triangular Wave

Figure 6.2(b) Electrolytic cell

..... 91-128

Figure 6.3(a) Cyclic Voltammogram of 10^{-2}M VOPPIXDME in CH_2Cl_2 containing 0.1M TBAP at room temperature. Scan rate =100mV/s

Figure 6.3(b) Cyclic Voltammogram of 10^{-3}M VOPPIXDME in CH_2Cl_2 containing 0.1M TBAP at room temperature. Scan rate =100mV/s

Figure 6.3(c) Cyclic Voltammogram of 10^{-4}M VOPPIXDME in CH_2Cl_2 containing 0.1M TBAP at room temperature. Scan rate =100mV/s

Figure 6.4(a) Cyclic Voltammogram of 10^{-2}M MnPPIXDME in CH_2Cl_2 containing 0.1M TBAP at room temperature. Scan rate =100mV/s

Figure 6.4(b) Cyclic Voltammogram of 10^{-3}M MnPPIXDME in CH_2Cl_2 containing 0.1M TBAP at room temperature. Scan rate =100mV/s

Figure 6.4(c) Cyclic Voltammogram of 10^{-4}M MnPPIXDME in CH_2Cl_2 containing 0.1M TBAP at room temperature. Scan rate =100mV/s

Figure 6.4(d) Cyclic Voltammogram of 10^{-5}M MnPPIXDME in CH_2Cl_2 containing 0.1M TBAP at room temperature. Scan rate =100mV/s

Figure 6.5(a) Cyclic Voltammogram of 10^{-2}M CoPPIXDME in CH_2Cl_2 containing 0.1M TBAP at room temperature. Scan rate =100mV/s

Figure 6.5(b) Cyclic Voltammogram of 10^{-3}M CoPPIXDME in CH_2Cl_2 containing 0.1M TBAP at room temperature. Scan rate =100mV/s

Figure 6.5(c) Cyclic Voltammogram of 10^{-4}M CoPPIXDME in CH_2Cl_2 containing 0.1M TBAP at room temperature. Scan rate =100mV/s

Figure 6.6(a) Cyclic Voltammogram of 10^{-2}M NiPPIXDME in CH_2Cl_2 containing 0.1M TBAP at room temperature. Scan rate =100mV/s

Figure 6.6(b) Cyclic Voltammogram of 10^{-3}M NiPPIXDME in CH_2Cl_2 containing 0.1M TBAP at room temperature. Scan rate =100mV/s

Figure 6.7 Cyclic Voltammogram of 10^{-3}M CuPPIXDME in CH_2Cl_2 containing 0.1M TBAP at room temperature. Scan rate =100mV/s

Figure 6.8(a) Cyclic Voltammogram of 10^{-2} M ZnPPIXDME in CH_2Cl_2 containing 0.1M TBAP at room temperature. Scan rate =100mV/s

Figure 6.8(b) Cyclic Voltammogram of 10^{-4}M ZnPPIXDME in CH_2Cl_2 containing 0.1M TBAP at room temperature. Scan rate =100mV/s

Figure 6.8(c) Cyclic Voltammogram of 10^{-5}M ZnPPIXDME in CH_2Cl_2 containing 0.1M TBAP at room temperature. Scan rate =100mV/s

Figure 6.9a Cyclic Voltammogram of 10^{-3}M SnPPIXDME in CH_2Cl_2 containing 0.1M TBAP at room temperature. Scan rate =100mV/s

Figure 6.9b Cyclic Voltammogram of 10^{-4}M SnPPIXDME in CH_2Cl_2 containing 0.1M TBAP at room temperature. Scan rate =100mV/s

Figure 6.10a Cyclic Voltammogram of 10^{-2}M VOMPIXDME in CH_2Cl_2 containing 0.1M TBAP at room temperature. Scan rate =100mV/s

Figure 6.10b Cyclic Voltammogram of 10^{-3}M VOMPIXDME in CH_2Cl_2 containing 0.1M TBAP at room temperature. Scan rate =100mV/s

Figure 6.10c Cyclic Voltammogram of 10^{-4}M VOMPIXDME in CH_2Cl_2 containing 0.1M TBAP at room temperature. Scan rate =100mV/s

Figure 6.11 Cyclic Voltammogram of 10^{-2}M MnMPIXDME in CH_2Cl_2 containing 0.1M TBAP at room temperature. Scan rate =100mV/s

Figure 6.12a Cyclic Voltammogram of 10^{-2} M CoMPIXDME in CH_2Cl_2 containing 0.1M TBAP at room temperature. Scan rate =100mV/s

Figure 6.12b Cyclic Voltammogram of 10^{-3} M CoMPIXDME in CH_2Cl_2 containing 0.1M TBAP at room temperature. Scan rate =100mV/s

Figure 6.12c Cyclic Voltammogram of 10^{-5} M CoMPIXDME in CH_2Cl_2 containing 0.1M TBAP at room temperature. Scan rate =100mV/s

Figure 6.13a Cyclic Voltammogram of 10^{-2} M NiMPIXDME in CH_2Cl_2 containing 0.1M TBAP at room temperature. Scan rate =100mV/s

Figure 6.13b Cyclic Voltammogram of 10^{-5} M NiMPIXDME in CH_2Cl_2 containing 0.1M TBAP at room temperature. Scan rate =100mV/s

Figure 6.14a Cyclic Voltammogram of 10^{-2} M CuMPIXDME in CH_2Cl_2 containing 0.1M TBAP at room temperature. Scan rate =100mV/s

Figure 6.14b Cyclic Voltammogram of 10^{-4} M CuMPIXDME in CH_2Cl_2 containing 0.1M TBAP at room temperature. Scan rate =100mV/s

Figure 6.14c Cyclic Voltammogram of 10^{-5} M CuMPIXDME in CH_2Cl_2 containing 0.1M TBAP at room temperature. Scan rate =100mV/s

Figure 6.15a Cyclic Voltammogram of 10^{-2} M VOMPIXdiHCl in CH_2Cl_2 containing 0.1M TBAP at room temperature. Scan rate =100mV/s

Figure 6.15b Cyclic Voltammogram of 10^{-3} M VOMPIXdiHCl in CH_2Cl_2 containing 0.1M TBAP at room temperature. Scan rate =100mV/s

Figure 6.15c Cyclic Voltammogram of 10^{-4} M VOMPIXdiHCl in CH_2Cl_2 containing 0.1M TBAP at room temperature. Scan rate =100mV/s

Figure 6.15d Cyclic Voltammogram of 10^{-5} M VOMPIXdiHCl in CH_2Cl_2 containing 0.1M TBAP at room temperature. Scan rate =100mV/s

Figure 6.16 Cyclic Voltammogram of 10^{-2} M VOHPIXDME in CH_2Cl_2 containing 0.1M TBAP at room temperature. Scan rate =100mV/s

Figure 6.17 Cyclic Voltammogram of 10^{-3} M MnHPIXDME in CH_2Cl_2 containing 0.1M TBAP at room temperature. Scan rate =100mV/s

Figure 6.18 Cyclic Voltammogram of 10^{-2} M NiHPIXDME in CH_2Cl_2 containing 0.1M TBAP at room temperature. Scan rate =100mV/s

Figure 6.19 Cyclic Voltammogram of 10^{-2} M CuHPIXDME in CH_2Cl_2 containing 0.1M TBAP at room temperature. Scan rate =100mV/s

..... 130

Figure 6.20 Plot of Conductance vs Concentration of some Metalloporphyrins

PREFACE

Porphyrins and Metalloporphyrins such as Metalloprotoporphyrin-IX DME,Mesoporphyrin-IXDME and Hematoporphyrin –IXDME are naturally occurring compounds. Some porphyrinic metallocycles are well known as molecular building blocks of one dimensional "molecular metals". The large ring porphyrinic metallomacrocycles exhibit high electrical conductivities at room temperature. Tin porphyrins have been shown to possess some beneficial biological properties.Tin-heme have been used in the treatment of jaundice and in the photodynamic therapy of cancer.

The aggregation of porphyrins and metalloporphyrins are well studied and well documented in the literature. Even on oxidation they dimerise.Our earlier studies have shown that VOPP-IXDME,VOMP-IXDME and VOHP-IXDME form dimers on oxidation. However, at what range of concentrations they exist as dimers were not properly investigated.This prompted us to study the concentration dependent dimerisation of porphyrins and metalloporphyrins and their oxidation products.

This thesis consists of six chapters. The differentiation between monomer and dimers and their physico-chemical properties are highlighted in the introduction.

Chapter 1 briefly discusses the review on dimerisation and aggregation of porphyrins.

All the experimental details employed in the course of the investigation are described in Chapter 2.

Chapter 3 deals with the visible absorption study on the dimerisation of metalloprotoporphyrin-IX dimethyl ester.

Chapter 4 embodies the visible absorption studies of metal complexes of mesoporphyrin-IX dimethyl ester.

Chapter 5 deals with the visible absorption studies of metallohematoporphyrin-IX dimethyl ester.

Chapter 6 embodies the cyclic voltammeter and conductance studies of some metalloporphyrins.

Chapters 3, 4, 5 and 6 are framed with introduction, results, discussions and conclusions.

INTRODUCTION

INTRODUCTION

Porphyrins are naturally occurring compounds. Their metal complexes do occur in biological systems and are biologically very important. Magnesium coordinating porphyrins occur in green plants as chlorophyll and in photosynthetic cyano-bacteria. Iron coordinated porphyrins are known as heme which occurs in the red blood cells. Porphyrins and metalloporphyrins are therefore, widely studied compounds and their chemistry is quite old. However, with the advent of new techniques newer results and information are still pouring in. Porphyrins such as protoporphyrin IX, mesoporphyrin IX and hematoporphyrin IX are naturally occurring compounds. Their compounds with transition metals are widely studied group of compounds. Such metalloporphyrins aggregate in the form of dimers and oligomers. The aggregation of porphyrins and metalloporphyrins are well studied and well documented in the literature[1-3]. Even on oxidation they dimerise. Our earlier studies[30,31] on vanadyl protoporphyrin IX - dimethyl ester, vanadyl mesoporphyrin IX - dimethyl ester, and vanadyl hematoporphyrin IX - dimethyl ester have shown that they form dimers on oxidation. However, at what range of concentrations they exist as dimers were not properly investigated. Therefore, we were prompted to carry out this thesis work in which we present the studies and results of dimerisation of vanadyl porphyrins at different concentration range; in other words differentiation between monomer and dimers and their physico-chemical properties. The electron transfer processes in monomer and dimer are quite different. We have restricted our investigation within the available facilities such as UV-visible spectroscopy and cyclic voltammetry.

CHAPTER – 1

A BRIEF REVIEW ON DIMERISATION AND AGGREGATION OF PORPHYRINS

CHAPTER – 1

A BRIEF REVIEW ON DIMERISATION AND AGGREGATION OF PORPHYRINS

Homo and hetero dimer formation in metalloporphyrins were studied by ESR[4-6]. Aggregation of metalloporphyrins causes a decrease in the electronic relaxation leading to the broadening of linewidth at room temperature. From the ESR studies it has been found that the planar metalloporphyrin complexes form face- to - face dimer type with direct metal - metal interaction. On the other hand, square pyramidal derivatives such as VOP and FePCl, the homo dimer formation constants were found to be one fourth of those of the planar complexes.

Pasternacks and co-workers[7,8] have studied the dimerization of some water soluble porphyrin such as tetra phenyl porphine sulphonate ($TPPS_3$), tetra carboxy phenyl porphine (TCPP) and tetra (N-methyl tetra pyridyl) porphine (TMPyP) by UV-Visible spectroscopy. Beer's Law studies were done and found that the deviation from the Beer's Law as an indication of higher aggregation. It was concluded that none of these porphyrins aggregate at pH~7.5 in 80% Ethyleneglycol - water mixture within the concentration range 10^{-5}M to 10^{-6}M. Further, it was observed that the peripherial groups did have profound effect on the acidity and basicity of the porphyrin ring. It was concluded that the cationic porphyrins such TMPyP and TPyP do not aggregate in water while the anionic porphyrins aggregate. This is generally so for the meso substituted porphyrins. Anionic porphyrins also dimerises in presence of inorganic salts. Such an

ionic porphyrin has shown additional property by forming J- aggregates under the acidic condition or in the presence of cationic polymers like protonated polypeptide.

Recently a report appeared in the literature[9] on the self aggregation of cationic porphyrins like PCnPy and TPOCnPy (pyridyl porphyrins) in aqueous media. The absorbance of the soret band of PC_3Py ($5x10^{-6}M$) at 412 nm decreases with decreasing pH, with a simultaneous appearance of a new band at 417 nm with an isosbestic point at 414 nm. It is known that the soret band of face- to -face dimers and higher H-type aggregates appear at shorter wavelength [8,10 -15] while edge- to - edge aggregates (J- type) appear at longer wavelength compare to their corresponding monomers. Further, higher aggregates other than J- aggregates exhibit a broad band near the soret band[9]. The absorption spectra of PC_3Py in water ($5X10^{-4}moldm^{-3}$) shows λ_{max} = 398nm at lower temperature which changes to λ_{max} = 412 nm with an isosbestic point at 404 nm upon increasing the temperature. This change in the spectrum was attributed to the dissociation of the face - to - face dimer to its monomer. A solution of $PC_3Py(5X10^{-6}mol\ dm^{-3})$ exhibited the formation of dimer at room temperature(25°C) on addition of KNO_3.

Ibers and co- workers[16] have reported the synthesis and characterization of quinone- substituted octaalkyl porphyrin monomers and dimers. They have synthesized both gable and flat dimer. Some of the porphyrins were metallated by metals zinc, copper etc. UV-Visible spectrum of such metalloporphyrins show "split soret" band typical of phenyl-linked bis-porphyrinyl benzenes. However, the trend is more pronounce in the case of gable dimer and less in the flat dimer. The split in the soret band was attributed to the excitonic interactions[17] between the two adjacent porphyrinic sub units. This excitonic

interaction was more pronounced in the case of gable – type dimer. Similar observations were reported by Osuka et.al[18] in directly linked porphyrin arrays. They observed the electronic interaction between the neighboring porphyrin were quite low inspite of a direct covalent linkage between them. This was due to the orthogonal conformation of meso-meso linked porphyrin arrays that disrupted the π – electron conjugation. The soret band of the zinc complex exhibited split. This has been attributed to the excitonic interaction between the adjacent porphyrin units.

Protoporphyrins, Hematoporphyrins, Mesoporphyrins and deuteroporphyrins aggregate forming dimer and oligomers. Walter[19] has found that the Fe(III) deuteroporphyrin dimethyl ester disulphonate form dimers over the range of pH below 13. He proposed that the species contain two water molecules as additional axial ligands on a μ- oxo oligomer. It was pointed out that below pH 13 high spin Fe (III) porphyrins oligomer was formed without additional ligands while above pH 13 low – spin oligomer with two added hydroxide ligands were formed. Berdnarski and Jordan[20,21] reported that the Fe (III) protoporphyrin exits in dimeric form in the entire pH range of 7-13. In this case also the addition of hydroxide ions outside the co-ordination sites of the oligomers inducing low – spin iron was proposed. It has been proposed that the Vinyl groups in the protoporphyrin enhanced the aggregation substantially. The μ– oxo oligomer of Fe (III) protoporphyrin IX-dimethyl ester exhibited a shorter distance between the two porphyrin rings compared to that of the Fe(III) tetra phenyl porphyrin.

Mac Cragh et.al[22] studied a large number of copper and silver porphyrins by ESR in non-aqueous solvent. Boyd et.al[23] have found the distance between Cu-Cu to be 3.5 - 4.5 Å between the sandwich copper porphyrins in $CHCl_3$. They also found that copper hematoporphyrin dimethyl ester exist in trimers.

It is to be noted that the absorption spectrum of the monomeric porphyrins depend upon the environment eg. solvents etc[24] in which it exists. It has been observed that more polar environment leads to blue shift of the soret band. This observation was made in aqueous solution with greater ionic strength. Addition of tetra methyl ammonium perchlorate leads to a red shift indicating a more organic environment due to ion pairing with the TCP an ionic site[24].

Krishnan et.al[25,26] reported that addition of cation such as NH_4^+ , K^+, Cs^+ ,and Ba^{2+} to a solution of TCP (meso- tetrakis (benzo-5-crown-5) porphyrin) dimerises the porphyrins. They reported that addition of K^+ has a strong effect causing (i) a decrease in the absorbance of the soret band as well as the Q bands, (ii) broadening and red shifted Q bands and (iii) broadening and blue shifted soret band. Chandrashekar and Willegen et.al.[27] reported similar effect in the absorption spectrum of ZnTCP. Similar observations were reported by Chang and Kagan et.al for TCP and for covalently linked porphyrins. The blue shifts of the soret band due to dimerization were attributed to the effect of dipole –dipole coupling between the transition moments in the two porphyrins. The Coulombic exciton coupling give rise to a shift ($\Delta\xi$) given by[17]

$$\Delta\xi = DGR^{-3} \quad \ldots\ldots\ldots\ldots\ldots\ldots\ldots\ldots (1.1)$$

where D = Transition dipole moment in the monomer, G = Geometric factor accounting for the relative orientation of the dipoles in the dimer constituents and R= center-center distance between the rings.

It is to be noted that there is no simple relationship between dimerization effect and the geometric structure[27]. The shifts in soret and Q bands cannot be readily interpreted. However, it was attributed tentatively to the perturbation of the electronic energy levels by the $\pi - \pi$ interaction between the porphyrins.

Gross et.al[28] reported that for bisporphyrinic tweezer, a cofacial porphyrin dimer have shown a blue shift of the Soret band by 2 nm and 3 nm for the free base and the metallo – porphyrin respectively. Slight broadening of the Soret band was also observed.

Kadish et.al[29] reported the synthesis, electrochemical and photophysical study of covalently linked porphyrin dimers with two different macrocycles. They observed that the UV-visible spectrum of H_2 [p-(TPP-DEHMP)] H_2 is also similar to super imposed UV-visible spectra of monomeric $(TPP)H_2$ and $(OEP)H_2$. They concluded that the electronic interactions between the two subunits are very weak. Thus, they described the electronic absorption spectra and electrochemical properties of the dimers as superposition of the two monomeric subunits.

Subramanian et.al[30,31] reported the ESR and electrochemical studies of Vanadyl protoporphyrin IX - dimethyl ester, mesoporphyrin IX- dimethyl ester and hematoporphyrin IX -dimethyl ester. Splits in the soret band were observed and also a slight blue shift in the soret band was observed on oxidation.

REFERENCES

1. W. I. White, in "The Porphyrins", Edited by D. Dolphin (Academic press, New York,1979),Vol, V. part C, p 303 and references therein.
2. A. E. Alexander, J.Chem.Soc.p-1813(1937)
3. J. A. Beyeron,G. L. Gaines, Jr and W. D. Bellamy, J. Colloid Interface Sci., 25, 97(1967)
4. W. E. Blumberg and J. Peisach, J. Biol. Chem., 240, 870(1965)
5. P. D. W. Boyd, T. D. Smith, J. H. Price and J. R. Pilbrow, J. Chem. Phys., 56, 1253(1972)
6. Lucia Banci, Inorg. Chem. 24, 782(1985) and references therein.
7. R. F. Pasternack, L. Francesconi, D. Raff and E. Spiro, Inorg. Chem., 12, 2606 (1973)
8. R. F. Pastersnack, P. R. Huber, P. Boyd, G. Engasser, L. Francisconi, E.Gibbs, P. Fasella, G. C. Ventaro, and L.de C.Hinds, J. Am. Chem. Soc., 94, 4511(1972) and references therein.
9. K. Kano, K. Fukuda, H. Wakani, R. Nishiyabu and R. F. Pasternack, J. Am. Chem. Soc., 120, 7494(2000) and references therein.
10. E. Ojadi, R. Selzer and H. Linschitz, J. Am. Chem. Soc,107,7783(1985).
11. K. Kano, M. Takei and S. Hashimoto, J. Phys. Chem., 94, 2181(1990) and references therein.
12. R. F. Pastersnack, C. Bustamanti, P. J. Collings, A. Giannetto, E. J. Gibbs, J. Am. Chem. Soc. Chem. Communn., 115. 5393(1993)
13. J. M. Ribo, J. Crusats, J. A. Ferrera, M. I. Valeso, J. Chem. Soc. Chem. Communn 681, 682 (1994).
14. N. C. Maiti, M. Ravikant, S. Majumdar, N, PeriaSamy, J. Phys. Chem., 99, 17192 (1995).
15. D. I. Akins, H. R. Zhu, C. Guo, J. Phys. Chem, 100, 5420(1996)
16. J. I. Sessler, M.R. Johnson, S.E. Creager, J. C. Fettinger and J. A. Ibers, J. Am. Chem. Soc. 112, 9310 (1990)

17. M. Kasha, H. R. Rawls and M. El-Bayoumi, Pure, Appl. Chem., 11, 371 (1965)
18. A. Osuka, K. Maruyama, J. Am. Chem. Soc., 110, 4454 (1988)
19. R. I. Walter, J. Biol. Chem., 196, 151 (1952)
20. J. Jordan and T. M. Bednarski, J. Am. Chem. Soc., 86, 5690 (1964)
21. T. M. Bednarski and J. Jordan, J. Am. Chem. Soc. 89, 1552 (1967)
22. A. Mac Cragh, C. B. Storm and W. S. Koski, J. Am. Chem. Soc., 87, 1470 (1965)
23. P. D. W. Boyd, T. D. Smith, J. H. Price and J. R. Pilbrow, J. Am. Chem. Soc., 56, 1253 (1972)
24. S. E. Clarke, C. L. Wamser and H. E. Bell, J. Phys. Chem. A, 106, 3235 (2002)
25. V. Thanabal, V. Krishnan, J. Am. Chem. Soc., 104, 3643 (1982)
26. V. Thanabal, V. Krishnan, Inorg. Chem., 21, 3606 (1982)
27. T. K. Chandrashekar, H. V. Willigen and M. A. Ebersole, J. Phys. Chem. 89, 3453 (1985) and references therein
28. J. Brettar, J. P. Gisselbrecht, M. Gross and N. Solladie, Chem. Communn, 733 (2001).
29. K.M. Kadish, N. Guo, E.V. Caemelbecke, A. Froiio, R. Paolesse, D. Monti, P. Tagliatesta, T. Boseln, L. Prodi, F. Bolletta and N. Zaccheroni, Inorg. Chem., 37, 2358 (1998)
30. A. Lemtur, B. K. Chakravorty, T. K. Dhar and J. Subrananian, J. Phys. Chem. 88, 5603 (1984)
31. J. Subramanian, V. P. Shedbalkar, A. Lemtur, R. Chakravorty and T. N. Saloi, J. Phys. Chem., 100, 4770 (1996)

CHAPTER – 2

EXPERIMENTAL PROCEDURE

CHAPTER – 2

EXPERIMENTAL PROCEDURE

2.1. INTRODUCTION

This chapter consists of synthesis of metalloporphyrin, preparation of supporting electrolyte for Cyclic Voltammetric (CV) measurements, purification of reagents and chemicals. It also includes a brief instrumental description of CV, UV and Conductance.

2.2. PURIFICATION OF REAGENTS AND SOLVENTS

2.2.1. Methanol: Methanol (MERCK) was distilled twice at its boiling point and stored over molecular sieves (Linde-4Å) and used.

2.2.2. Chloroform: Chloroform (MERCK) was purified by passing through a column of basic alumina. The eluate was stored over molecular sieves (Linde-4Å) and used.

2.2.3. Dichloromethane: Dichloromethane (MERCK) was refluxed with CaH_2 for three hours and allowed to stand overnight. The supernatant was decanted, distilled, stored over molecular sieves (Linde-4Å) and used.

2.2.4. Dimethyl formamide: DMF (MERCK) was distilled under reduced pressure and stored over molecular sieves (Linde-4Å) prior to use.

2.2.5. Pyridine: Pyridine (MERCK) was distilled twice under N_2 and over CaH_2 prior to use.

2.2.7. Protoporphyrin IX - dimethyl ester (Aldrich Chem. Co.), Mesoporphyrin IX - dimethyl ester (Aldrich Chem. Co.), Hematoporphyrin IX - dimethyl ester ((Aldrich Chem. Co.) and Mesoporphyrin IX -diHCl (Sigma) were purchased and used as received.

2.3. PREPARATION OF SUPPORTING ELECTROLYTE (TBAP): Tetrabutylammonium perchlorate was prepared by method of House[1] and recrystallized thrice from methanol.

2.4. SYNTHESIS OF METALLOPORPHYRINS

2.4.1. Vanadyl Protoporphyrin IX-dimethyl ester: VO(PROTO) was synthesized according to the methods of Uneo[2] and Erdman[3] by refluxing 100mg of protoporphyrin IX-dimethyl ester, 20ml of glacial acetic acid, 10ml of pyridine and 300mg of vanadyl sulphate for five hours in a silicon oil bath. The reaction mixture was cooled at room temperature, extracted with dichloromethane, washed with water in order to remove the unreacted vanadyl sulphate and dried over anhydrous sodium sulphate. The crude product was filtered and evaporated to dryness. The resulting VO (PROTO) was purified by column chromatography on silica gel with the mixture of dichloromethane and methanol (9:1) elution. The product was recrystallized from dichloromethane and methanol mixture. The purity of the product was checked by TLC and UV – Visible Spectroscopy.

λ_{max}: 410, 540, 579 (10^{-6}M)

Similarly Vanadyl mesoporphyrin IX-dihydrochloride and Vanadyl mesoporphyrin IX-dimethyl ester were synthesized by the same method described above.

λ_{max}: 405, 532, 570 (10^{-6}M) and

λ_{max}: 391, 533, 570 (10^{-6}M) respectively.

Vanadyl Hematoporphyrin: Vanadyl Hematoporphyrin gives poor yield by the above procedure. It was also synthesized by refluxing 100mg of Hematoporphyrin, 20ml glacial acetic acid, 30 ml of sodium acetate and 200mg of vanadyl sulphate for 12 hours then continued as before.

λ_{max}: 412, 538, 575 (10^{-6}M)

2.4.2. Copper(II) protoporphyrin IX-dimethyl ester: Cu(PPIXDME) was synthesized according to the method of Adler[4] by refluxing 150 mg of Protoporphyrin IX- dimethyl ester in chloroform and saturated solution of copper acetate in methanol. The cooled reaction mixture was extracted with chloroform, washed with water till the water layer was colourless and dried over anhydrous sodium sulphate. It was filtered and evaporated to dryness the product was purified by column chromatography and recrystallized from dichloromethane-methanol mixture. The purity of the compound was checked by TLC and UV- Visible spectroscopy.

λ_{max}: 380, 537, 571 (10^{-6}M)

Similarly Copper(II) mesoporphyrin IX-dimethyl ester was synthesized by the same method described above.

λ_{max}: 396, 524, 560 (10^{-6}M)

Copper (II) hematoporpohyrin was synthesized by refluxing 150 mg of hematoporphyrin, 20ml of chloroform, 10 ml of glacial acetic acid and saturated solution of copper acetate in methanol for 2 hours then continued as before.

λ_{max}: 400, 527, 562 (10^{-6}M)

2.4.3. Nickel(II) protoporphyrin IX-dimethyl ester: The compound was synthesized by the method of Adler[4]. The product was chromatographed on silica gel by using chloroform-methanol (9:1) mixture as eluent. It was recrystallized from chloroform-methanol mixture. The purity of the compound was checked by TLC and UV-visible spectroscopy.

λ_{max}: 389, 523, 558 (10^{-6}M)

Similarly Nickel(II) mesoporphyrin IX-dimethyl ester was prepared. The purity of the compound was checked by TLC and UV-visible spectroscopy.

λ_{max}: 407, 514, 550 (10^{-6}M)

Nickel(II) hematoporphyrin IX-dimethyl ester: The compound was synthesized by refluxing 150mg of hematoporphyrin, 300mg of nickel acetate in N, N-dimethylformamide for 30 minutes. The cooled reaction mixture was extracted with chloroform and washed with water till the water layer was cleared, and then continued as before.

λ_{max}: 377, 521, 555 (10^{-6}M)

2.4.4. Manganese(II) protoporphyrin IX-dimethyl ester: It was prepared by the method of Adler[4]. Similarly Manganese(II) mesoporphyrin IX-dimethyl ester was also prepared by method of Adler[4]. As before the purity were checked by TLC and UV-Visible Spectroscopy.

λ_{max}: 362,476, 566, 598 (10^{-6}M) and

λ_{max}: 366,471, 557, 584 (10^{-6}M) respectively.

Manganese(II) hematoporphyrin IX –dimethyl ester was synthesized by refluxing 150mg of Hematoporphyrin and 250mg of Manganese acetate in N, N-Dimethyl-formamide for 30 minutes and then continued as before.

λ_{max}: 367, 470, 558 (10^{-6}M)

2.4.5. Cobalt(II) protoporphyrin IX-dimethyl ester: The compound was synthesized by the method of Adler[4]. Cobalt(II) mesoporphyrin IX-dimethyl ester was also synthesized by the same method. Cobalt(II) hematoporphyrin was synthesized as Mn (II) hematoporphyrin. The purity were checked as above.

λ_{max}: 385, 559 (10^{-6}M)

λ_{max}: 393, 529,552 (10^{-6}M) and

λ_{max}: 417, 529, 560 (10^{-6}M) respectively.

2.4.6 Zinc(II) protoporphyrin IX-dimethyl ester: It was synthesized by method of Adler [4] and proceeded as before.

λ_{max}: 390, 539, 575 (10^{-6}M)

2.4.7 Tin(II) protoporphyrin IX-dimethyl ester: The compound was synthesized by method of Adler[4]. Purification was done as other compounds.

λ_{max}: 405, 539, 576 (10^{-6}M)

2.5 INSTRUMENTATION

2.5.1. CYCLIC VOLTAMMETRIC MEASUREMENTS:

Cyclic Voltammograms were obtained with three electrode electrolytic cell using CH1 (620B) Electrochemical analyzer CH Instruments. CH1(102) Platinum electrode and Platinum disk were used as auxiliary electrode and working electrode respectively.

Potentials were measured and reported against a saturated calomel electrode (SCE) which was separated from the bulk solution by means of a fritted-glass disk junction. Measurements were done at room temperature by bubbling N_2 gas through the solution in the cell before recorded. In these measurements the compounds were prepared solution in CH_2Cl_2. TBAP(0.1M) was used for all cyclic voltammetric measurements.

2.5.2. UV-VISIBLE MEASUREMENTS:

Measurements were done with Du* 650 Spectrophotometer using a quartz cuvette. The spectra were recorded, absorbance (A) versus wavelength in the range 350-700 nm. All spectra were measured at room temperature by using CH_2Cl_2 as solvent. The radical cations were generated by using $SbCl_5$ (0.1M in CH_2Cl_2) and reduction were also generated by using Diethylamine.

2.5.3. CONDUCTANCE MEASUREMENTS:

Conductivity Meter type 304 was used to measure the specific conductivity of the porphyrin solution using conductivity cell at room temperature. It was digital panel Meter and the accuracy of the measurement is ± 1 count.

REFERENCES

1. H.O. House, Feng, Edith and N.P. Peet, *J.Org.chem* 36(16) 2371-2374. (1971)
2. A.D.Adler, F.R.Longo, J.D. Finarelli, J. Goldmacher, J.Assour and l. Karkakoff, *J.Org.Chem.*32, 476 (1967)
3. G.M. Badger, R.A. Jones and R.L. Laslet, *Aust. J.Chem.*17, 1028 (1964)
4. A.D. Adler, F.R. Longo, F. Kampus and J. Kim, *J.Inorg.Nucl.Chem.* 32, 2443 (1970)

CHAPTER – 3

VISIBLE ABSORPTION STUDY ON THE DIMERISATION OF METALLOPROTOPORPHYRIN IX DIMETHYL ESTER (MPPIXDME), M=VO, Mn, Co, Ni, Cu, Zn and Sn

CHAPTER – 3

VISIBLE ABSORPTION STUDY ON THE DIMERISATION OF METALLOPROTOPORPHYRIN IX DIMETHYL ESTER (MPPIXDME), M=VO, Mn, Co, Ni, Cu, Zn and Sn

3.1. INTRODUCTION

The theoretical foundations and hence the spectroscopic background for porphyrins and metalloporphyrins were laid down by Martin Gouterman sometimes in 1960s[1-3]. Currently the most acceptable interpretation of the absorption spectra of porphyrins are attributed to $\pi \rightarrow \pi^*$ transitions and not due to $n \rightarrow \pi^*$ transition[4]. This is because of the symmetry of the n-orbitals and the antisymmetry of the π-orbitals with respect to the plane of the molecule[5]. The lower energy transitions give rise to Q bands (in the visible region) while the stronger energy transition gives rise to soret band i.e. the B band (near UV). The structure of free base porphyrin and metalloporphyrin are presented in figure 3.1(a) and 3.1(b) and their energy level diagram are presented in the figure 3.2[6]. The porphyrin ligands which we have used in our study broadly falls into two types[7-11] viz (i) Those which do not have any substituents in the meso positions such as octaethylporphyrins(OEP), protoporphyrins (Proto), hematoporphyrins (HP) and other naturally occurring porphyrins are categorized as Etio type. (ii) Those ligands which have substituents in the meso position are categorized as TPP type (mesotetraphenyl porphyrins). The UV-Visible absorption spectrum of Etio-type porphyrin is shown in

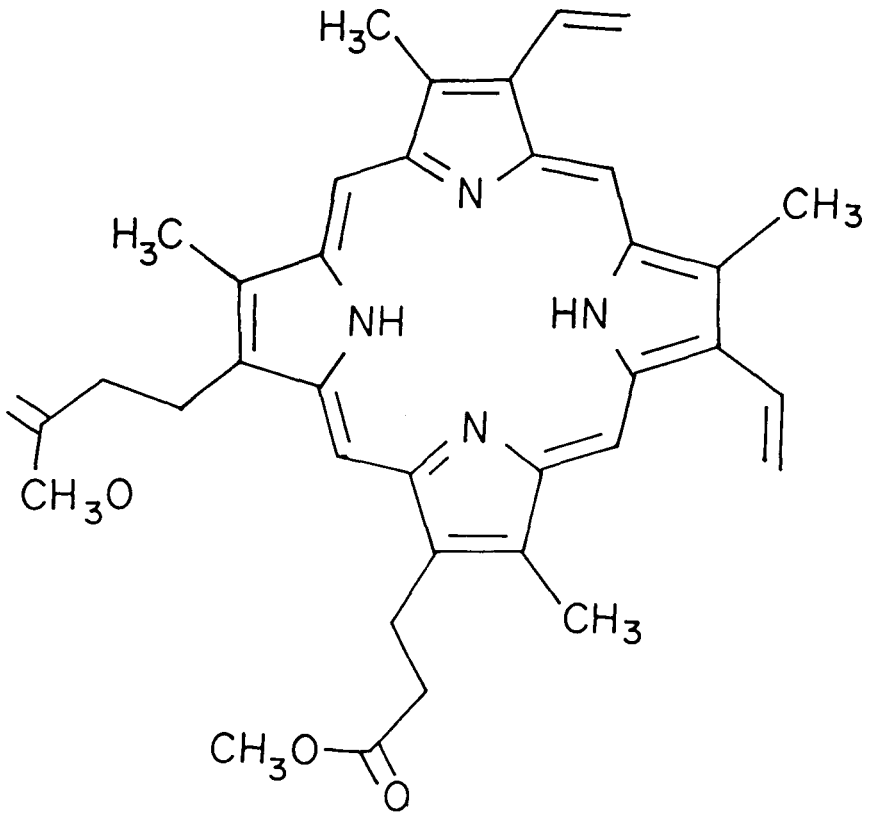

Figure 3.1a Structure of free base protoporphyrin IX-dimethyl ester

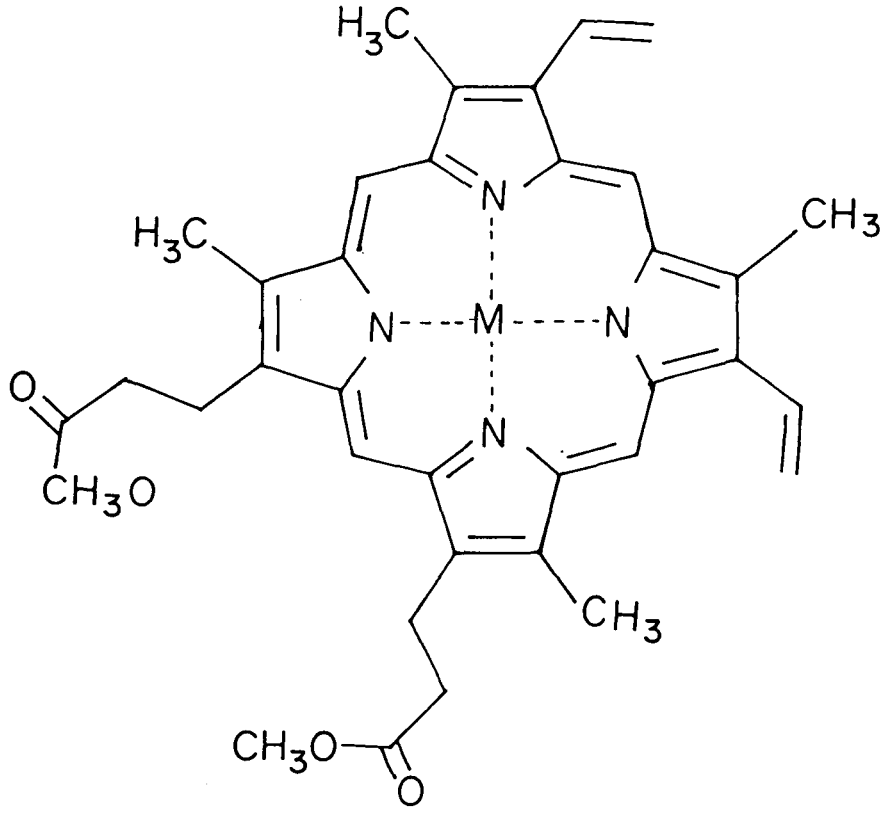

Figure 3.1b Structure of metalloprotoporphyrin IX-dimethyl ester

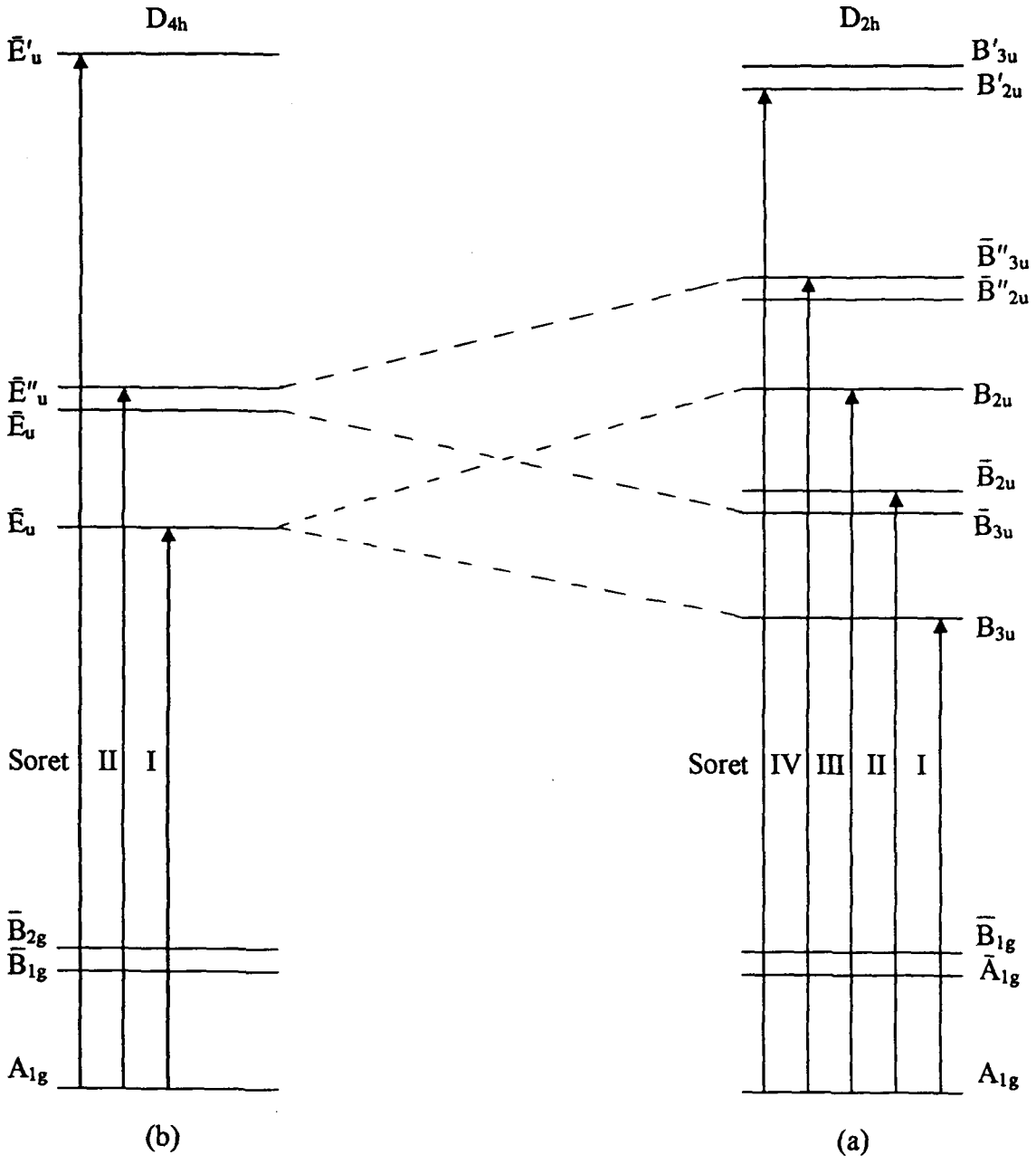

Figure 3.2 Energy levels of (a) Free base porphyrin (FBP) with D_{2h} symmetry (b) Metalloporphyrin (MP) H_2PH^{2+} and P^{2-} with D_{4h} symmetry. The bar indicates a vibrational satellite.

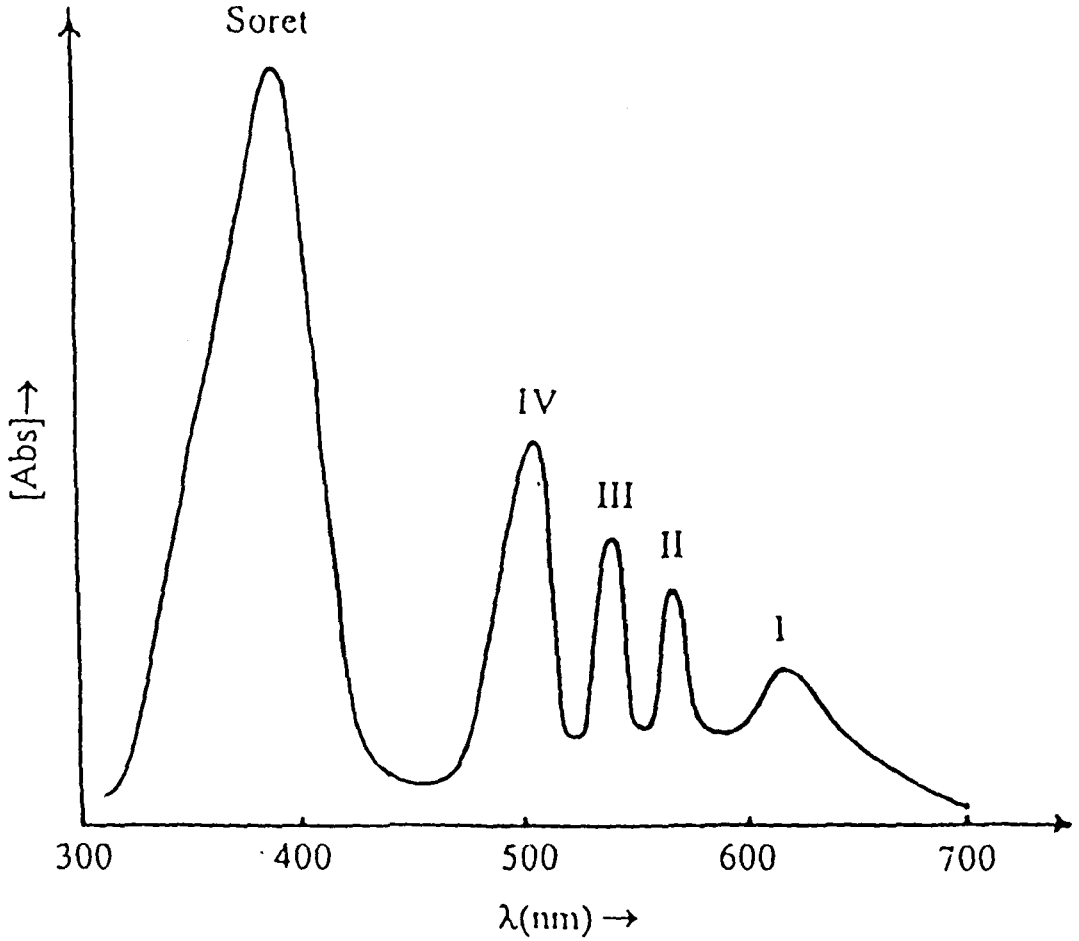

Figure 3.3 UV-Visible absorption spectra of Etio-type porphyrin (characteristic bands)

figure 3.3. Generally a free base porphyrin possesses D_{2h} symmetry (around the four pyrrole rings). The strong soret band near UV region is due to $^1A_{1g} \rightarrow {}^1E'_u$ transition. Absorption bands I and III in the visible region are due to quasi forbidden electronic transition $^1A_{1g} \rightarrow B_{3u}$ and $^1A_{1g} \rightarrow B_{2u}$ (the allowedness of these transitions are still not well understood). Generally, in the substituted porphyrins E'_u splits into B'_{2u} and B'_{3u} states which are very close lying. The electronic transitions to state E'_u (B'_{2u} or B'_{3u}) are allowed giving rise to intense soret band. Bands II and IV are of vibrational origin (vibrational satellite bands of I and III).

In case of metalloporphyrins (MP), the protonation to H_2PH^{2+} or ionization to P^{2-}, the energy levels B_{2u} and B_{3u} combine into a single doubly degenerate levels E_u. This is because of the change in symmetry of the porphyrin from D_{2h} to D_{4h}. As a result, bands I and III merge into one. The degeneracy of E_u is not easily lifted on substitution of the porphyrin ring. In MP bands II and IV disappear because B_{2u} and B_{3u} become degenerate and a new vibrational satellite band emerges corresponding to E_u state.

3.2. EXPERIMENTAL DETAILS

Solutions of metalloporphyrins in CH_2Cl_2 (dichloromethane) were prepared in the following concentrations: 10^{-4} M, 10^{-5} M and 10^{-6} M. We did not attempt to prepare concentrations beyond 10^{-6}M because the solution becomes very faint and could not obtain good spectra. Oxidations were carried out with $SbCl_5$ (0.1M) in CH_2Cl_2. All measurements were done at room temperature i.e. 20°C. We present here the visible absorption spectra study of metalloprotoporphyrin IX dimethyl ester (henceforth we will use MPPIXDME).

3.3. RESULTS

Results of visible un-oxidized MPPIXDME (M = VO, Mn, Co, Ni, Cu, Zn and Sn) absorption spectra are presented in the table 3.1.

As we go from the concentration 10^{-4}M to 10^{-6}M, the soret band exhibits a blue shift (table 3.1). From 10^{-4}M to 10^{-5}M the soret bands are usually broad and show splitting (figure 3.4 (a, b, c and d)). But we could not observe the splitting in the case of MnPPIXDME (figure 3.5).The soret band becomes sharper at 10^{-6} M (figure 3.6). For CoPPIXDME, NiPPIXDME, CuPPIXDME and ZnPPIXDME, the soret bands are more blue shifted (for 10^{-6}M solution) while SnPPIXDME shows the same wavelength to that of the 10^{-4}M solution. The Q bands do not show appreciable changes on dilution for all MPPIXDME.

3.4. OXIDATION OF MPPIXDME

Oxidation of MPPIXDME with $SbCl_5$ show slight blue shifts of the soret band except for MnPPIXDME, CoPPIXDME and ZnPPIXDME (10^{-5}M) in which soret bands are red shifted. Some of the MPPIXDME exhibit splitting in the soret band on oxidation. Q bands of all MPPIXDME are red shifted except for VOPPIXDME and MnPPIXDME (10^{-5}M). VOPPIXDME, CoPPIXDME and CuPPIXDME show isosbestic points on oxidation with $SbCl_5$ (figure 3.7(a, b,), 3.4(a, b) and 3.8 respectively and table 3.2). The oxidized products of MPPIXDME with $SbCl_5$ on reduction with diethylamine, all the bands come back towards the unoxidised species (table 3.1).

3.5. Beer's law experiment

Beer's law experiments were conducted for the un-oxidized MPPIXDME. We chose the absorbance of one of the Q band (550-601 nm) because the intensity of the soret band for higher concentrations go out of the range. The results are presented in the table 3.3. Plots of absorbance vs. concentrations are also presented in figure 3.9. In all cases linearity breaks down after 10^{-5}M concentrations.

3.6. DISCUSSION

It is well known that MPPIXDME dimerises face - to – face[12] or back – to – back like sandwich. From the visible absorption spectra it is quite evident that MPPIXDME exists as dimers between the concentration10^{-4}M to 10^{-5}M. From 10^{-5}M concentration and below we observed that the soret band is blue shifted. This may be due to the dissociation of dimer to monomers. Most of the dimerization studies reported in the literature were done in the water soluble porphyrins (mostly TPP systems) and observed split in the soret band accompanied by blue shift on dimerization[13]. Further, it was also reported that the Q bands were slightly red shifted. Earlier report of the visible absorption spectrum of VOPPIXDME(10^{-5}M) have shown the split in the soret band[17]. We can invoke the exciton theory to explain the shift in the soret band as well as the shift in the Q bands. According to the exciton theory there can be a very small shift in the Q bands[16]. The exciton splitting for oblique transition dipole is expressed as $E = 2|M|^2r^2(\cos\gamma + 3\cos^2\theta)$, where θ and γ define the orientation of one porphyrin relative to other with respect to the axis through the centers of the dimer constituents. According to the above equation it is evident for parallel planes, the maximum splitting will be when x and y axis of each

porphyrins have the same orientation and hence no shift because x and y axis are orthogonal. Thus, it cannot explain the shift in the soret band. Further, our findings are quite opposite to that of the water soluble porphyrins. From the table it is evident that at higher concentrations the soret band occurs at longer wavelength and for that of the lower concentrations at shorter wavelength and is also sharper. It is to be noted that at higher concentrations the soret band is broad and shows splitting. At the moment we cannot explain why the soret band of the dimer occur at longer wavelength with respect to that of the monomer.

Oxidations with TFA and perchloric acid have shown broadening of the soret band and blue shift[17]. The Q bands are also shifted slightly towards longer wavelengths. Oxidation with $SbCl_5$ shows slight blue shift for the soret band and slight red shift for the Q bands. (Table 3.1). This may be explained by the exciton theory. On the contrary ZnPPIXDME(10^{-5}M) shows red shifts for both the soret band and the Q bands on oxidation with $SbCl_5$. This cannot be explained by the exciton theory alone. In order to explain the experimentally observed visible absorption spectra may be we have to consider charge transfer along with the excitonic interactions. This may require some extensive theoretical approach. Currently, there is no clear theory to explain the blue shift in the soret band and red shifts in the Q bands on dimerization[14-16]. In the absence of any clear theory we attribute the blue shift in the soret band as due to dissociation of dimers to monomers in the case of unoxidised system.

3.7. CONCLUSION

From the visible absorption studies of MPPIXDME, we conclude the followings:

(i) Unoxidised MPPIXDME systems exist as dimers above the concentration range 10^{-5}M in the neutral solvents such as Dichloromethane.

(ii) Below 10^{-5}M it exists as monomer. This is supported by the Beer's law experimental results[7] and

(iii) On oxidation with $SbCl_5$, dimerization occurs even below 10^{-5}M

However, it is to be noted that detail experimental studies with different techniques are necessary to substantiate the above observations. Proper theoretical formulations and approach are required to explain the experimental observations.

Table 3.1 UV-Visible absorption data of Unoxidised, Oxidised and Reduced products of metalloprotoporphyrin IX-dimethyl ester, metal = VO, Mn, Co, Ni, Cu, Zn, and Sn in CH_2Cl_2 containing 0.1M $SbCl_5$ (at room temperature)

		λ_{nm}					
Metal	Conc. (M)	Unoxidised		Oxidised		Reduction of the oxidized species with diethylamine	
		Soret	Q	Soret	Q	Soret	Q
	10^{-4}	419	539, 578	416	539, 579	420	538, 577
VO	10^{-5}	412	539, 578	410	538, 577	409	538, 577
	10^{-6}	410	540, 579				
	10^{-4}	374	475, 569, 597	370	479, 558, 587	373	475, 568, 598
	10^{-5}	364	476, 567, 598	376	474, 554, 584	363	477, 567, 599
Mn	10^{-6}	362	476, 566, 598				
	10^{-4}	418	539, 558	419,436	530, 561	419	540, 560
Co	10^{-5}	392	540, 559	414,406	545, 562	418	541, 561
	10^{-6}	385	559				
	10^{-4}	420	523, 559	419	524, 560	421	526, 559
Ni	10^{-5}	400	523, 559	381, 406	524, 560	397	523, 559
	10^{-6}	389	523, 558				
	10^{-4}	423	537, 571	423	536, 572	424	536, 570
Cu	10^{-5}	412	536, 571	407	534, 572	414	537, 571
	10^{-6}	380	537, 571				
	10^{-4}	424	540, 574	421	552, 590	425	540, 575
Zn	10^{-5}	413	539, 575	414	551, 589	415	540, 576
	10^{-6}	390	539, 575				
	10^{-4}	419	539, 577	414	537, 579	420	540, 578
Sn	10^{-5}	407	539, 577	401	538, 580	414	539, 578
	10^{-6}	419	539, 576				

Table 3.2 UV- Visible *absorption* data of *metalloprotoporphyrin* IX-dimethyl ester, metal = VO, Co and Cu indicating isosbestic points in CH_2Cl_2 containing 0.1M $SbCl_5$ (at room temperature)

λ_{nm}		
MPPIXDME	Concentration	
	10^{-4}M	10^{-5}M
VO	---- 523, 592	392, 432, 526, 590
Co	450, 511, 583	439, 511,586
Cu	439, 521, 599	----------

Table 3.3 UV- Visible data of Absorbance and concentration of metalloprotoporphyrin IX-dimethyl ester, metal=VO, Mn, Co, Ni Cu, Zn and Sn (at room temperature).

MPPIX DME	Conc.(M)	Abs.	Q- Band	MPPIX DME	Conc.(M)	Abs.	Q- Band
VO	$1x10^{-6}$	0.02	579	Cu	$1x10^{-6}$	0.12	571
	$2x10^{-6}$	0.1	578		$2x10^{-6}$	0.32	571
	$1x10^{-5}$	0.23	578		$4x10^{-6}$	0.47	571
	$3x10^{-5}$	0.34	578		$1x10^{-5}$	0.65	571
	$4x10^{-5}$	0.76	578		$4x10^{-5}$	0.92	571
	$1x10^{-4}$	1.32	578		$6x10^{-5}$	1.34	571
					$8x10^{-5}$	1.55	571
					$9x10^{-5}$	2.6	571
Mn	$1x10^{-6}$	0.02	598	Zn	$1x10^{-6}$	0.2	575
	$6x10^{-6}$	0.033	598		$8x10^{-6}$	0.28	575
	$8x10^{-6}$	0.05	598		$1x10^{-5}$	0.4	575
	$9x10^{-6}$	0.09	598		$4x10^{-5}$	0.5	575
	$1x10^{-5}$	0.2	598		$8x10^{-5}$	0.71	575
	$6x10^{-5}$	0.21	597		$1x10^{-4}$	1.1	574
	$8x10^{-5}$	0.24	597		$2x10^{-4}$	1.32	574
	$1x10^{-4}$	1.2	597				
Co	$1x10^{-6}$	0.07	559	Sn	$2x10^{-6}$	0.01	576
	$8x10^{-6}$	0.08	559		$4x10^{-6}$	0.02	577
	$1x10^{-5}$	0.17	559		$6x10^{-6}$	0.03	577
	$6x10^{-5}$	0.34	558		$8x10^{-6}$	0.04	577
	$8x10^{-5}$	0.67	558		$1x10^{-5}$	0.06	577
	$1x10^{-4}$	1.6	558		$2x10^{-5}$	0.09	577
	$2x10^{-4}$	2.27	558		$4x10^{-5}$	0.16	577
					$6x10^{-}$	0.38	577
Ni	$1x10^{-6}$	0.06	558				
	$8x10^{-6}$	0.20	558				
	$1x10^{-5}$	0.28	559				
	$6x10^{-5}$	0.4	559				
	$8x10^{-5}$	0.7	559				
	$9x10^{-5}$	1.31	559				
	$1x10^{-4}$	2.4	559				

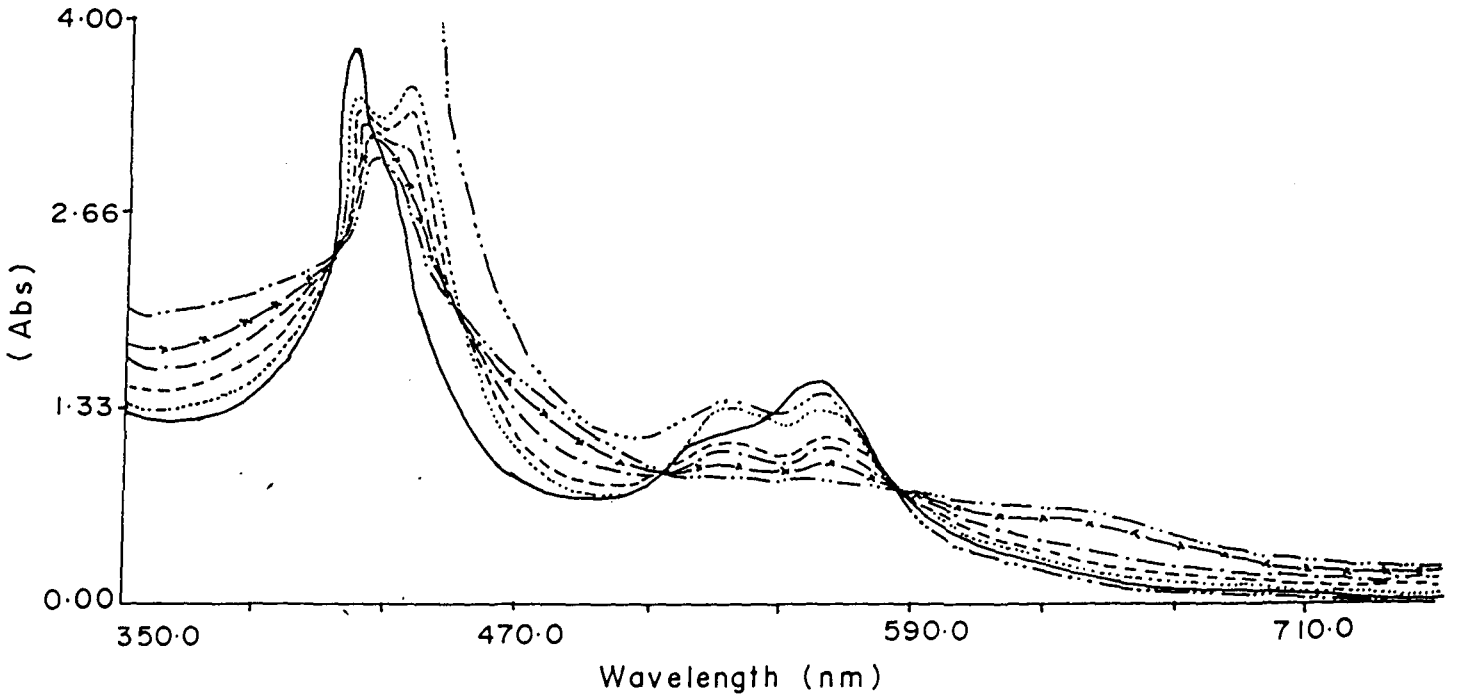

Figure 3.4a UV-Visible absorption spectra of CoPPIXDME (10^{-4}M) solution in CH_2Cl_2 unoxidised (—) oxidised(with 0.1M $SbCl_5$) ····, ----, — ·, — x . — · · and reduced (with diethyl amine) — · · ·

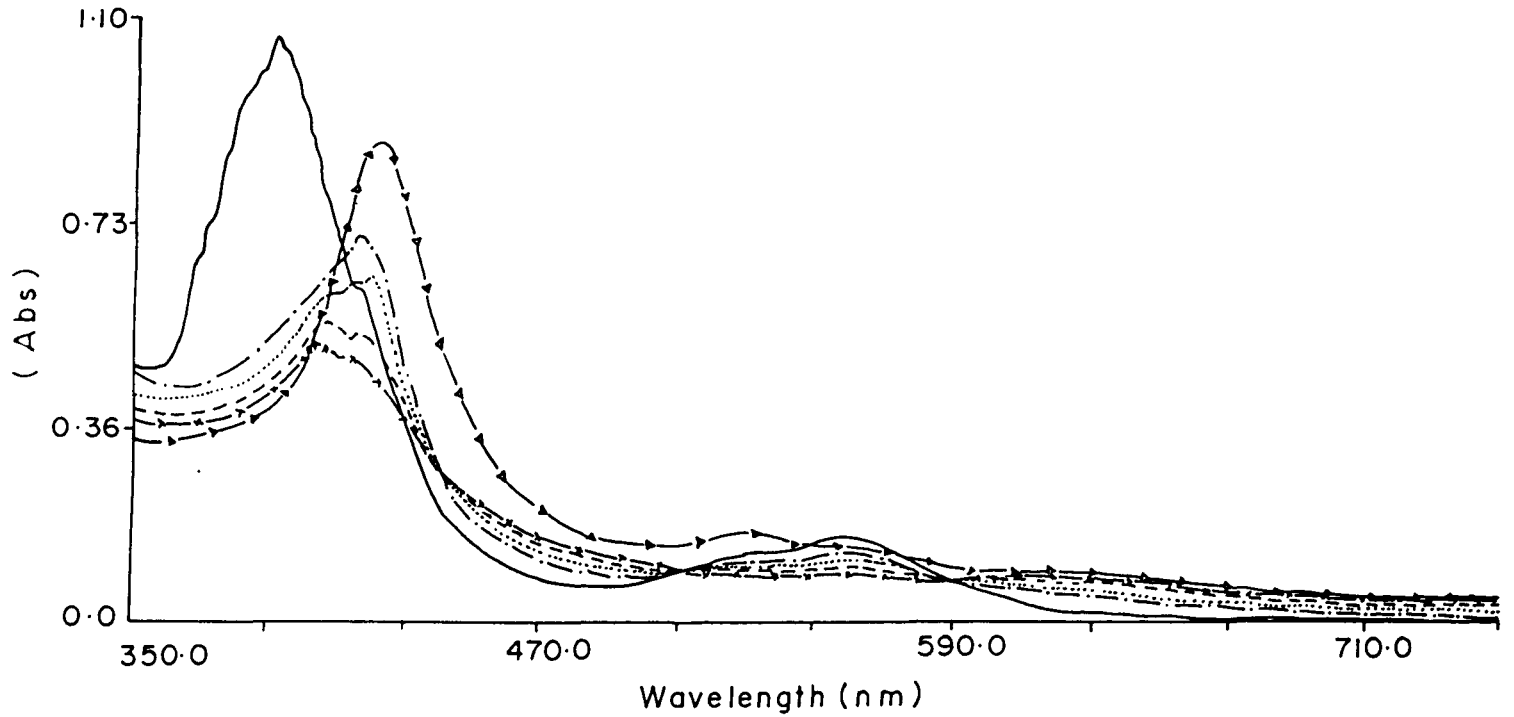

Figure 3.4b UV-Visible absorption spectra of CoPPIXDME (10^{-5}M) solution in CH_2Cl_2 unoxidised (—) oxidised(with 0.1M $SbCl_5$) — ·, ····, ----, — x and reduced (with diethyl amine) — Δ

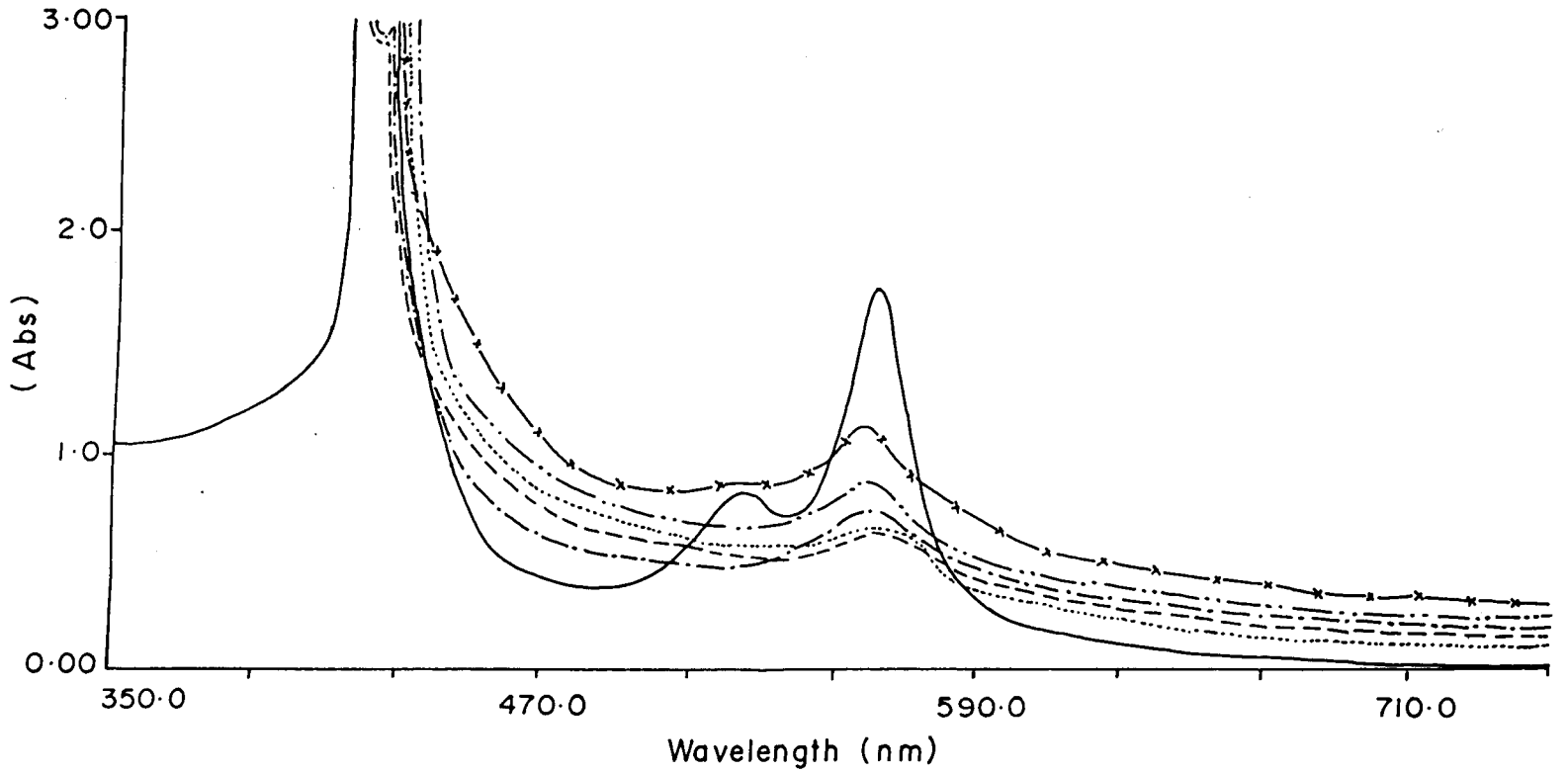

Figure 3.4c UV-Visible absorption spectra of NiPPIXDME (10^{-4}M) solution in CH_2Cl_2 unoxidised (—) oxidised(with 0.1M $SbCl_5$) —·, ----, ····, — · · ·, and reduced (with diethyl amine) — x

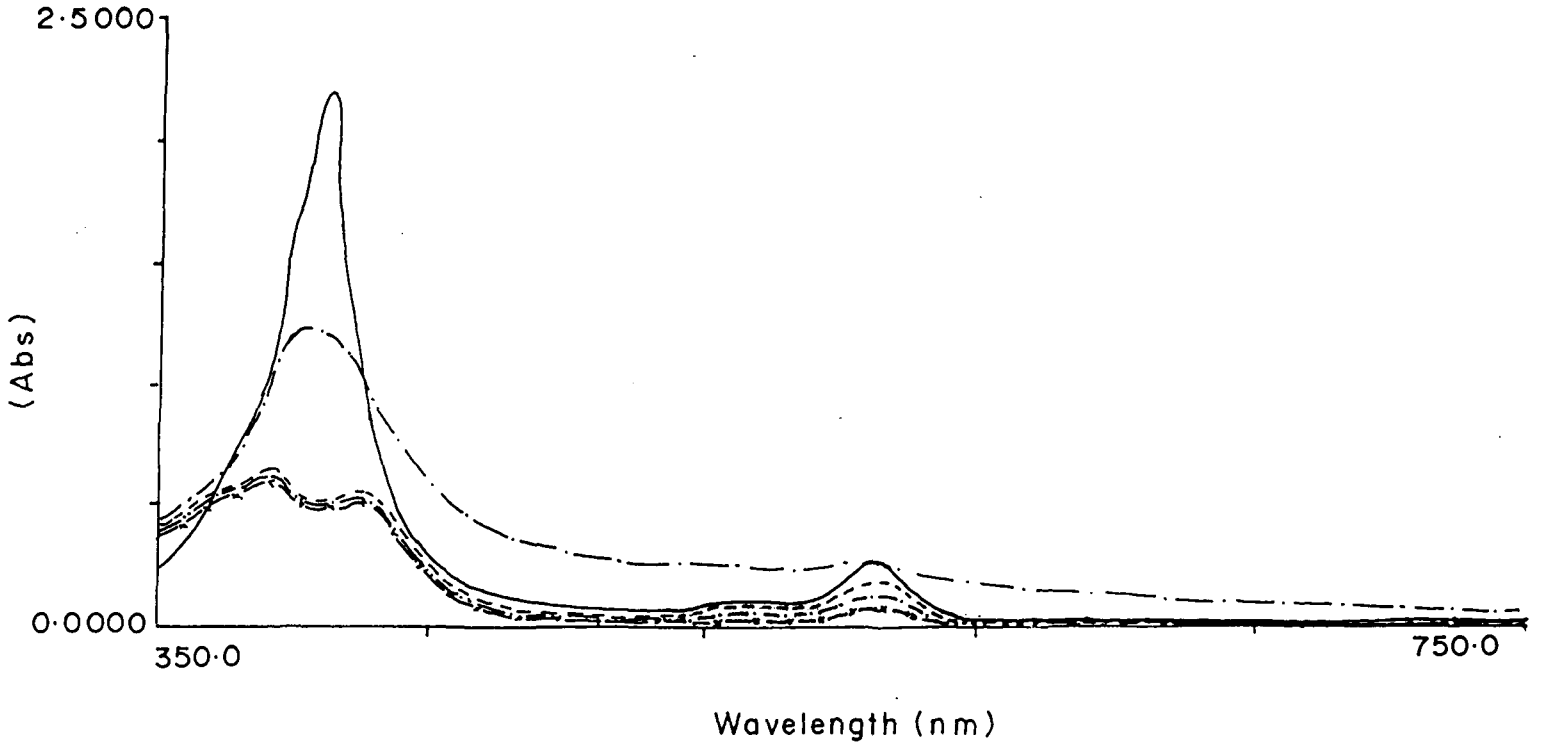

Figure 3.4d UV-Visible absorption spectra of NiPPIXDME (10^{-5}M) solution in CH_2Cl_2 unoxidised (—) oxidised(with 0.1M $SbCl_5$) —x. —·, ····, ---- and reduced (with diethyl amine) — · ·

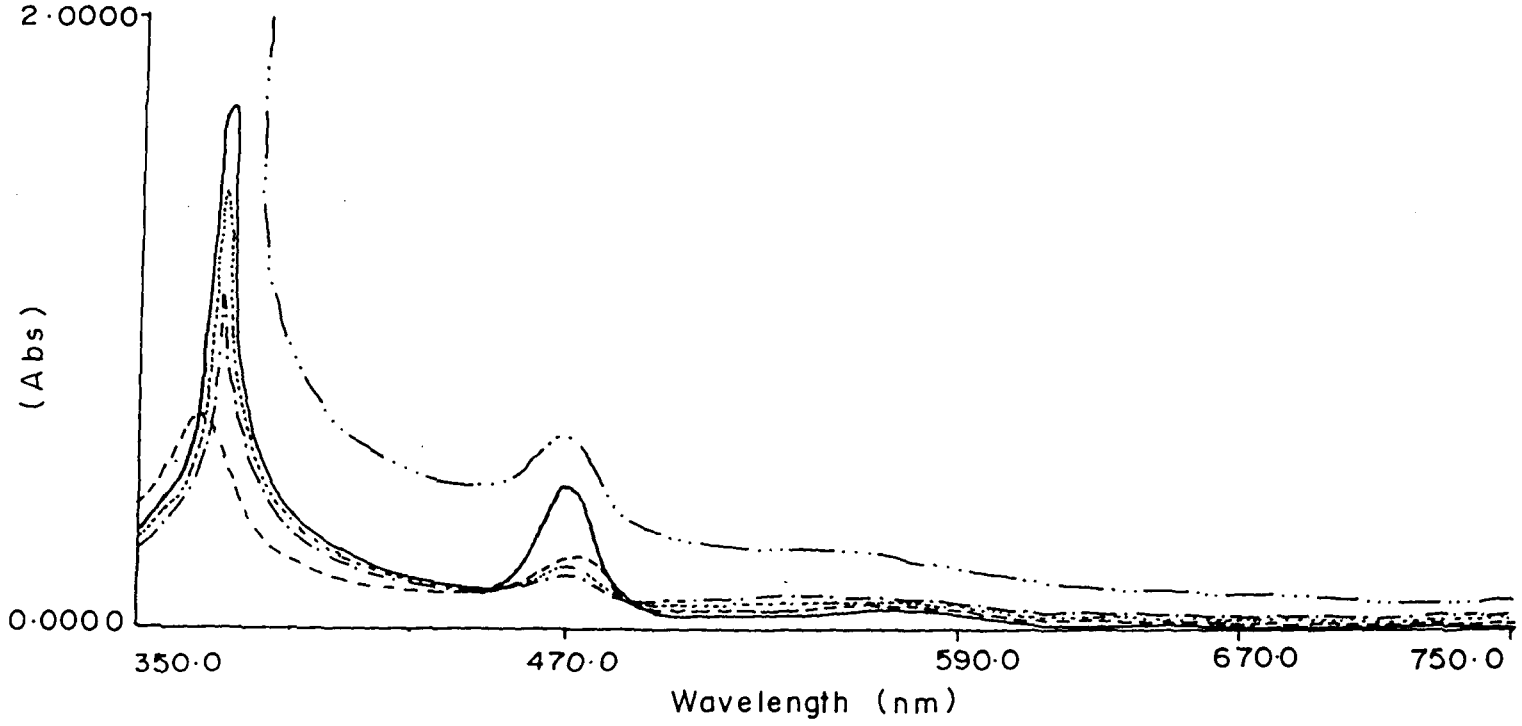

Figure 3.5 UV-Visible absorption spectra of MnPPIXDME (10^{-5}M) solution in CH_2Cl_2 unoxidised (—) oxidised(with 0.1M $SbCl_5$) · · · ·, — ·, ---- and reduced (with diethyl amine).— · · ·

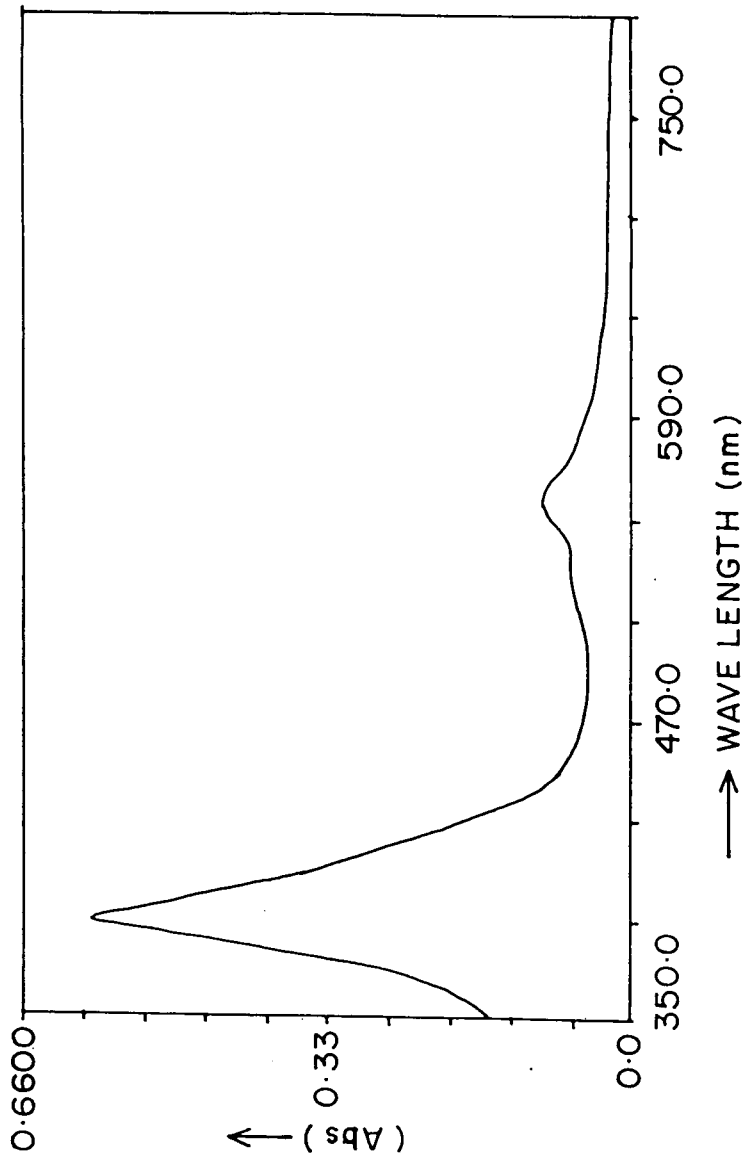

Figure 3.6 UV-Visible absorption spectra of CoPPIXDME (10^{-6}M) solution

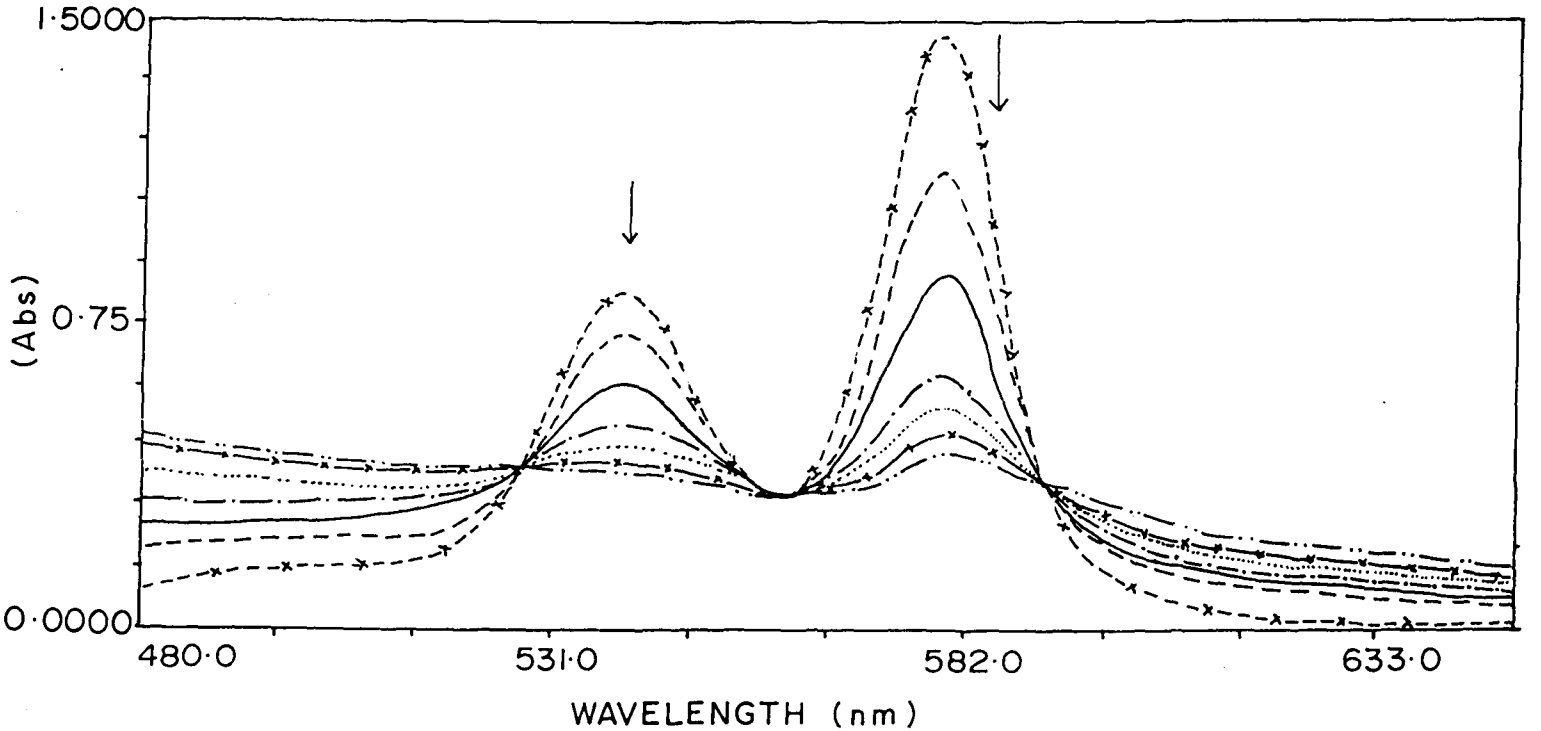

Figure 3.7a UV-Visible absorption spectra of VOPPIXDME (10^{-4}M) solution in CH_2Cl_2 indicating isosbestic point

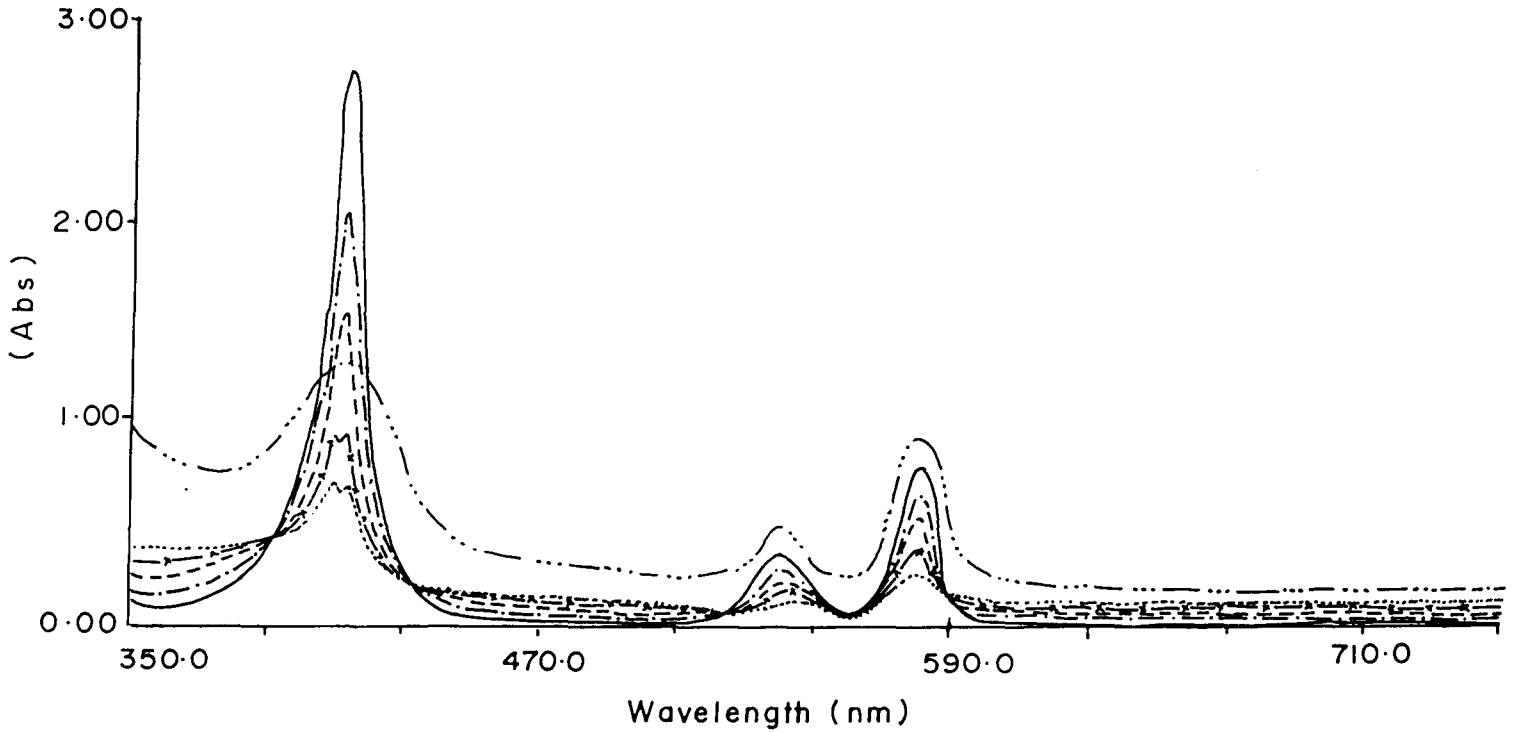

Figure 3.7b UV-Visible absorption spectra of VOPPIXDME (10^{-5}M) solution in CH_2Cl_2 indicating isosbestic point, unoxidised (—) oxidised (with 0.1M $SbCl_5$) —·, ---, —x·· and reduced (with diethyl amine) — ···

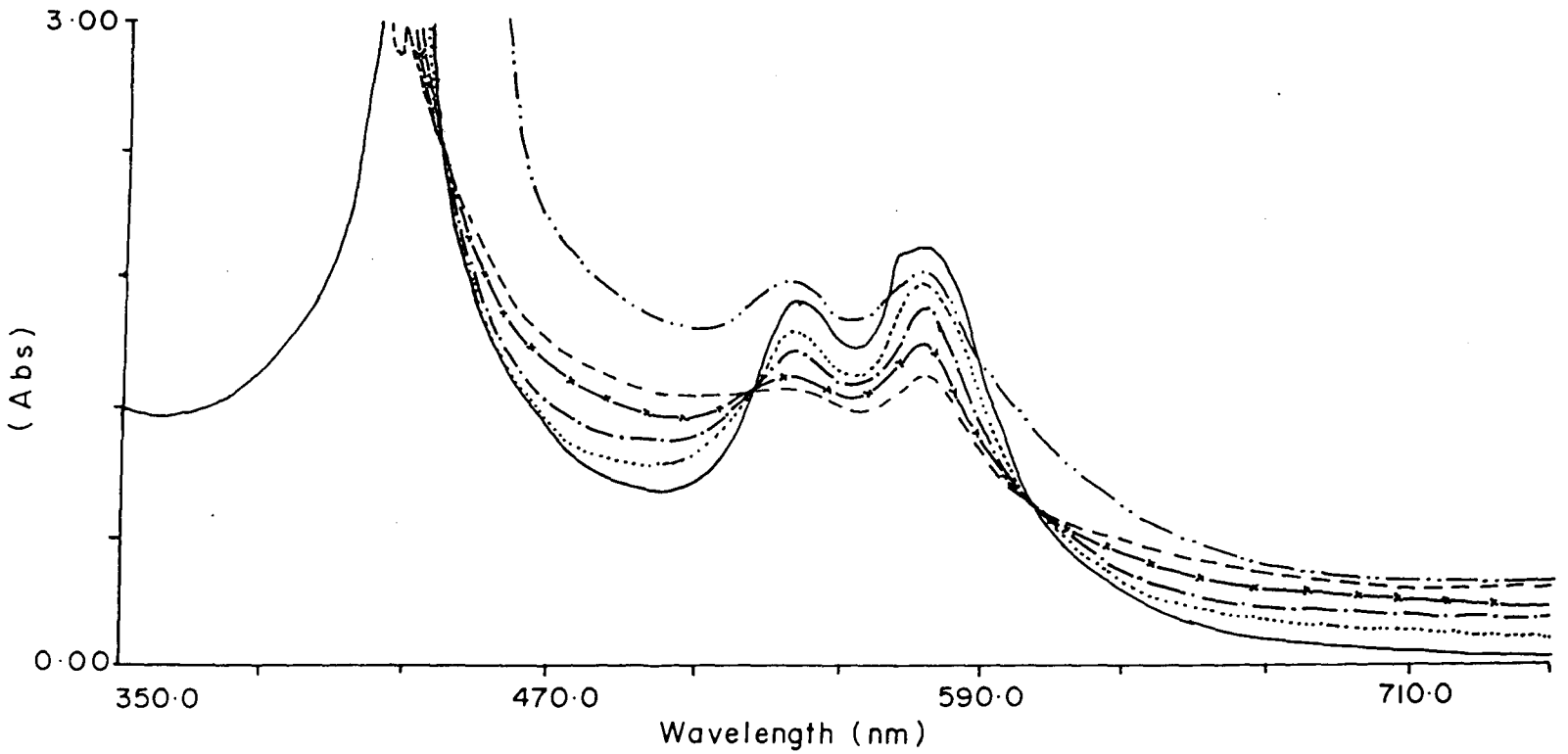

Figure 3.8 UV-Visible absorption spectra of CuPPIXDME (10^{-4}M) solution in CH_2Cl_2 indicating isosbestic point, unoxidised (—) oxidised (with 0.1M $SbCl_5$ ····, — ·, —x, --- and reduced (with diethyl amine) — ··

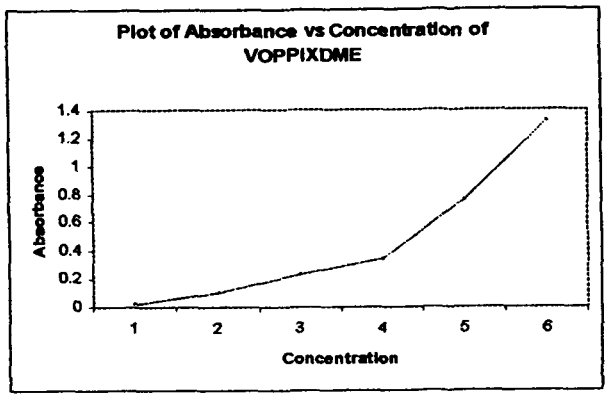

(a)

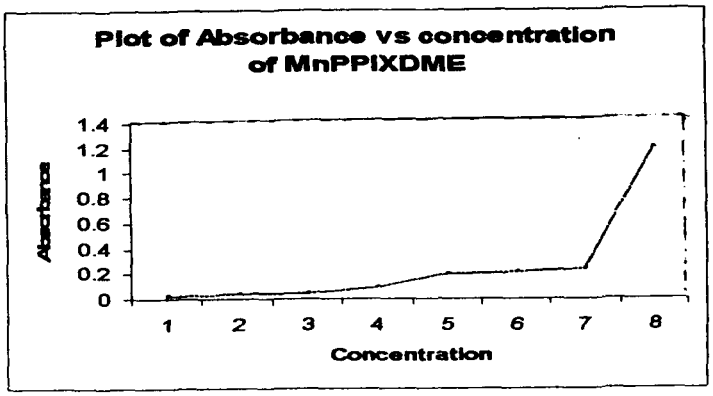

(b)

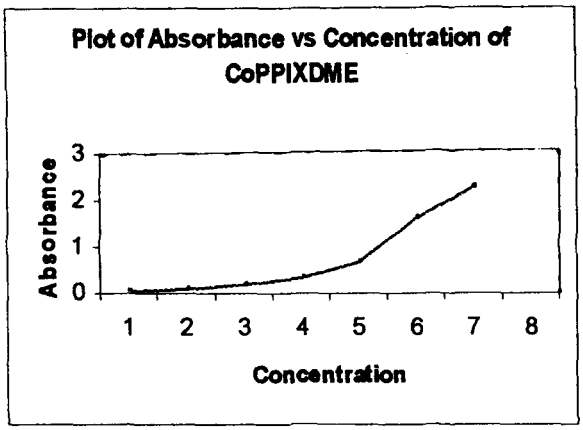

(c)

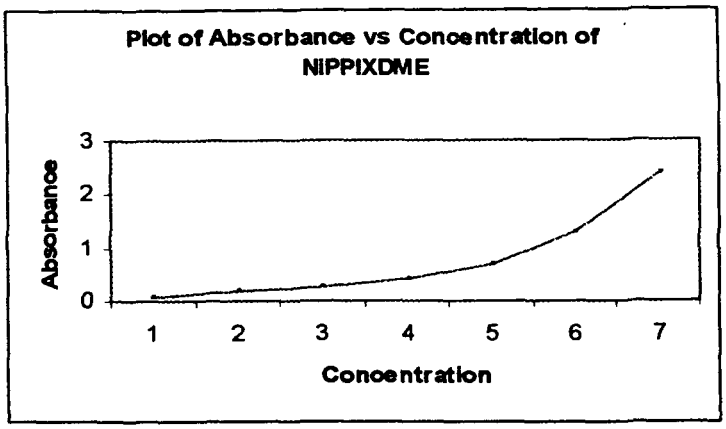

(d)

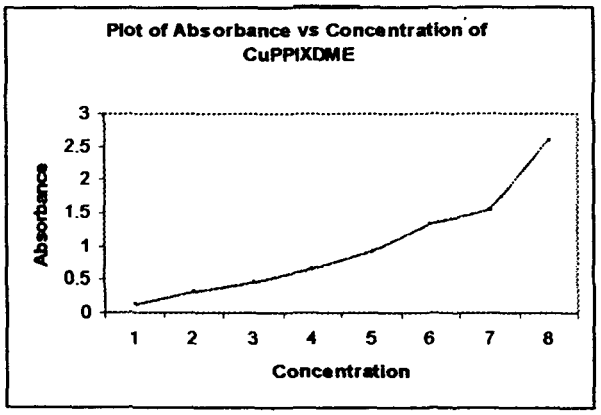

(e)

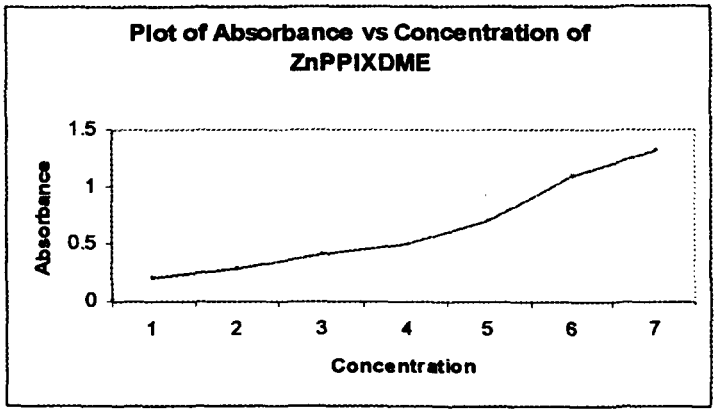

(f)

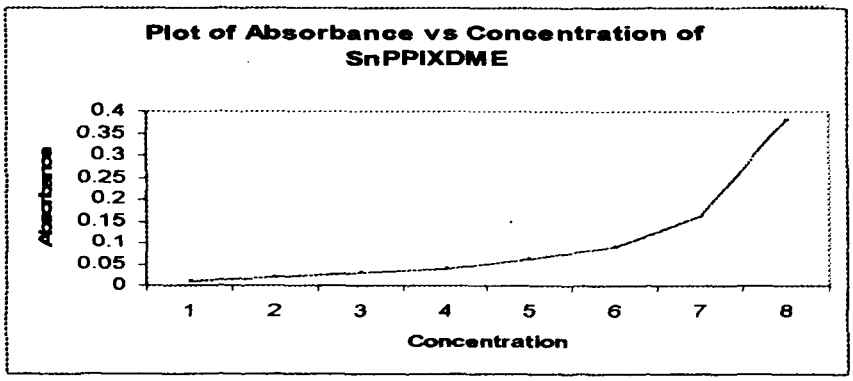

(g)

Fig 3.9(a-g) Plot of Absorbance vs concentration of MPPIXDME

REFERENCES

1. M. Gouterman, J. Chem. Phys., 30, 1139 (1959)
2. M. Gouterman, J. Mol. Spectroscopy. 6, 138 (1961)
3. M. Gouternam, in " the Porphyrins" Edited by D. Dolphin (Academic Press, New York 1979) Vol. III, Part A, and references therein
4. A. H. Crown, A. B. Chivis, W. R. Poor, D.G. Whitten and E.W. Baker, J. Am. Chem. Soc., 90, 6577 (1968)
5. T. Hashimoto, Y. K. Choe, H. Nakano and K. Hirao, J. Phys. Chem., A, 103, 1894 (1999)
6. B.D. Berezin, " Co-ordination Compounds of porphyrins and Phthalocyanines" Willy Interscience, Chicherter 1981
7. K. M. Smith, in " Porphyrin and metalloporphyrins" Edited by K. M. Smith (Elsevier, Amsterdam, 1975) p.3. and references therein
8. J. Fajer, D.C. Borg, A. Forman, D, Dolphin and R.H. Felton, J. Am. Chem. Soc., 92, 3451 (1970)
9. J. H. Furhop and D. Manzerall, J. Am. Chem. Soc., 90, 3875 (1968)
10. R. H. Felton, D. Dolphin, D.C. Borg and J. Fajer, J. Am. Chem. Soc. 91, 196 (1969)
11. R. H. Felton, "The Porphyrins" Edited by D. Dolphin (Academic Press. New York, 1978) Vol. V, p. 81 and references therein
12. A. Hughes, Proc. R. Soc. London, Ser. A., 155, 710 (1936)

13. K. Kano, K. Fukuda, H. Wakami, R. Shiyabu and R.F. Pasternack, J. Am. Chem. Soc., 122, 7494 (2000) and references therein

14. T. K. Chandrashekar, H.V. Willegen and M.H. Ebessole, J. Phys. Chem., 89, 3453 (1985) and references therein

15. M. Y. Choi, J. A. Pollard, M. A. Webb and J. L. McHale, J. Am. Chem. Soc., 125, 810 (2003)

16. M. Ravikant, D. Reddy and T. K. Chandrashekar, J. Chem. Soc. Dalton Trans., 2103 (1991) and references therein

17. A. Lemtur, B. K. Chakravorty, T. K. Dhar and J. Subramanian, J. Phys. Chem., 88, 5603(1984)

CHAPTER – 4

VISIBLE ABSORPTION STUDIES OF METAL COMPLEXES OF MESOPORPHYRIN IX- DIMETHYL ESTER, METAL = VO, Mn, Co, Ni and Cu.

CHAPTER-4

VISIBLE ABSORPTION STUDIES OF METAL COMPLEXES OF MESOPORPHYRIN IX- DIMETHYL ESTER, METAL = VO, Mn, Co, Ni and Cu.

4.1 INTRODUCTION

The structure of free base and metallomesoporphyrin IX-dimethyl ester is shown in figure 4.1a and 4.1b. Metallomesoporphyrin IX- dimethyl esters do form dimer and aggregates[1]. But the aggregation is not as extensive as in the case of MPPIXDME. Monomeric and dimeric species exists at room temperature. Earlier report have shown that at around 10^{-2} M concentration (in CH_2Cl_2) VOMPIXDME aggregates (dimer) in the similar way as in the case of VOPPIXDME, while it shows monomeric form below the concentration 10^{-3} M. On careful examination we observe that metallomesoporphyrin IX-dimethyl ester exists as dimer on oxidation with $SbCl_5$ (at room temperature) even at a concentration around 10^{-5}M (in CH_2Cl_2)

4.2 EXPERIMENTAL DETAILS

Solutions of metallomesoporphyrin IX- dimethyl ester of different concentrations 10-4M, 10-5M and10-6M were prepared in dichloromethane. Visible absorption spectra were recorded at room temperature. Oxidations were carried out using 0.1M solution of $SbCl_5$ in dichloromethane. The oxidised species were reduced by using diethyl amine.

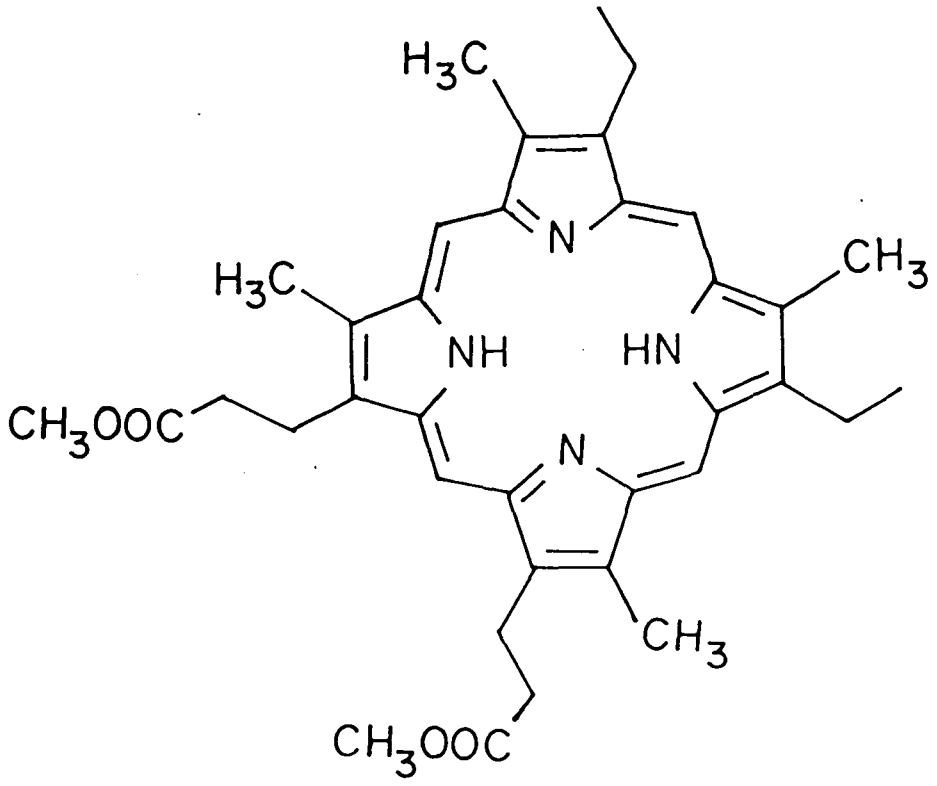

Figure 4.1a Structure of free base mesoporphyrin IX-dimethyl ester

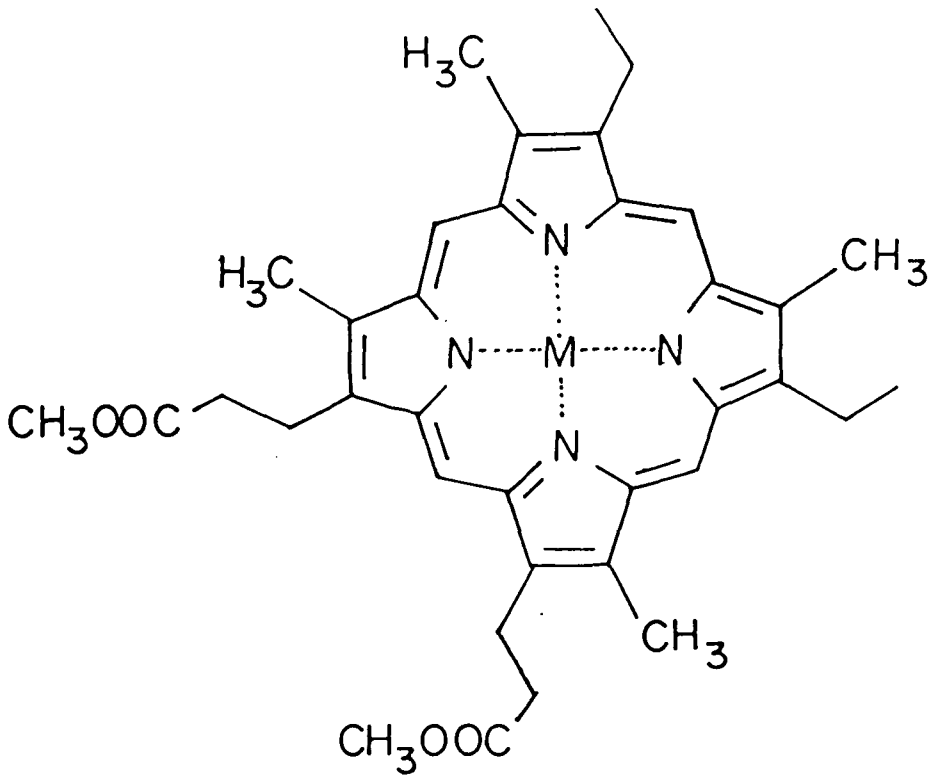

Figure 4.1b Structure of metallomesoporphyrin IX-dimethyl ester

4.3 RESULTS

Visible absorption spectra and results are presented in the figures 4.2(a, b, c, d, e, f and g) and the table 4.1. At 10^{-4}M all the soret bands show some splitting. The soret band of all the metallomesoporphyrin IX-dimethyl ester have shown blue shift on dilution except for Vanadylmesoporphyrin IX- dihydrochloride. Visible bands show no appreciable shift. On oxidation with $SbCl_5$, the soret band of all the complexes show slight blue shift for the soret band while Q bands show slight red shift. The blue shift of the soret band on oxidation with $SbCl_5$ is more pronounced in the case of VOMPIXDME. As we go on adding $SbCl_5$ (1drop of capillary tube of size 1mm) the intensity of the Soret band as well as that of the Q bands decreases exhibiting isosbestic points at 542, 554, 581 for10^{-4} M and 429, 519, 542, 555, 577 for 10^{-5}M. CoMPIXDME(10^{-5}M) and VOMPIXdiHCl also exhibit isosbestic points (see figure 4.2a, b, f and g and table 4.2). The soret band also exhibits splitting.

Beers law experiments indicate a break in the linearity at 10^{-5}M. (figure 4.3 and table 4.3)

4.4 DISCUSSION

The results imply that metallomesoporpyrin IX dimethyl ester exists as dimer within the concentration range 10^{-4}M to 10^{-5}M. Below 10^{-5}M it exists as monomer. This is clear from the Beer's law experiments. The presence of isosbestic points[3,4] on oxidation of 10^{-5}M solution of metallomesoporphyrin IX - dimethyl ester with $SbCl_5$ indicates the presence of two species. This may be due to monomer-dimer co-existence. The slight blue shift in the soret band and very slight red shift in the Q bands may be

well within the frame work of the exciton theory[5]. However, for the unoxidised metallomesoporphyrin IX dimethyl ester, the observed blue shift in the soret band due to dilution cannot be explained by the exciton theory[6,7]. It is our observations that at higher concentration it exists in dimeric form while it dissociates to monomers at lower concentrations.

4.5 CONCLUSION

From the visible absorption study we conclude the following:

(i) For un-oxidized metallomesoporphyrin IX-dimethyl ester, the blue shift of the soret band on dilution cannot be explained by the exciton theory. Therefore, we qualitatively attribute it to the dissociation of the dimer to monomer at around 10^{-5}M concentration.

(ii) Even at concentration 10^{-5}M due to the presence of $SbCl_5$, metallomesoporphyrin IX-dimethyl ester dimerises and show shifts as predicted by exciton theory.

Table 4.1 UV- Visible absorption data of Unoxidised, Oxidised and Reduced products of metallomesoporphyrin IX -dimethyl ester, metal = VO, Mn, Co, Ni and Vanadyl mesoporphyrin IX-dihydrochloride in CH_2Cl_2 containing 0.1M $SbCl_5$ (at room temperature)

		λ_{nm}					
Metal	Conc (M)	Unoxidised		Oxidised		Reduction of the oxidized species with diethylamine	
		Soret	Q	Soret	Q	Soret	Q
VO	10^{-4}	416	533, 572	414	516, 573	417	533, 571
	10^{-5}	402	532, 571	395	533, 572	405	532, 570
	10^{-6}	391	533, 570				
Mn	10^{-4}	414	471, 556, 586	411	479, 567, 594	415	470, 555, 585
	10^{-5}	370	471, 555, 586	368	468, 550, 582	373	471, 554, 584
	10^{-6}	366	471, 557, 584				
Co	10^{-4}	421	529, 551	419	531, 553	422	530, 552
	10^{-5}	415	529, 553	412	525, 556	413	528, 552
	10^{-6}	393	529, 552				
Ni	10^{-4}	413	514, 550	406	496, 574	414	514, 550
	10^{-5}	409	514, 551	381	496, 577	390	513, 552
	10^{-6}	407	514, 550				
Cu	10^{-4}	398	524, 559	383	513, 572	398	524, 560
	10^{-5}	397	523, 560	382	521, 561	397	523, 560
	10^{-6}	396	524, 560				
VOM PIXdi HCl	10^{-4}	417	530, 567	415	530, 567	419	530, 567
	10^{-5}	403	530, 568	388	530, 568	398	530, 567
	10^{-6}	405	532, 570				

Table 4.2 UV- Visible absorption data of metallomesoporphyrin IX- dimethyl ester, metal= VO, and Co and Vanadyl mesoporphyrin IX-dihydrochloride indicating isosbestic points in CH_2Cl_2 containing 0.1M $SbCl_5$ (at room temperature)

	λ_{nm}	
M'MPIXDME(M'=metal)	Concentration	
	10^{-4}M	10^{-5}M
VO	542, 554, 581	429, 519, 542, 555, 577
Co	---------	400, 430, 508, 571
VOMPIXdiHCl	428, 521, 545, 556, 580	520, 543, 556, 580

Table 4.3 UV- Visible data of Absorbance and concentration of metallomesoporphyrin IX-dimethyl ester, metal=VO, Mn, Co, Ni Cu, and Vanadyl mesoporphyrin IX-dihydrochloride (at room temperature).

M'MP IX DME	Conc.(M)	Abs.	Q- Band	M'MP IX DME	Conc.(M)	Abs.	Q- Band
	$1x10^{-6}$	0.2	570		$1x10^{-6}$	0.06	560
	$2x10^{-6}$	0.28	571		$2x10^{-6}$	0.3	560
	$1x10^{-5}$	0.42	571		$4x10^{-6}$	0.6	560
VO	$2x10^{-5}$	0.55	571	Cu	$1x10^{-5}$	0.99	560
	$4x10^{-5}$	1.42	571		$2x10^{-5}$	1.5	559
	$1x10^{-4}$	2.5	572		$4x10^{-5}$	3.05	559
					$1x10^{-4}$	3.31	559
	$1x10^{-6}$	0.08	584		$1x10^{-6}$	0.03	570
	$2x10^{-6}$	0.09	584		$2x10^{-6}$	0.21	570
	$4x10^{-6}$	0.1	584		$4x10^{-6}$	0.39	570
Mn	$6x10^{-6}$	0.11	584		$1x10^{-5}$	0.6	568
	$1x10^{-5}$	0.12	585	VOMP	$2x10^{-5}$	0.93	568
	$2x10^{-5}$	0.2	585	IX	$4x10^{-5}$	1.51	567
	$4x10^{-5}$	0.37	585	diHCL	$1x10^{-4}$	2.5	567
	$6x10^{-5}$	0.86	585				
	$1x10^{-4}$	1.3	586				
	$1x10^{-6}$	0.03	552				
	$2x10^{-6}$	0.049	551				
	$4x10^{-6}$	0.05	551				
Co	$1x10^{-5}$	0.065	553				
	$2x10^{-5}$	0.15	552				
	$4x10^{-5}$	0.23	552				
	$1x10^{-4}$	1.8	551				
	$1x10^{-6}$	0.09	550				
	$2x10^{-6}$	0.16	550				
Ni	$4x10^{-6}$	0.25	551				
	$1x10^{-5}$	0.4	551				
	$2x10^{-5}$	0.74	550				
	$4x10^{-5}$	1.68	550				
	$1x10^{-4}$	1.7	550				

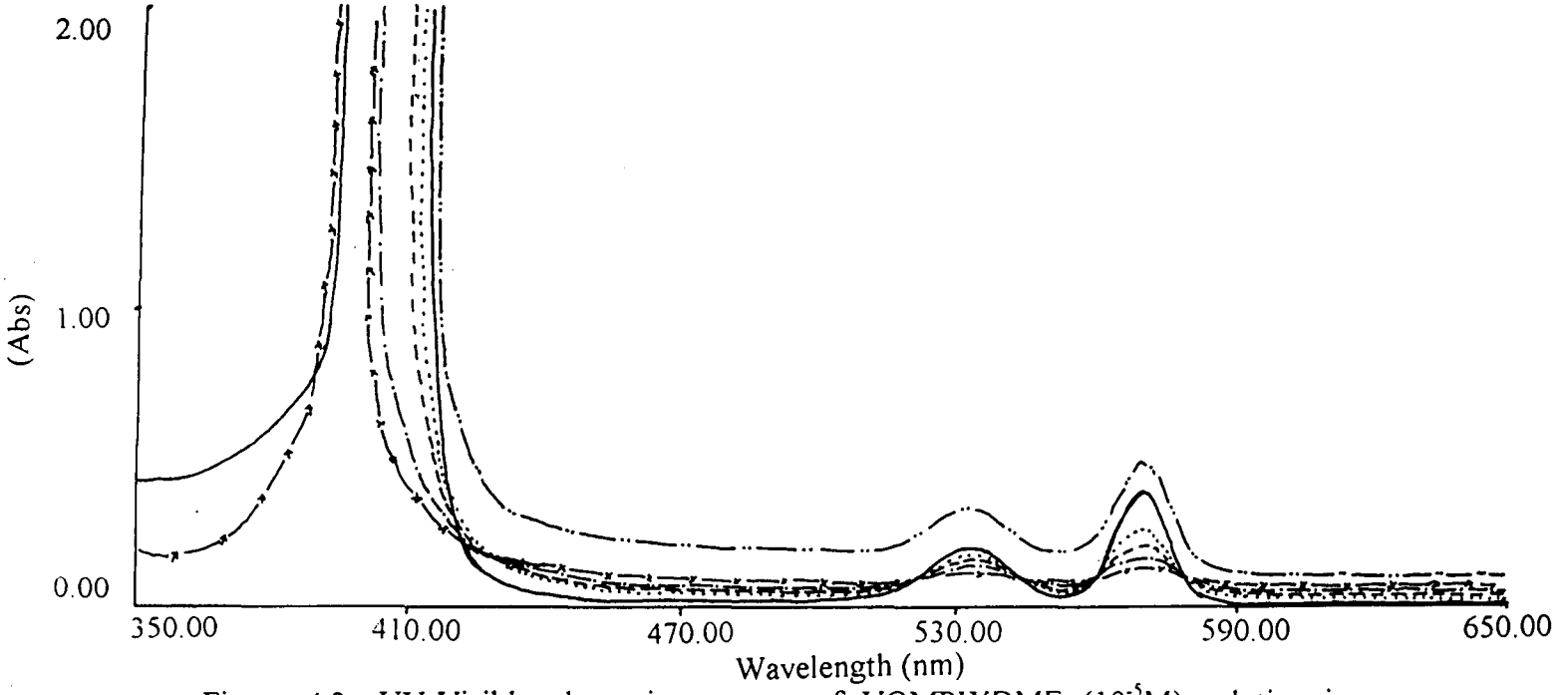

Figure 4.2a UV-Visible absorption spectra of VOMPIXDME (10^{-5}M) solution in CH_2Cl_2 unoxidised (—) oxidised(with 0.1M $SbCl_5$) ····, ----, — ·, — x and reduced (with diethyl amine) — · ·

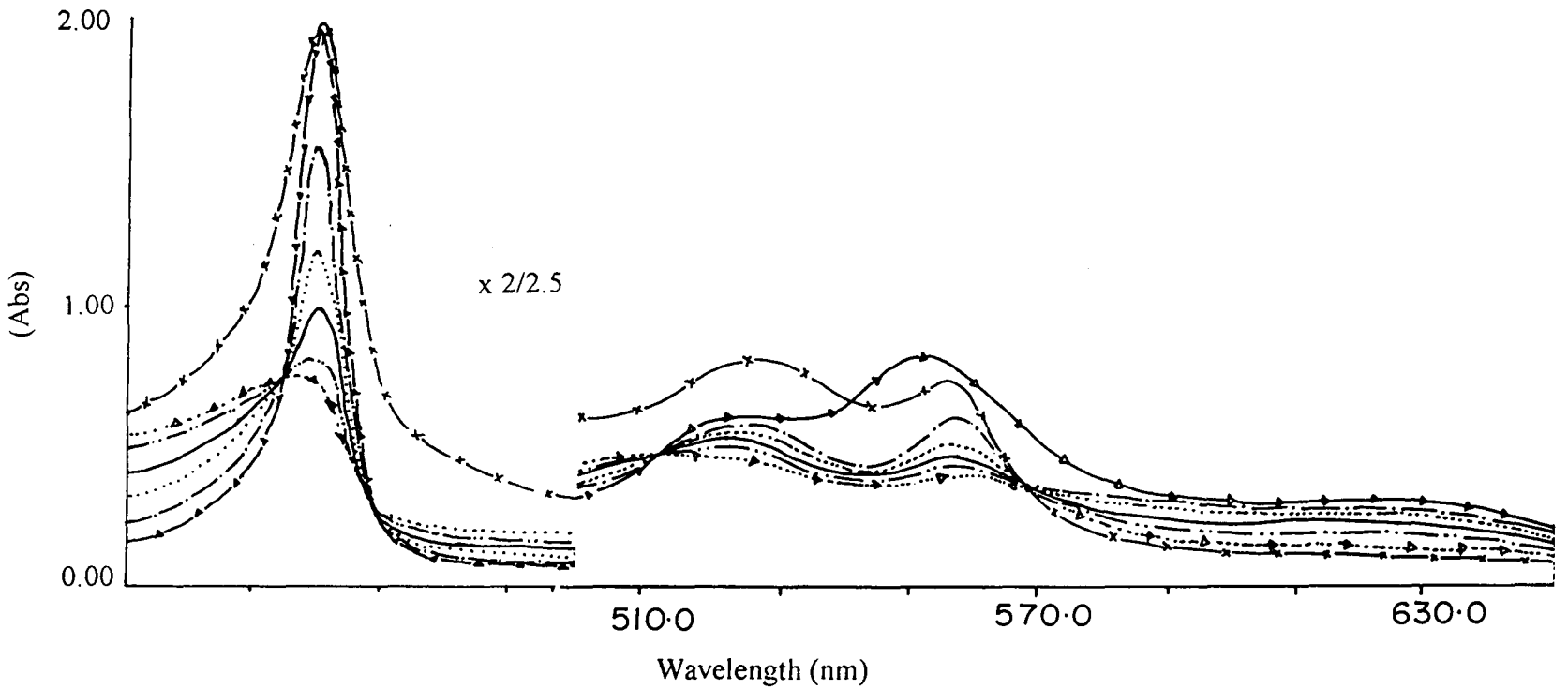

Figure 4.2b UV-Visible absorption spectra of CoMPIXDME (10^{-5}M) solution in CH_2Cl_2 unoxidised (—△) oxidised(with 0.1M $SbCl_5$) — ·, ····, —, — · ·, ····△····, and reduced (with diethyl amine) — x

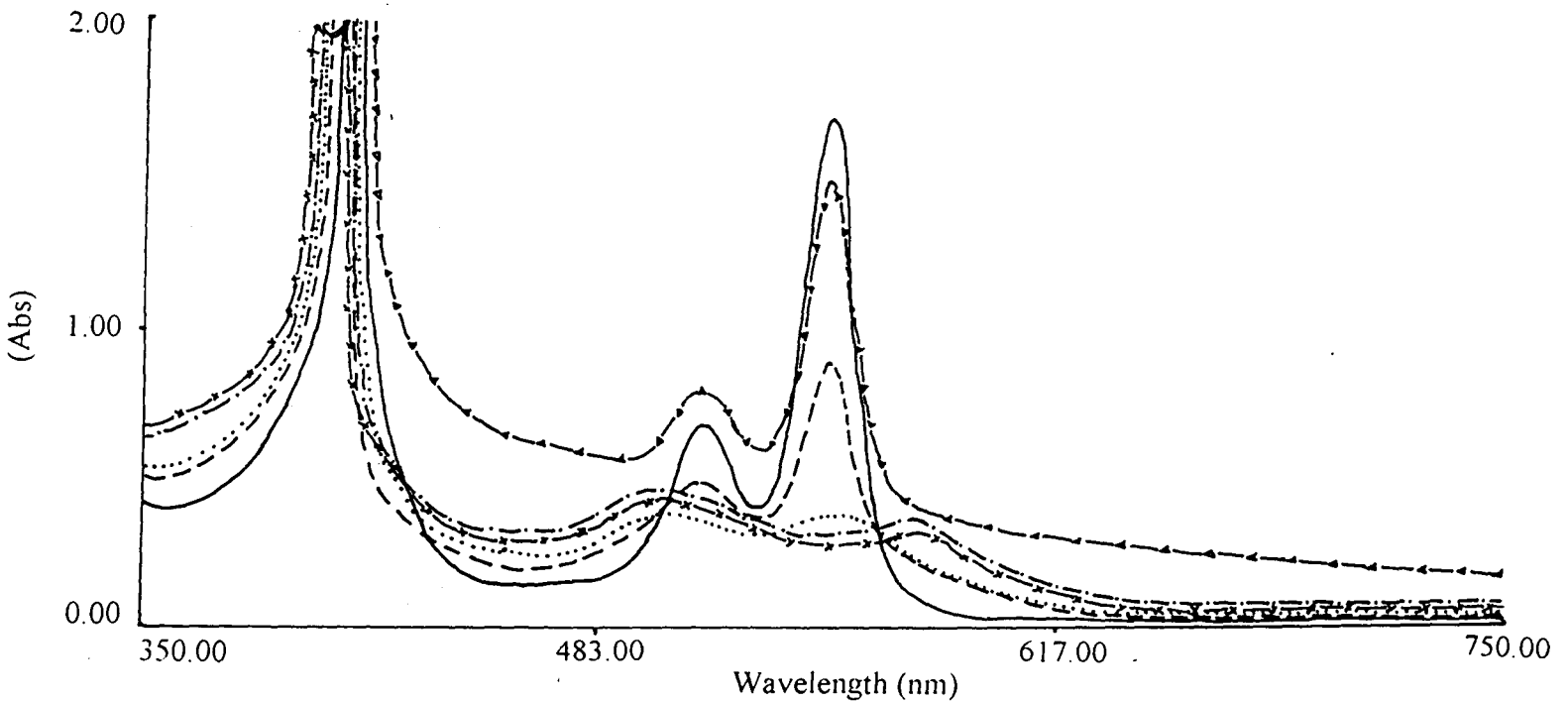

Figure 4.2c UV-Visible absorption spectra of NiMPIXDME (10^{-4}M) solution in CH_2Cl_2 unoxidised (—) oxidised(with 0.1M $SbCl_5$) ----, ····, —·, — x and reduced (with diethyl amine) —Δ

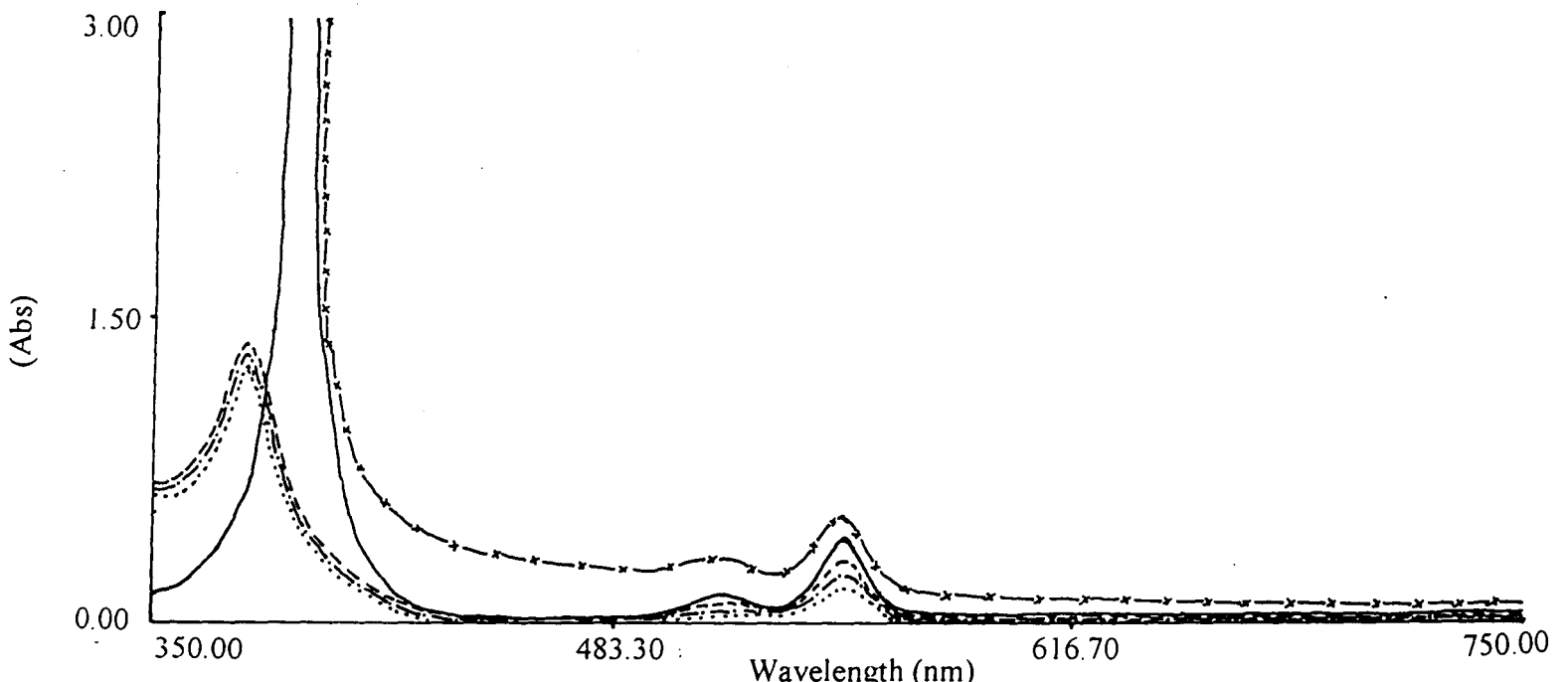

Figure 4.2d UV-Visible absorption spectra of NiMPIXDME (10^{-5}M) solution in CH_2Cl_2 unoxidised (—) oxidised(with 0.1M $SbCl_5$) ----, — ·, ···· and reduced (with diethyl amine) — x

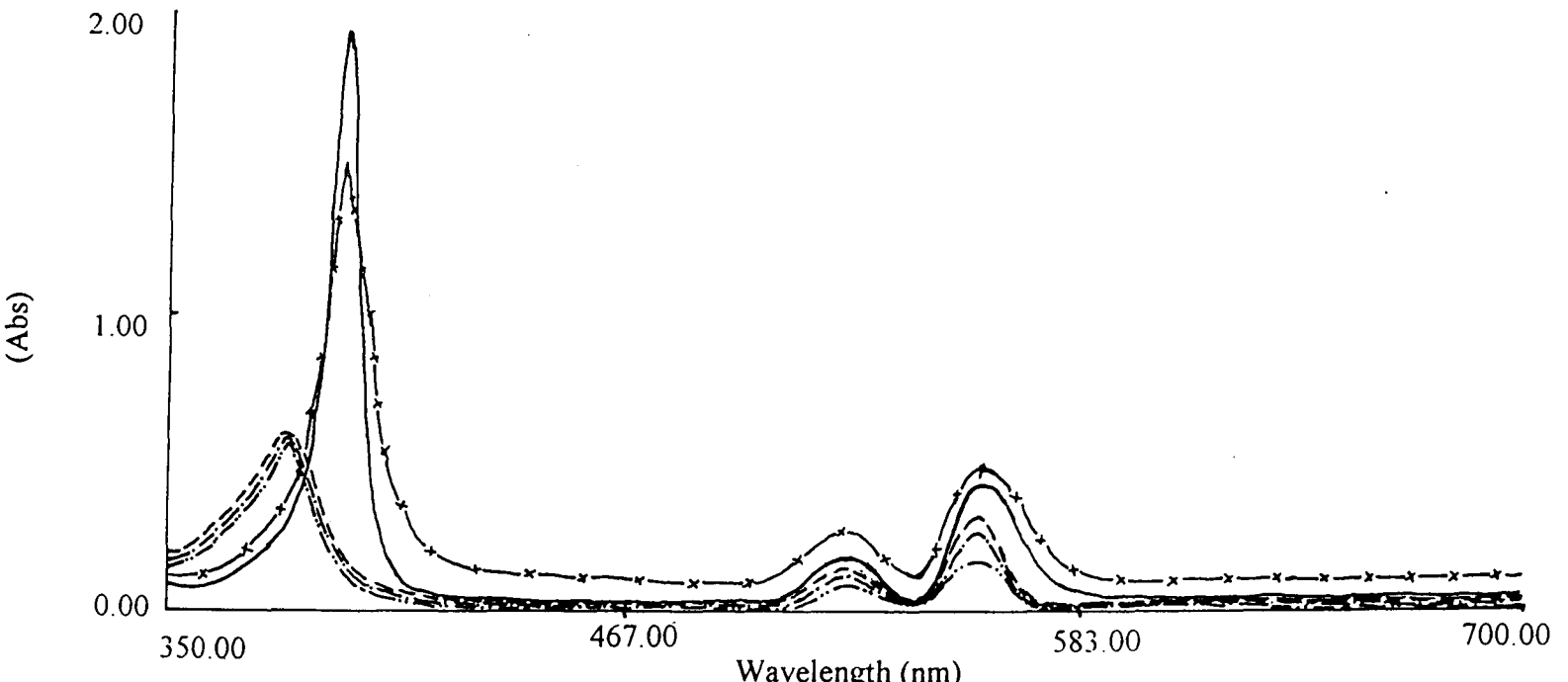

Figure 4.2e UV-Visible absorption spectra of CuMPIXDME (10^{-5}M) solution in CH_2Cl_2 unoxidised (—) oxidised(with 0.1M $SbCl_5$) ----, —·, —· · and reduced (with diethyl amine) — x

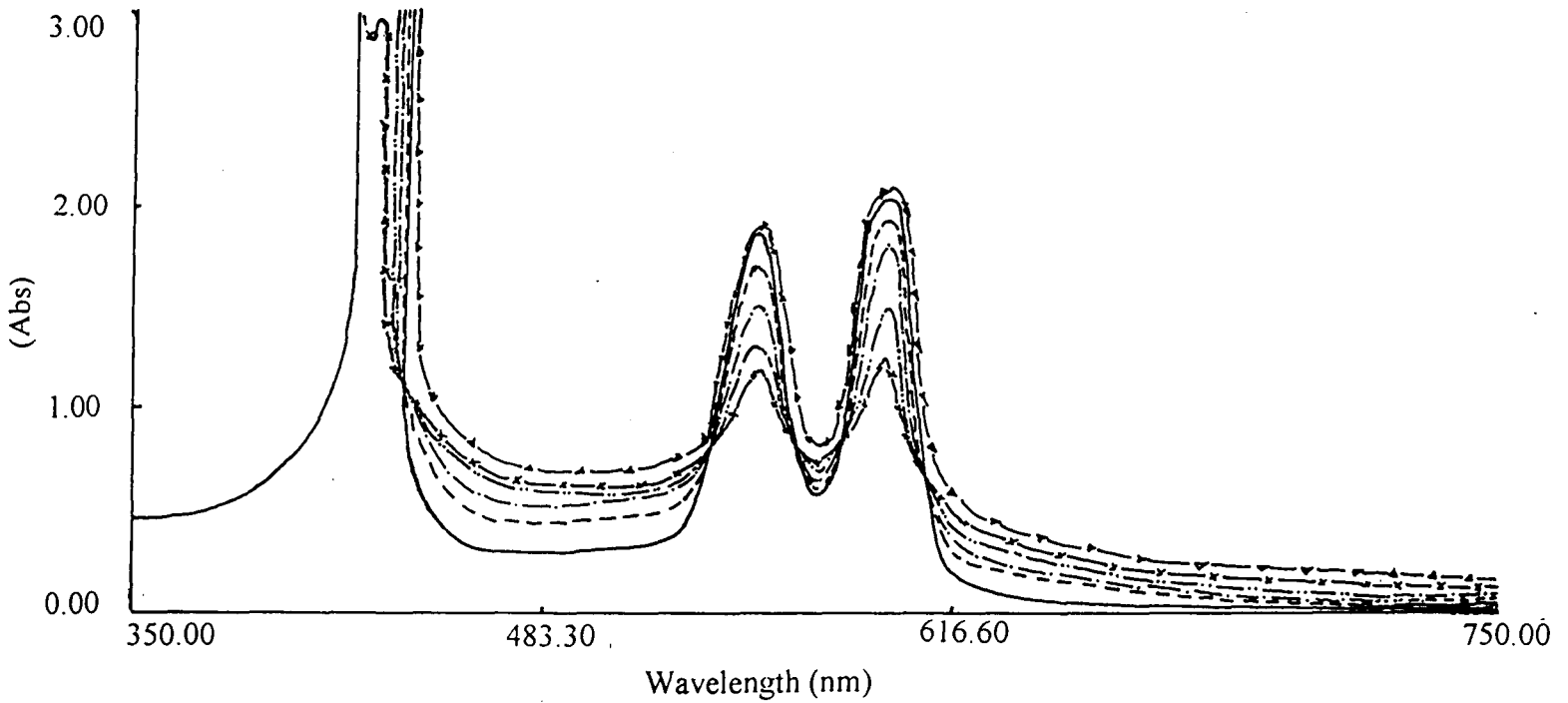

Figure 4.2f UV-Visible absorption spectra of VOMPIXdiHCl (10^{-4}M) solution in CH_2Cl_2 unoxidised (—) oxidised (with 0.1M $SbCl_5$) —x,—··, —·, ---- and reduced (with diethyl amine) —Δ

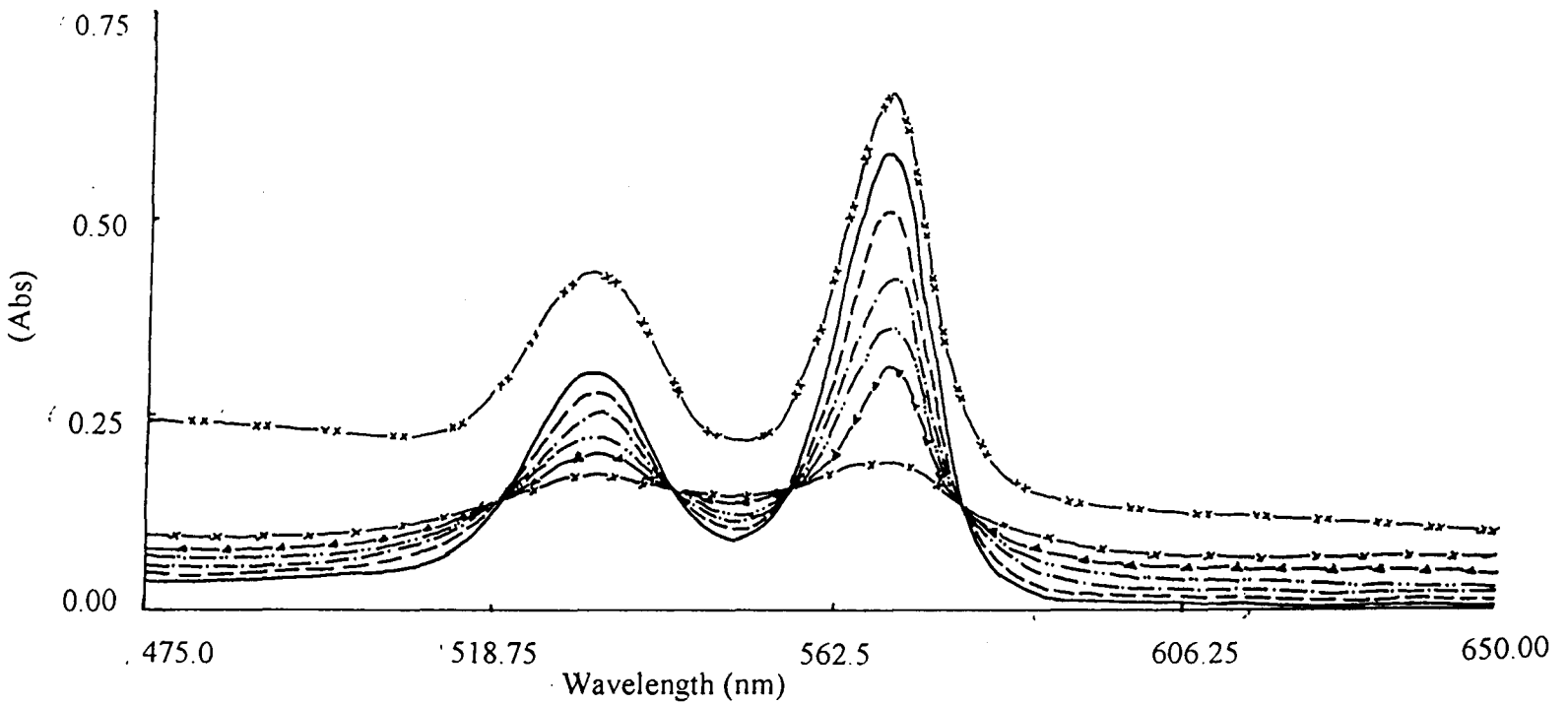

Figure 4.2g UV-Visible absorption spectra of VOMPIXdiHCl (10^{-5}M) solution in CH_2Cl_2 unoxidised (—) oxidised (with 0.1M $SbCl_5$) ----, —·, —··, — ∧ , —x and reduced (with diethyl amine) —x x

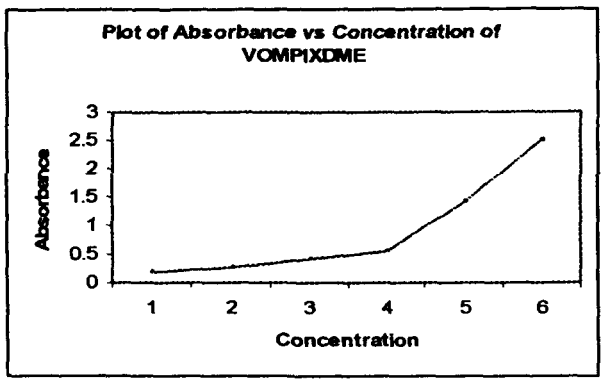

(a)

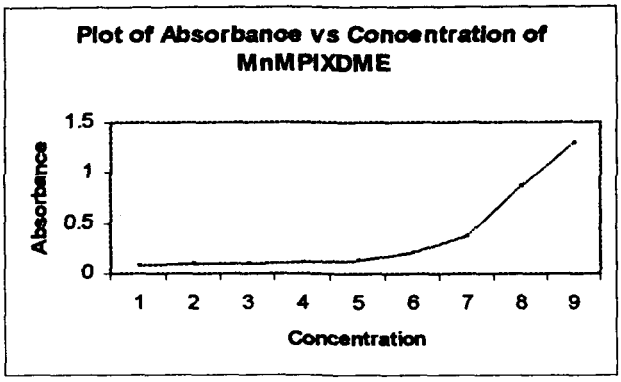

(b)

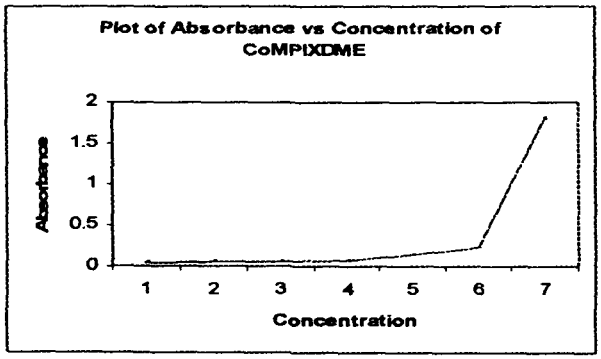

(b)

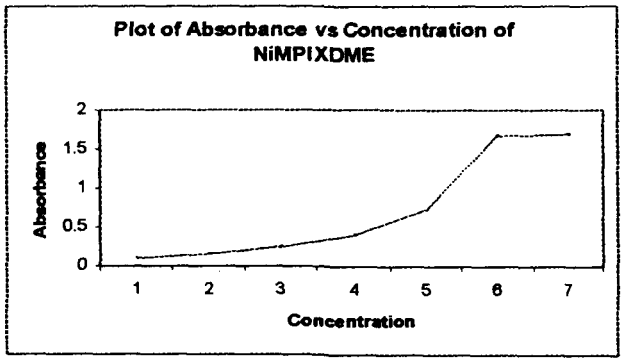

(d)

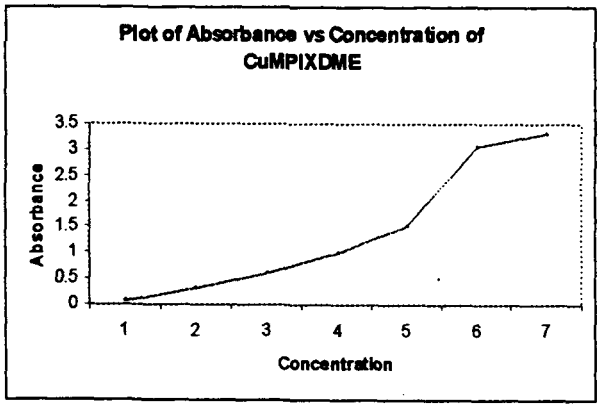

(e)

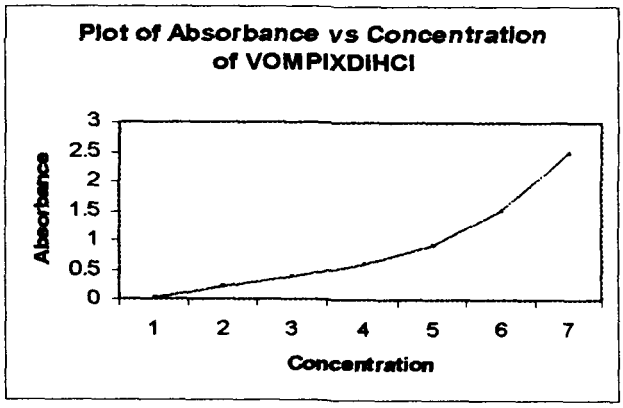

(f)

Figure 4.3(a-f) Plot of Absorbance vs. Concentration of M'MPIXDME and VOMPIXdiHCl

REFERENCES

1. A. E. Alexander, J. Chem. Soc. p. 1813 (1937)

2. J. Subramanian, V. P. Shedbalkar, A. Lemtur, R. Chakravorty and T. N. Saloi, J. Phys. Chem., 100, 4770(1996)

3. W. A. Gallagher and W.B. Elliott, Ann. N. Y. Acad. Sci., 206, 463(1973)

4. L.A. Bottomley, C. Ercolani, J. N. Gorce, G. Pennesi and G. Rossi, Inorg. Chem., 25, 2338 (1986) and references therein

5. M. Kasha, H. R. Rawls and M. El-Bayoumi, Pure Appl. Chem., 11, 371 (1965) and references therein

6. T. K. Chandrashekar, H.V. Willigen and M.H. Ebersole, J. Phys. Chem., 89, 3453(1985)

7. J. Brettar, J-P. Gisselbrecht, M.Gross, N. Solladie, Chem. Communn, 733(2001) and references therein.

CHAPTER – 5

VISIBLE ABSORPTION STUDIES OF METALLO HEMATOPORPHYRIN IX-DME (MHPIXDME), M = VO, Mn, Co, Ni and Cu.

CHAPTER - 5

VISIBLE ABSORPTION STUDIES OF METALLO HEMATOPORPHYRIN IX-DME (MHPIXDME), M = VO, Mn, Co, Ni and Cu.

5.1. INTRODUCTION

Earlier workers[1,2] have reported that Mn (II) hematoporphyrin aggregate in 0.1M KOH. Mn (III) hematoporphyrin also showed aggregation in $9.1x10^{-2}$M NaOH. It is also reported that Mn (IV) and Mn (III) hematoporphyrin do not aggregate in 0.1M KOH. On the contrary, we observed that MHPIXDME shows strong aggregation even in a mixture of organic solvents. Our investigation on MnHPIXDME aggregation in methanol- dichloromethane (30% and 70%) mixture is presented in this chapter along with other compounds which was prepared in dichloromethane. The free base and metallohematoporphyrin structure is presented in figure 5.1a and b.

5.2. EXPERIMENTAL DETAILS

The concentration range of 10^{-4}M, 10^{-5}M and 10^{-6}M solutions of MnHPIXDME were prepared in methanol – dichloromethane mixture (MnHPIXDME is also soluble in water) while the rest were prepared in dichloromethane. All measurements were carried out at room temperature. Oxidations were carried out using 0.1M solutions of $SbCl_5$ in dichloromethane. The oxidised species were then neutralised with diethyl amine.

5.3. RESULTS

Visible absorption spectra and results are presented in figure 5.2(a-e) and in table 5.1. The soret band of all the MHPIXDME shows blue shift on dilution. The range of shift varies from 11nm to 18nm. The soret band also exhibit splitting at higher concentration. However, the bands show very little changes, practically no shifts are

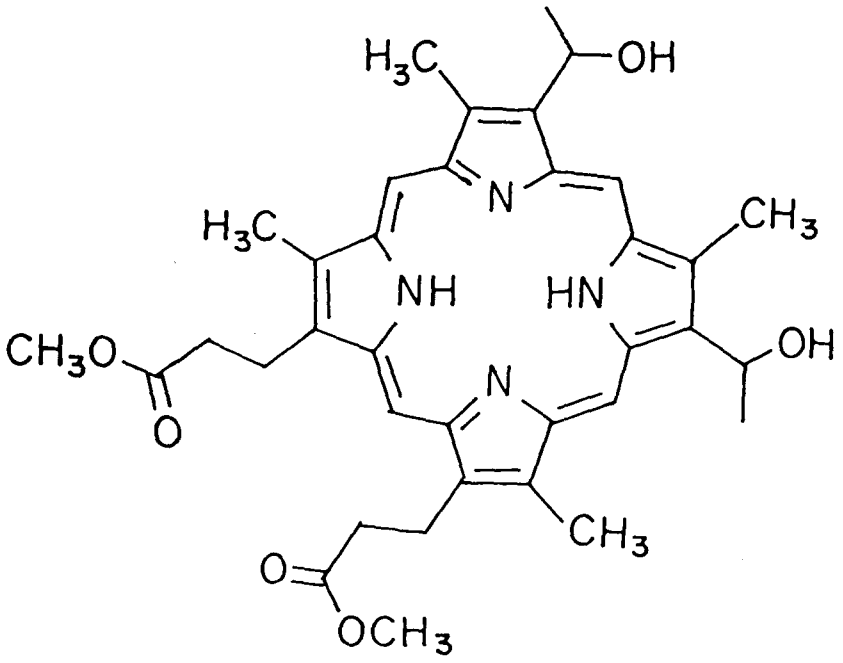

Figure 5.1a Structure of free base hematoporphyrin IX-dimethyl ester

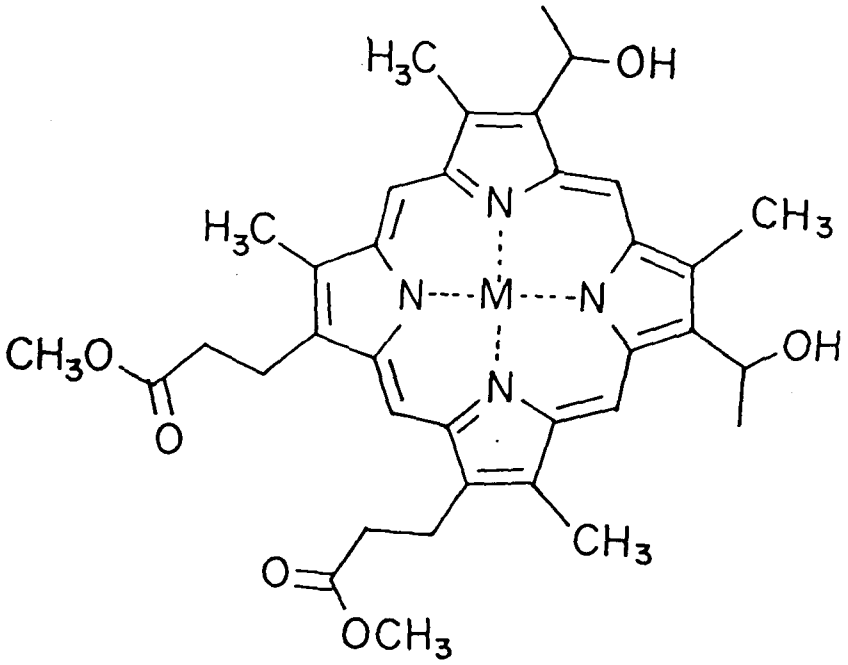

Figure 5.1b Structure of metallohematoporphyrin IX-dimethyl ester

observed. Almost all the complexes shift the base line and increase the intensity of the peaks on oxidation

Beer's Law experiment shows linearity breaks at 10^{-5}M for all MHPIXDME (table 5.3). Slight blue shifts in the position of the soret band are observed on the oxidation with $SbCl_5$. No appreciable shifts are observed as regard to the positions of the Q band. Isosbestic points are observed for NiHPIXDME 10^{-4}M and 10^{-5}M solutions at 430nm, 506nm, 574nm and 373nm, 420nm, 505nm and 577nm respectively (table 5.2 and figure 5.2d and 5.2e) on oxidation with $SbCl_5$. No isosbestic points are observed for other MHPIXDME we have studied.

5.4. DISCUSSION

From the results it is suggested that most of the MHPIXDME exist in dimeric form upto the concentration around 10^{-5}M, after which most of them shows monomeric form. It is expected that planar compounds such as Cu hemato, Ni hemato and Co hemato to form face-to-face dimer more readily than other MHPIXDME[3]. In VOhemato, VO is out of plane of the porphyrin ring by about 0.3Å and forms back-to-back dimer.

On oxidation with $SbCl_5$ all MHPIXDME show the soret bands are slightly blue shifted. These results are in accordance with that of the water soluble metalloporphyrins. Thus, on oxidation with $SbCl_5$, form dimers. The blue shift in the soret band cannot be readily explained within the frame work of excitonic theory[4]. May be excitonic theory needs improvement. The presence of isosbestic points[5,6] in the spectra of the oxidized NiHPIXDME indicate the presence of two species may be monomer – dimer.

5.5. CONCLUSION

From the visible absorption studies we draw some conclusions which are as follows:

(i) Most of the MHPIXDME exists as dimer at the concentration around 10^{-5}M. Below this concentration the dimer dissociate to monomers.

(ii) On oxidation almost all MHPIXDME, we have studied show dimerization.

Note: Since MnHPIXDME is water soluble, we need to pursue more studies.

Table 5.1 UV-Visible absorption data of Unoxidised, Oxidised and Reduced products of metallohematoporphyrin IX- dimethyl ester, metal = VO, Mn, Co, Ni and Cu in CH_2Cl_2 containing 0.1M $SbCl_5$ (at room temperature)

		λ_{nm}					
Metal	Conc. (M)	Unoxidised		Oxidised		Reduction of the oxidized species with diethylamine	
		Soret	Q	Soret	Q	Soret	Q
VO	10^{-4}	424	540, 575	421	544, 581	429	539, 576
	10^{-5}	418	541, 576	408	539, 577	421	539, 576
	10^{-6}	412	538, 575				
Mn	10^{-4}	374	463, 540, 576	379	465, 546, 579	371	470, 553, 592
	10^{-5}	370	470, 556, 589	364	465, 549, 584	374	467, 550, 572
	10^{-6}	367	470, 558				
Co	10^{-4}	425	528, 557	424	528, 559	427	527, 558
	10^{-5}	418	528, 558	413	524, 556	419	526, 558
	10^{-6}	417	529, 560				
Ni	10^{-4}	424	522, 555	423	521, 554	422	518, 553
	10^{-5}	392	521, 556	372, 404	522, 557	393	516, 554
	10^{-6}	377	521, 555				
Cu	10^{-4}	408	528, 563	405	525, 564	408	528, 562
	10^{-5}	402	527, 562	395	526, 562	402	526, 562
	10^{-6}	400	527, 562				

Table 5.2 UV-Visible absorption data of Nickel hematoporphyrin IX-dimethyl ester indicating isosbestic points in CH_2Cl_2 containing 0.1M $SbCl_5$ (at room temperature).

	λ_{nm}	
MHPIXDME	Concentration	
	10^{-4}M	10^{-5}M
Ni	430, 506, 574	373, 420, 505, 577

Table 5.3 UV- Visible data of Absorbance and concentration of metallohematoporphyrin IX-dimethyl ester, metal=VO, Mn, Co, Ni and Cu (at room temperature).

MHP IX DME	Conc.(M)	Abs.	Q- Band	MHP IX DME	Conc.(M)	Abs.	Q- Band
VO	$1x10^{-6}$	0.05	575	Cu	$1x10^{-6}$	0.1	562
	$2x10^{-6}$	0.18	575		$2x10^{-6}$	0.15	562
	$4x10^{-6}$	0.3	575		$4x10^{-6}$	0.21	562
	$6x10^{-6}$	0.4	575		$1x10^{-5}$	0.28	562
	$1x10^{-5}$	0.57	576		$2x10^{-5}$	0.41	562
	$2x10^{-5}$	0.571	575		$4x10^{-5}$	0.8	562
	$4x10^{-5}$	1.26	575		$1x10^{-4}$	1.2	563
	$1x10^{-4}$	2.09	575				
Mn	$1x10^{-6}$	0.06	589	Ni	$1x10^{-6}$	0.008	555
	$1x10^{-5}$	0.1	589		$2x10^{-6}$	0.01	556
	$2x10^{-5}$	0.2	589		$1x10^{-5}$	0.02	556
	$4x10^{-5}$	0.35	589		$2x10^{-5}$	0.2	556
	$1x10^{-4}$	0.9	576		$1x10^{-4}$	2.13	555
	$2x10^{-4}$	0.7	576				
Co	$1x10^{-6}$	0.08	560				
	$2x10^{-6}$	0.12	560				
	$4x10^{-6}$	0.2	558				
	$1x10^{-5}$	0.3	558				
	$2x10^{-5}$	0.83	557				
	$1x10^{-4}$	1.1	557				

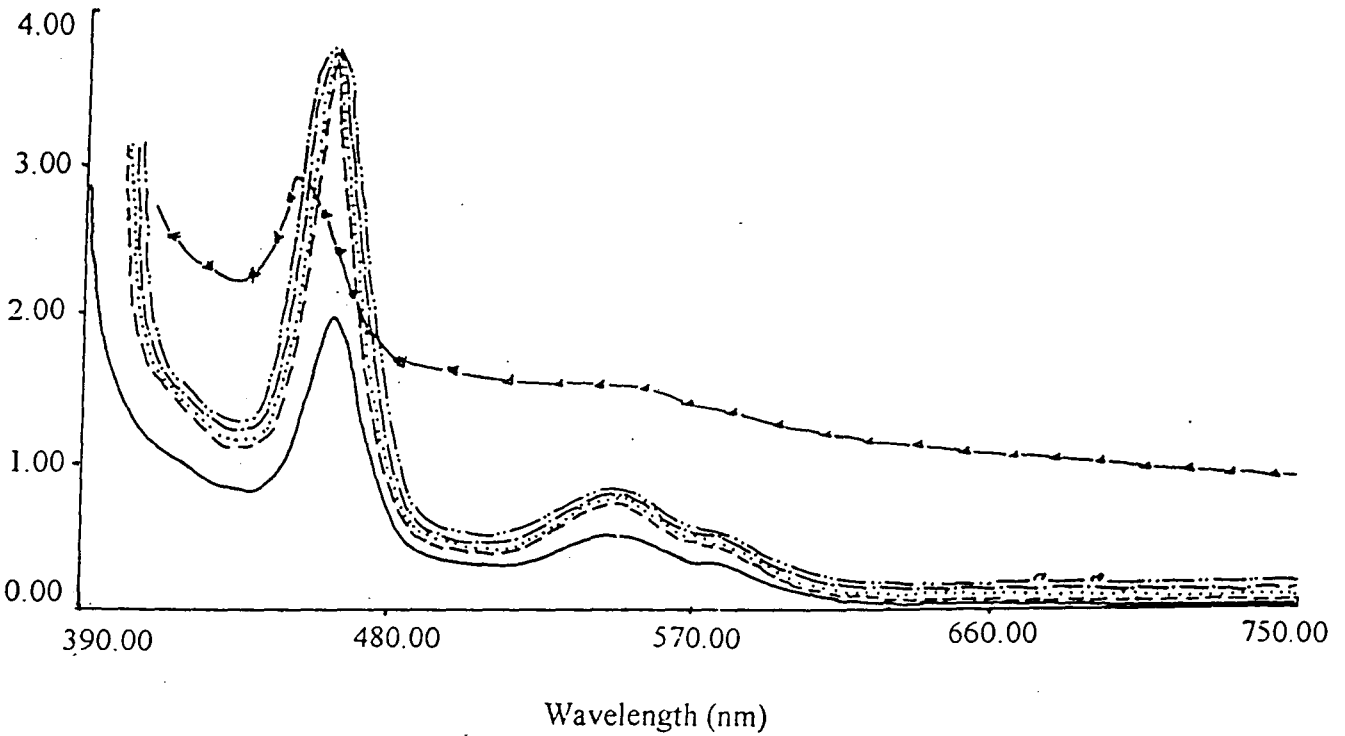

Figure 5.2a UV-Visible absorption spectra of MnHPIXDME (10^{-4}M) solution in CH_2Cl_2 unoxidised (—) oxidised(with 0.1M $SbCl_5$) ----, ····, — ·, — ··, and reduced (with diethyl amine) —▵

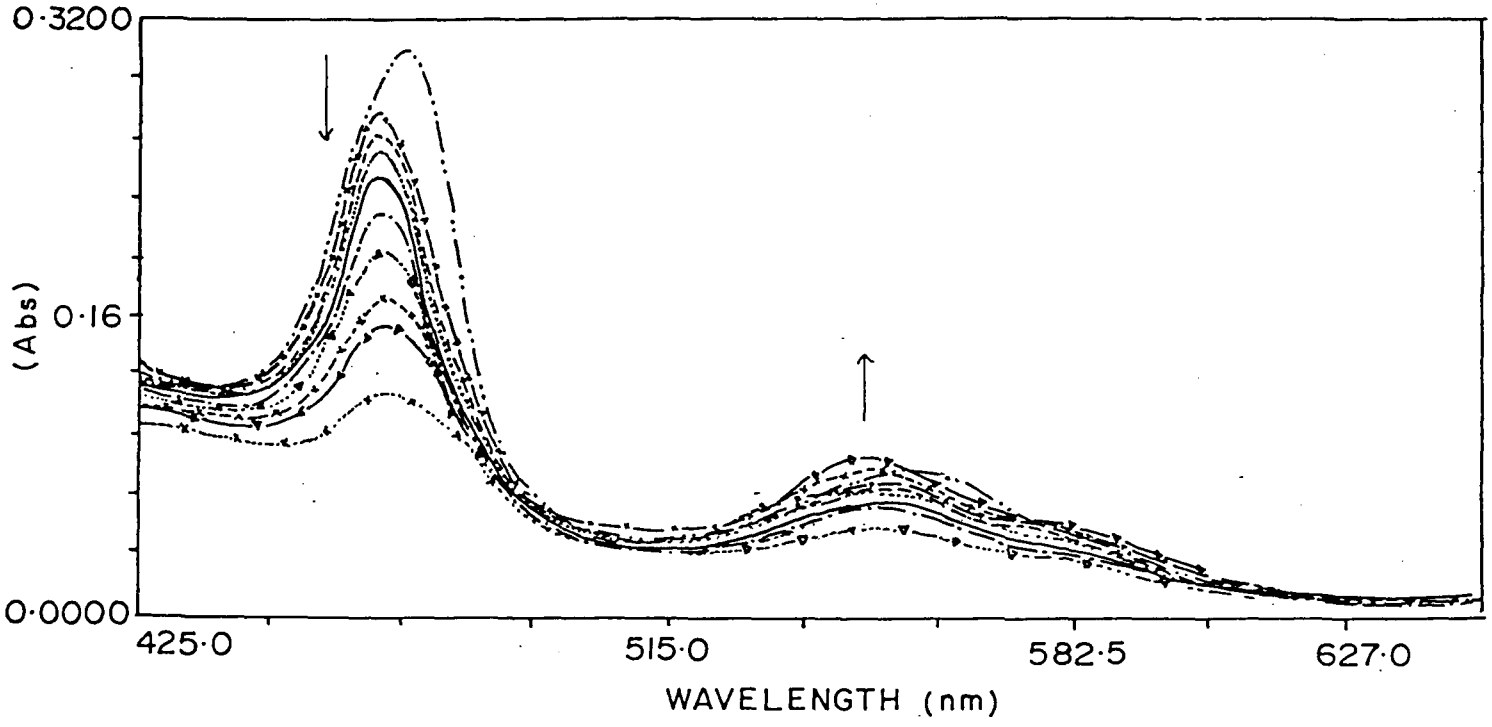

Figure 5.2b UV-Visible absorption spectra of MnHPIXDME (10^{-5}M) solution in CH_2Cl_2 unoxidised (····x) oxidised(with 0.1M $SbCl_5$) —Δ, -x-x-x-, · x· x·, — ·, — , ·····,----, —x and reduced (with diethyl amine) — · ·

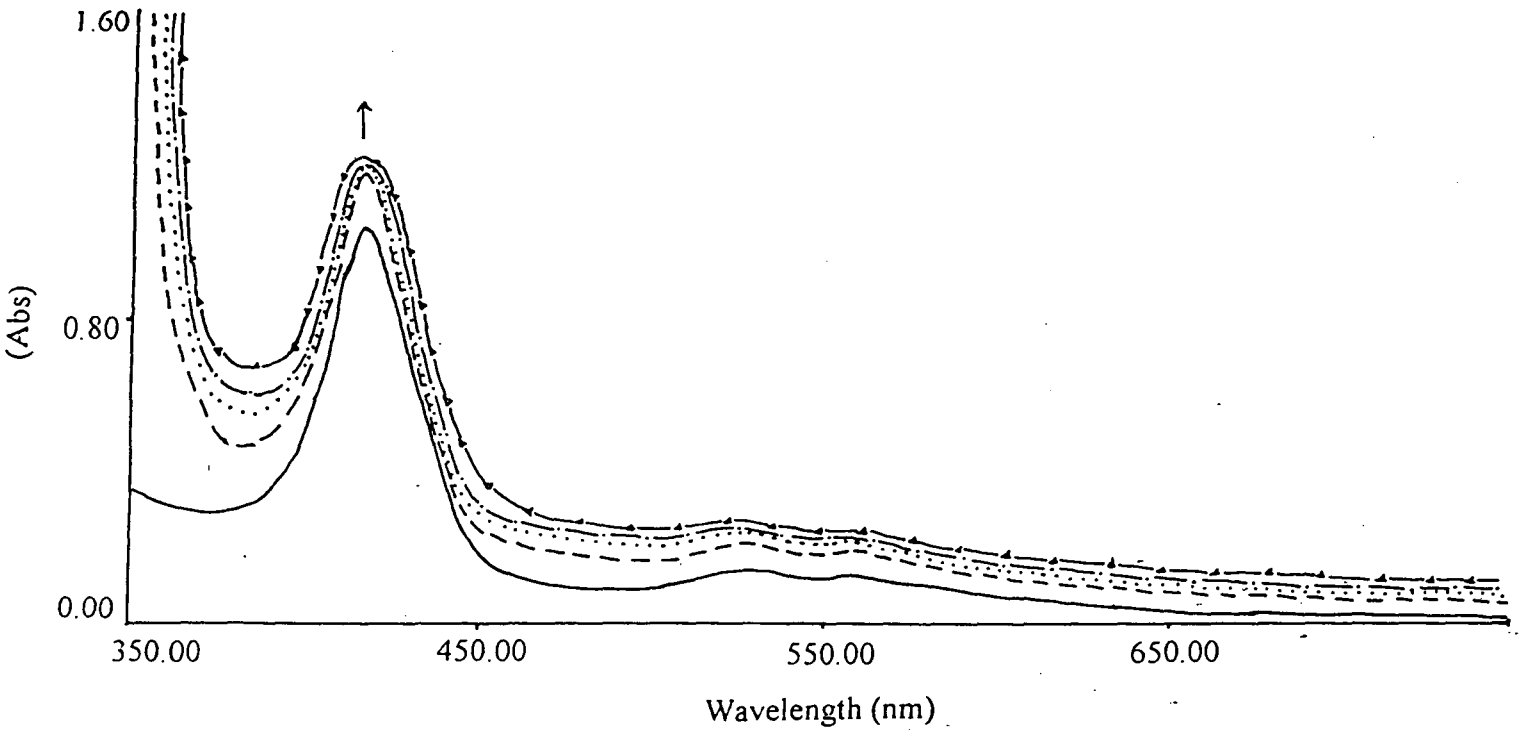

Figure 5.2c UV-Visible absorption spectra of CoHPIXDME (10^{-5}M) solution in CH_2Cl_2 unoxidised (--) oxidised(with 0.1M $SbCl_5$) ----, ····· , —·and reduced (with diethyl amine) —∧

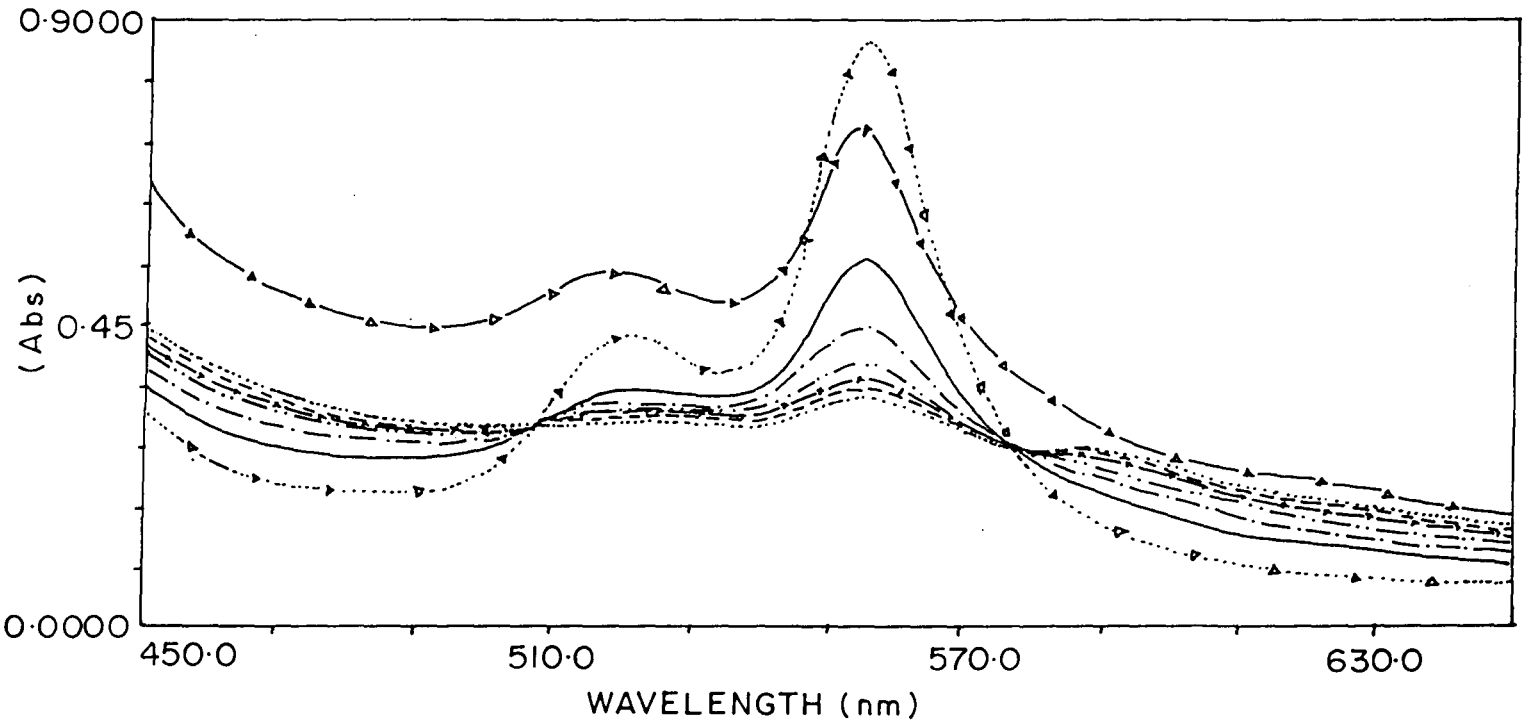

Figure 5.2d UV-Visible absorption spectra of NiHPIXDME (10^{-4}M) solution in CH_2Cl_2 unoxidised (···· Δ) oxidised(with 0.1M $SbCl_5$) —, — , — , — Δ , ----, ···· and reduced (with diethyl amine) — Δ

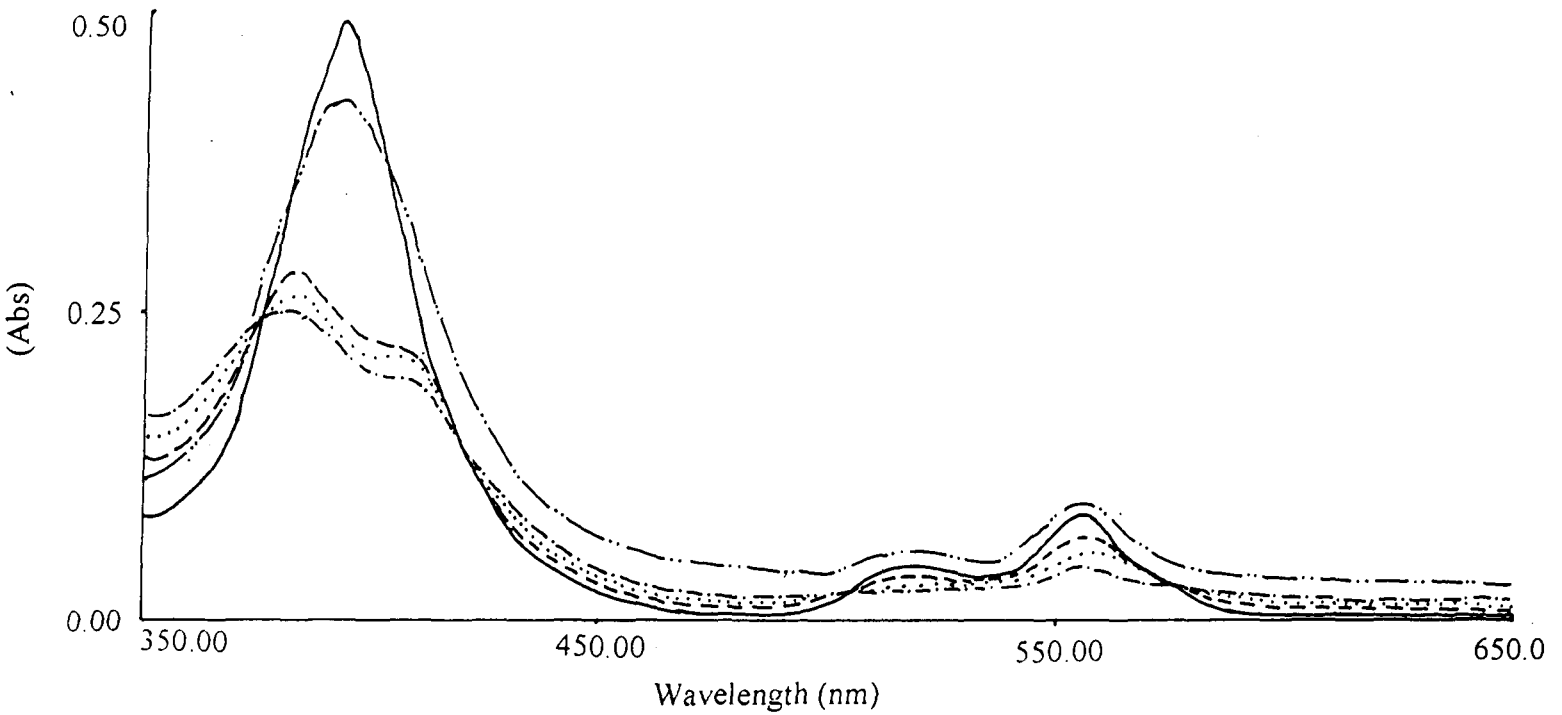

Figure 5.2e UV-Visible absorption spectra of NiHPIXDME (10^{-5}M) solution in CH_2Cl_2 unoxidised (—) oxidised(with 0.1M $SbCl_5$) ----, ····· , —·— and reduced (with diethyl amine) — ··

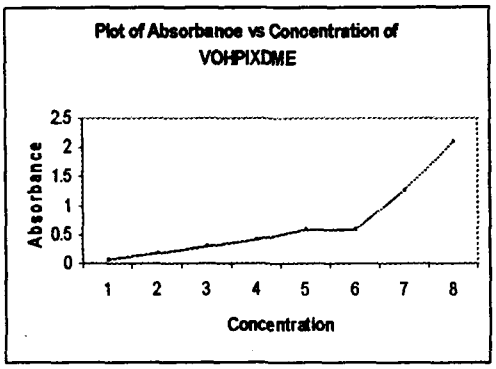

(a)

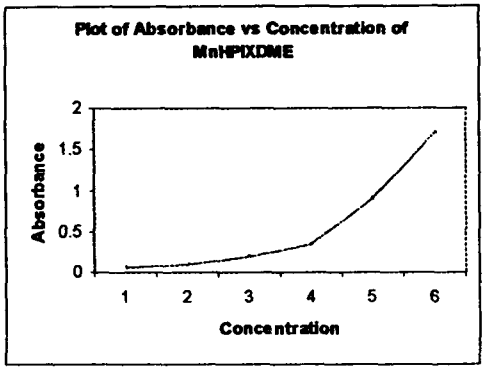

(b)

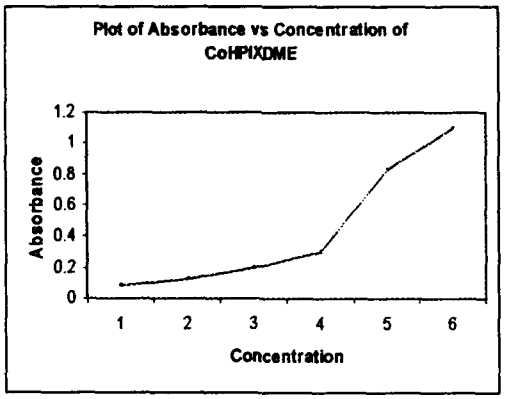

(b)

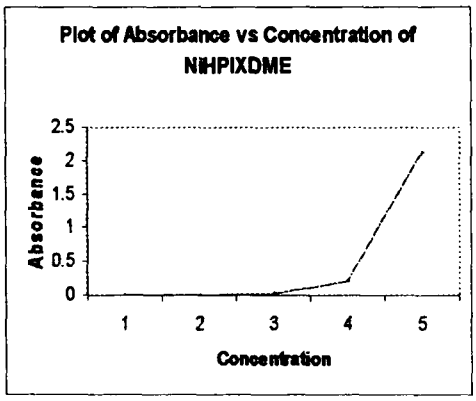

(d)

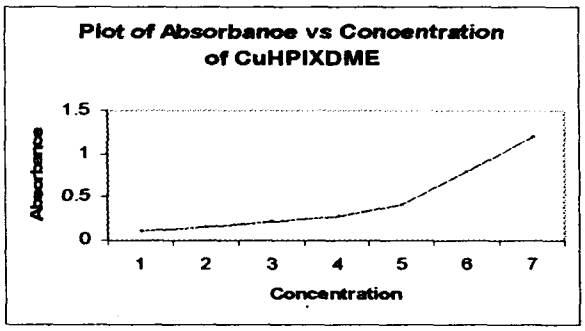

(e)

Figure 5.3 (a-e) Plot of Absorbance vs. Concentration of MHPIXDME

REFERENCES

1. J. James and P. Hembright, J. Coord. Chem. 3, 183 (1973)
2. D. G. Davis and J. G. Montalvo, Anal. Chem. 41, 1195 (1969)
3. P. D. W. Boyd, T. D. Smith, J. H. Price and J. R. Pilbrow, J. Bhem. Phys., 56, 1253 (1972)
4. M. Kasha, H. R. Rawls and M. El-Bayoumi, Pure. Appl. Chem., 11, 371 (1965)
5. M. Y. Choi, J. A. Pollard, M. A. Webb and J. L.Mehale, J. Am. Chem. Soc., 125, 810 (2003)
6. D. M. Chem, T. He, D. F. Cong, Y. H. Xhang, F. C. Liu, J. Phys. Chem. A., 105, 3981 (2001)

CHAPTER – 6

CYCLIC VOLTAMMETRIC AND CONDUCTANCE STUDIES OF SOME METALLOPORPHYRINS

CHAPTER-6

CYCLIC VOLTAMMETRIC AND CONDUCTANCE STUDIES OF SOME METALLOPORPHYRINS

6.1. INTRODUCTION

Electrochemistry in the form of cyclic voltammetry has become a very important technique in determining the redox behaviour of porphyrins and metalloporphyrins[1, 2]. The cyclic voltammetric technique is an undisputed technique in determining the redox potentials of chemical compounds in chemistry. Evidently, the technique provides us with very interesting information and insight about the chemical compound under investigation. The details about the cyclic voltammetry are available in the literature[3-6]. Therefore, we present here briefly the cyclic voltammetry, its principle and its technique which will help us in understanding the redox system of the metalloporphyrins.

6.2. CYCLIC VOLTAMMETRY IN BRIEF[5-7]

Principle: Cyclic voltammetry is an electrochemical technique in which the working electrode is swept with a triangular wave (potential) (figure 6.2a).One can sweep back and forth between the initial and the final potential. These two potentials are known as switching potentials whieh can be fixed arbitrarily. The potential at the working electrode is measured with respect to a saturated calomel electrode or a Ag/AgCl electrode. The sweep in which the potential is increased positively is known as positive

scan while the sweep in which the potential is increased negatively is known as negative scan. A plot of current vs. voltage gives the voltammogram. On removal of an electron from the system under investigation at the vicinity of the electrode (oxidation) a sudden rise in the current gives a peak while addition of an electron (reduction) to the system also gives a peak on the reverse scan. Thus, a redox couple is obtained.

Let E_{ox} be the oxidation potential and its corresponding reduction potential be E_{red}, then for an electrochemically reversible system,

$$\Delta E = E_{ox} - E_{red} = 0.059/n \text{ V} \quad \ldots\ldots (5.1)$$

where n is the number of electron transfer

Also, the half wave potential ($E_{1/2}$) is given by

$$(E_{1/2}) = \frac{E_{ox} + E_{red}}{2} \quad \ldots\ldots (5.2)$$

and the current (i_p) is given by

$$i_p = 3.01 \times 10^5 n(\alpha n)^{1/2} ACD^{1/2} v^{1/2} \quad \ldots\ldots (5.3)$$

at 25° C

where α is the transfer coefficient (its value is normally between 0.3 and 0.7) v is the scan rate in volts per second, A is the area of the planar electrode, D is the diffusion coefficient of the electroactive species and C is the concentration of the electroactive species.

For one electron transfer reversible process the ratio

$$i_a/i_c = 1 \quad \ldots\ldots (5.4)$$

where i_c is the cathodic peak current

i_a is the anodic peak current

Electrolytic cell:

The cell comprises of three electrodes viz. Working electrode (a platinum disc electrode), auxiliary electrode (a platinum wire) and a reference electrode (an SCE or Ag/AgCl electrode). All the electrodes are stationary in unstirred solution (figure 6.2b).

Before the electrolytic process is carried out, N_2 gas is bubbled through the solution for about 10-15 minutes to remove the dissolved O_2, and then the N_2 blanket above the solution is maintained during the measurements.

Supporting electrolyte: Depending on the conditions of the experiment a non-reacting salt which is soluble in the solvent is used as the supporting electrolyte.

6.3 CYCLIC VOLTAMMETRY OF METALLOPORPHYRINS[1,2,8]

Generally, a metalloporphyrin possesses D_{4h} or C_{4h} symmetry. In a metalloporphyrin the HOMO (highest occupied molecular orbital) which is a_{1u} and a_{2u} are nearly degenerate and the LUMO (lowest unoccupied molecular orbital) an e_g is truly degenerate. On oxidation, electrons are removed from the HOMO levels. This process may take place in the porphyrin ligand system or in the metal system or in both. This depends on the metal atom whether it is electroactive or non-electroactive. If the central metal atom is not electroactive (eg. Zn, Cu etc.), then the oxidation or reduction will occur in the porphyrin ligand. If the central metal atom is electro-active (eg. Fe, Co, Mn etc.), then oxidation and reduction may occur both in the ligand as well as in the metal center. This can be understood by considering the occupied energy levels of π-electrons and d electrons of the metal atom (figure 6.1) Case (i) contains electroactive metal center. Therefore, the redox process will occur in the metal.

Case (ii) contains non-electroactive metal center, hence the redox process will occur in the ligand system. In case (iii) both the energy level of the ligand and that of the metal atom are in the same level, hence the process will occur in both the systems.

Redox process in the ligand may be represented as follows; considering the metal to be bivalent.

$$M(II)P \xrightarrow[E^{ox}_{1/2}(1)]{-e} M(II)P^{+\cdot} \xrightarrow[E^{ox}_{1/2}(2)]{-e} M(II)P^{++}$$

$$M(II)P \xrightarrow[E^{red}_{1/2}(1)]{-e} M(II)P^{-\cdot} \xrightarrow[E^{red}_{1/2}(2)]{-e} M(II)P^{--}$$

$$\Delta_{ox} = E^{ox}_{1/2}(2) - E^{ox}_{1/2}(1)$$

$$\Delta_{red} = E^{red}_{1/2}(1) - E^{red}_{1/2}(2)$$

If the oxidation - reduction take place in the ligand, a constancy of Δ_{ox} and Δ_{red} were observed.

$\Delta_{ox} \approx 0.3$ eV while $\Delta_{red} \approx 0.5$eV.

Further, the quantity

$$\delta = E^{ox}_{1/2}(1) - E^{red}_{1/2}{}^{(1)}$$

is constant for a variety of metalloporphyrins (2.0 ± 0.15eV) though the absolute magnitude of the potentials varies widely. Independence of Δ_{ox}, Δ_{red} and δ of the metal is explained in terms of negligible mixing of the metal orbitals and the porphyrin π orbitals.

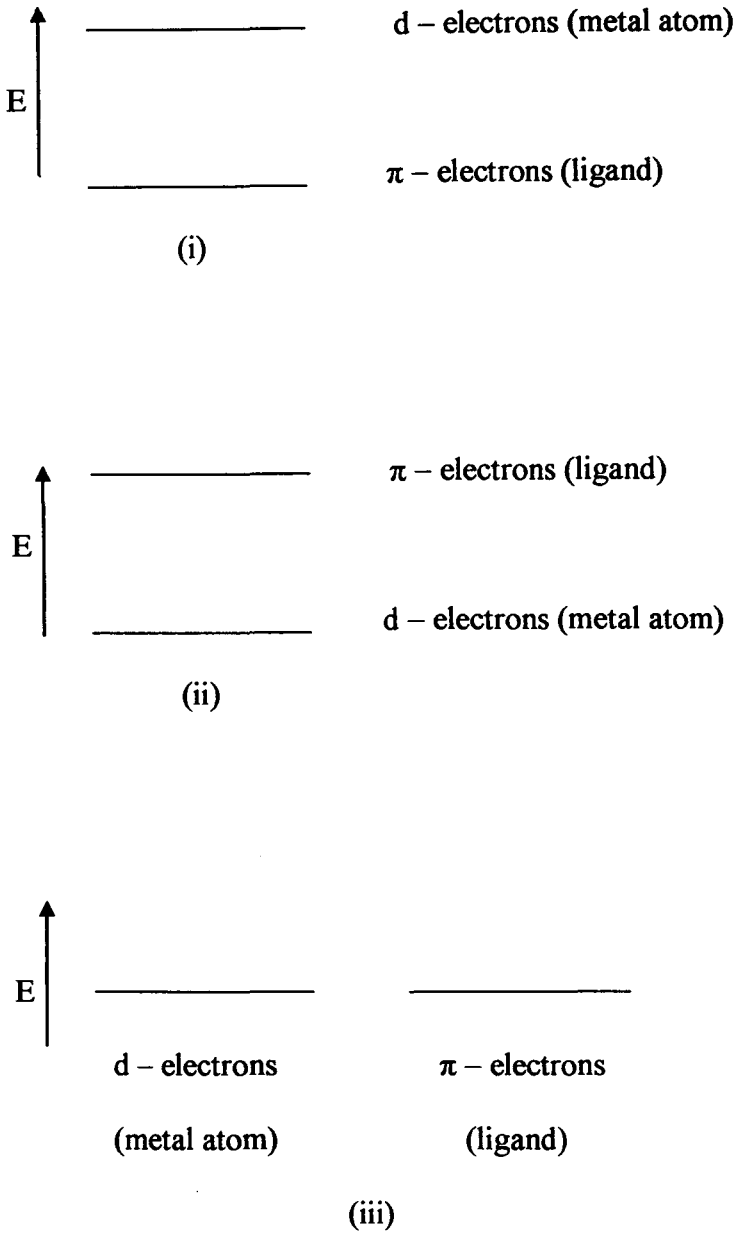

Figure 6.1 HOMO representation for metalloporphyrins

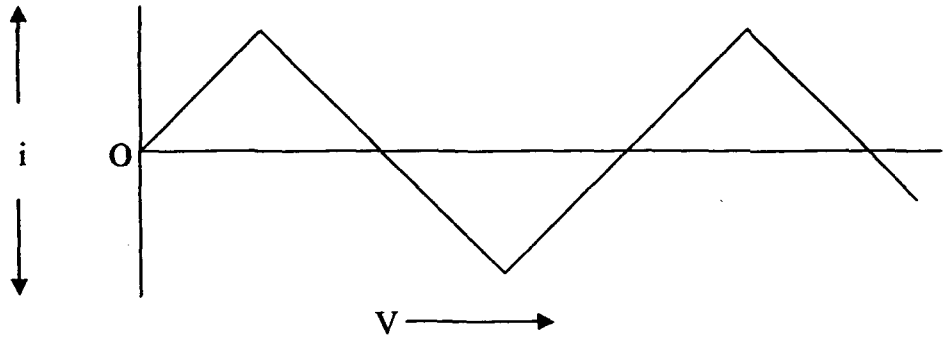

Figure 6.2(a) Tringular wave

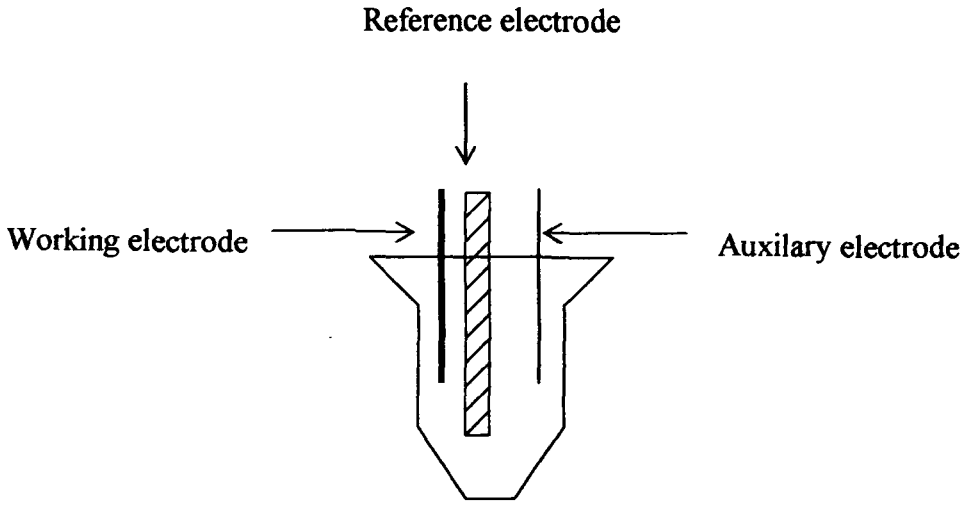

Figure 6.2(b) Electrolytic Cell

6.4 RESULTS

All redox parameters are presented in the table 1.

VOPPIXDME: The voltammogram of 10^{-2}M solution of VOPPIXDME shows two broad peaks on the oxidation sides while their corresponding reduction peaks are not properly resolved (figure 6.3a). The first oxidation peak at around 0.919V is broad and appears to consist of two peaks. The second oxidation peak around 1.320V is also broad and peak height is longer than the rest. Their corresponding reduction peaks occur at around 0.413V and 1.186V(table 6.1). The voltammogram of 10^{-3}M solution also exhibit the similar pattern with an additional reduction peak occurs at around 0.72V while the other reduction peaks broaden out (figure 6.3b). In fact both oxidation peaks are also broaden out. The voltammogram of 10^{-4}M solution shows three oxidation peaks around 0.652V, 1.0V and 1.389V and a very broad reduction peak at around 0.273V which appears to contain two peaks (figure 6.3c). The reduction peak comprises of two peaks. The voltammogram of the 10^{-5}M solution exhibits two oxidation peaks around 1.005V and 1.40V and a very broad reduction peak around 0.252V (table 6.1). The peaks are not well resolved. This may be due to dilution.

MnPPIXDME: The voltammogram of 10^{-2}M solution show three oxidation peaks around 0.45V and 1.2V and 1.516V (figure 6.4a). The corresponding reduction peaks are observed at around 0.483V and 0.899V. Addition to these, one more reduction peak is observed at 0.577V. The voltammogram of 10^{-3}M is also more or less the same (figure 6.4b). 10^{-4}M solution show similar features except the peaks are broadened and shifted. Oxidation occurs around 0.933V and 1.426V while reduction occurs around 1.026V and

0.306V (figure 6.4c). 10^{-5}M solution exhibit two broad oxidation peaks at around 0.773V and 1.346V and two broad reduction peaks at around 1.113V and 0.279V. As the scanning progresses a low intensity broad peak develop at around 0.633V (figure 6.4d). Reduction peaks show more than one peak although they are not resolved.

CoPPIXDME: 10^{-2}M solution gives the voltammogram consisting of three oxidation peaks at around 0.546V, 1.013V and 1.459V and a very broad reduction peak around 0.306V (figure 6.5a). The reduction peak show splitting into two peaks. 10^{-3}M solution show two broad oxidation peak around 0.846V and 1.340V and a broad reduction peak around 0.453V(figure 6.5b). The voltammogram of 10^{-4}M solution show no difference than that of 10^{-3}M solution (figure 6.5c). The voltammogram of 10^{-5}M solution show two broad oxidation peaks and a splitted reduction peak. The oxidation peak could not be located exactly but observed around 0.6V and 1.373V.

NiPPIXDME: 10^{-2}M solution gives a voltammogram consisting of one broad oxidation around 1.027V and a broad reduction peak around 0.719V. The oxidation peak moves towards the higher potential and also the reduction peak moves towards the lower potential in the process (figure 6.6a and table 6.1). 10^{-3}M solution gives two oxidation peaks and two reduction peaks but not well resolved (figure 6.6b). 10^{-4}M solution give a voltammogram consisting of two oxidation peaks around 0.341V and 0.741V and two reduction peaks around 0.647V and 0.447V. The voltammogram of 10^{-5}M solution is not well resolved which may be due to dilution. It shows two broad oxidation peaks around 0.257V and 0.694V and two reduction peaks around 0.621V and 0.368V.

CuPPIXDME: The voltammogram of 10^{-2}M solution show three oxidation peaks around 0.736V, 0.821V and 1.421V and their corresponding reduction peaks observed around 1.074V, 0.521V and 0.305V (figure 6.7). All the peaks are not well resolved. 10^{-3}M solution gives two oxidation peaks around 0.813V and 1.387V and corresponding two reductions observed around 0.473V and 0.326V. These peaks are also broad. 10^{-4}M and 10^{-5}M solutions give two very broad oxidaton peaks and two reduction peaks. The two reduction peaks are not well resolved.

ZnPPIXDME: 10^{-2}M solution gives a voltammogram with two very broad oxidation peaks at around 0.566V and 1.273V along with one broad reduction peak around 0.4V. All these peaks seem to contain more than one peak (figure 6.8a). 10^{-3}M solution show two broad oxidation peak and one broad reduction peak. All features are similar to that of the voltammogram of 10^{-2}M solution. Practically, no difference between the two voltammograms are observed. The voltammogram of 10^{-4}M solution also shows similar features and no difference were observed (figure 6.8b). In the voltammogram of 10^{-5}M the reduction peak is splitted into two (figure6.8c) .

SnPPIXDME: The voltammogram of 10^{-2}M solution show two oxidation peak around 0.670V and 1.4V while reduction peak is broad and occur around 0.376V. 10^{-3}M solution also gives similar voltammogram(figure 6.9a). The voltammogram of 10^{-4}M solution show similar pattern. Both oxidation and reduction peaks show to contain two peaks each (figure 6.9b). The voltammogram of 10^{-5}M solution gives almost the same voltammogram as that of the 10^{-4}M solution. Oxidation comprises of two peaks around

0.779V and 0.926V and the reduction side contain two peaks at around 0.421V and 0.258V.

VOMPIXDME: The voltammogram of 10^{-2}M shows three oxidation peaks and three reduction peaks. The first and third oxidation peaks are not well resolved (figure 6.10a). The voltammogram of 10^{-3}M solution gives two well resolved oxidation peaks occur around 0.973V and 1.360V and the corresponding reduction peak occurs at 1.053V and 0.640V (figure 6.10b), 10^{-4}M solution do not give well resolved oxidation and reduction peaks. The first reduction peak merges to the second reduction peak in the process(figure 6.10c). 10^{-5}M solution show a very broad oxidation peak in the range of 0.3V-0.5V and another peak at 0.879V. The two reduction peaks are not well resolved and their peak positions are 0.6V and 0.319V.

MnMPIXDME: For all concentrations i.e. 10^{-2}M (figure 6.11), 10^{-3}M, 10^{-4}M and 10^{-5}M, we could not obtain well resolved voltammograms. All voltammograms are featureless and very broad. Therefore, we need to investigate the system carefully and properly.

CoMPIXDME: 10^{-2}M and 10^{-3}M solutions give similar voltammograms with two broad oxidation peaks around 0.663V and 1.363V while the reduction side give two very broad peaks around 0.726V and 0.363V. The broad peak around 0.363V exhibits splitting. (figure 6.12a,b). The voltammogram of 10^{-4}M solution is almost similar. On the other hand 10^{-5}M solution gives a voltammogram with two broad oxidation peaks around 0.788V and 1.411V. The reduction show almost three peaks of which the one around 0.505V show splitting(figure 6.12c).

NiMPIXDME: The voltammogram of 10^{-2}M solution exhibit two broad oxidation peaks around 1.046V and 1.538V and two broad reduction peaks around 0.80V and 0.253V (figure 6.13a). 10^{-3}M solution also gives almost the same voltammogram. The oxidation peaks around 0.773V and 1.213V and their corresponding reduction peaks around 0.853V and 0.466V are observed. 10^{-4}M and 10^{-5}M solutions produce very broad featureless voltammograms(figure 6.13b).

CuMPIXDME: The voltammogram of 10^{-2}M solution comprises of two oxidation peaks occuring around 0.8V and 1.357V and two reduction peaks around 1.126V and 0.432V (figure 6.14a). The peak around 0.432V is broad and higher in height. The peak seems to contain more than one. 10^{-3}M solution gives a voltammogram containing two oxidation peaks around 0.880V and 1.439V while their corresponding reduction peaks around 0.920V and 0.333V. The peaks are not sharp due to dilution. The voltammogram of 10^{-4}M solution give four peaks, two oxidation peaks occuring around 0.940V and 1.70V. The two oxidation peaks are broad and not well resolved while the reduction peak at 0.946V is higher in height and the one at 0.346V is broad (figure 6.14b) . 10^{-5}M solution give voltammogram almost the same with that of the 10^{-4}M solution but the oxidation peak at higher potential is more resolved (figure 6.14c and table 6.2)

VOMPIXdiHCl: 10^{-2}M solution gives a voltammogram with two redox couples.Two broad oxidation peaks at around 0.541V, 1.210V and their corresponding reduction peaks at around 0.729V and 0.270V on repeated scans, the overlay voltammograms exhibit shift in the oxidation and reduction potential with reduced peak heights. The first oxidation potential shift from 0.541V to 0.523V, while the reduction potentials shift from

0.729V to 0.7V and 0.270V to 0.258V (figure 6.15a). The voltammogram of 10^{-3}M solution show the second oxidation and its corresponding reduction peak are broad and increased in height. On the other hand the first oxidation and its reduction peak are broaden out without proper resolution. The first oxidation and its corresponding reduction peak occurs around 0.422V and 0.354V respectively.The second oxidation occurs around 0.900V and its corresponding reduction peak occurs at around 0.654V. Repeated scan show shift for both the oxidations and reductions.The first oxidation peak flattens out and its corresponding reduction peak is shifted to 0.301V. The second oxidation and its reduction peak decreases in height and shifted from 0.900V to 0.825V and from 0.654V to 0.701V. The voltammograms of 10^{-5}M solution are similar to that of the 10^{-3}M solution. Here again the first oxidation peak at around 0.946V flattens out on repeated scan.Its peak point shift from 0.946V to 0.80V.The second oxidation occur around 1.601V and shift to 1.520V on repeated scan.The peak is broad and the height is quite low.The first reduction occur at around 1.033V and shift to 1.119V on repeated scan.The height of the first reduction peak is almost triple that of its oxidation.On the other hand the second reduction peak is broad and do not show any shift.The height of the first oxidation and its reduction peak are same and their ratio is more or less unity.

VOHPIXDME: The voltammogram of 10^{-2}M gives one broad oxidation peak around 1.386V while the reduction give three very close peaks which is centered around 0.493V (figure 6.16). 10^{-3}M also gives the same voltammogram. 10^{-4}M and 10^{-5}M solutions give very broad voltammograms with no proper resolution of peaks.

MnHPIXDME: 10^{-2}M and 10^{-3}M(figure 6.17) solutions give similar voltammograms with one very broad oxidation and one reduction peak. 10^{-4}M and 10^{-5}M solutions give featureless voltammograms.

NiHPIXDME: The voltammogram of 10^{-2}M consists of two broad oxidation peaks occuring around 0.820V and 1.587V. The reduction part of the voltammogram show one very broad peak which seems to contain three peaks and is centered around 0.3V(figure 6.18). The voltammogram of 10^{-3}M is more or less the same. For 10^{-4}M and 10^{-5}M, we obtain similar voltammogram but very broad without any sharp features.

CuHPIXDME: The voltammogram of 10^{-2}M solution exhibit two broad oxidation peaks at around 0.642V and 1.4V(figure 6.19 and table 6.3). 10^{-3}M solution gives more or less the same voltammogram. The voltammograms of 10^{-4}M and 10^{-5}M solutions are very broad without any sharp features. The voltammograms are all similar.

6.5 DISCUSSION

In the voltammogram of 10^{-2}M solution of VOPPIXDME, we observed two broad oxidation peaks around 0.919V and 1.320V. The corresponding reduction peaks around 0.413V and 1.186V which are also broad and not uniform. The height of the oxidation peak at 1.320V is double of the rest (i.e. $i_c/i_a>1$). The ΔE values are 0.506V and 0.134V (see table6.1). The ΔE = 0.506V is too high for reversibility and also the reduction peaks are not well resolved. The results imply that electron transfer processes are not uniform. The peak height indicates that more than one electron transfers processes are taking place simultaneously. The peaks are also broad and look like superimpose of more than one electron transfer peak. If there are two or three (or more) one electron transfer having

very close potentials taking place in the system, then these peaks may merge together giving rise to a broad peak. Also, if more than one electron transfer takes place simultaneously almost at closeby potentials, then the peak height will also increase. Further, the peak potential which we observed may not be accurate and leads to incorrect ΔE values. Thus, we obtain the voltammogram of the dimer accompanied by higher degree of aggregation. As the concentration decreases we observed separation of peaks on the oxidation sides without any further resolution on the reduction side. In the voltammogram of 10^{-4}M solution we observed three oxidation peaks. In fact we anticipated four redox couples from the dimer. These processes are stepwise and should reflect in the voltammogram. However, we observed only three oxidation peaks while the fourth one is not resolved. Also, we observed a broad reduction peak consisting of two peaks. This voltammogram can be of the dimer. Thus, we conclude that at this concentration the dimeric species are more dominant. For 10^{-5}M concentration we observed two oxidation peaks around 1.005V and 1.40V, the values of which are not the same as that of 10^{-2}M, 10^{-3}M and 10^{-4}M (see table). It may be due to monomer which is predominant at this concentration.

The voltammograms of MnPPIXDME are observed to be similar with that of VOPPIXDME. 10^{-2}M solution gives rise to a voltammogram consisting of three oxidation peaks and two reduction peaks. We could not observe the metal oxidation clearly. Perhaps the metal oxidation (Mn(II) $\longrightarrow$ Mn(III)) is overlapped with the first oxidation peak. The possibility of the Mn(II) $\longrightarrow$ Mn(III) is reflected in the low reduction potential (0.483V for 10^{-2}M, 0.306V for 10^{-4}M and 0.279V for 10^{-5}M). The

voltammogram of 10^{-2}M solution is predominantly that of the dimer. The voltammogram of 10^{-5}M solution which consist of two oxidation and two reduction peaks arise out of the monomer.

10^{-2}M solution of CoPPIXDME gives three oxidation peaks and one reduction peak. The ΔE value is very large. This may be due to overlapping of more than one electron transfer in the process. All the oxidation peaks are broad.10^{-3}M, 10^{-4}M and 10^{-5}M solutions give two oxidation and two reduction peaks. The intensity of the first oxidation peak in all the cases is very low.

10^{-2}M solution of NiPPIXDME gives a voltammogram consisting of one broad oxidation peak and a broad reduction peak. The ΔE value (table 6.1) is also too large for one electron reversibility process. It appears to us that both oxidation and reduction peak are not of a single transfer process. These peaks are most likely due to more than one electron transfer processes which potentials are close by. This is most likely that of the dimer. On the other hand the voltammogram of 10^{-5}M solution exhibit two oxidation peaks and two reduction peaks. Obviously this voltammogram is from the monomer.

Three oxidation peaks and three reduction peaks are observed for 10^{-2}M CuPPIXDME solution. The voltammogram of 10^{-5}M shows two broad oxidation peaks and splitted reduction peak. The broadness of these peaks may be due to dilution. At this concentration the voltammogram is most likely due to monomeric species.

In the case of ZnPPIXDME we observed only two broad oxidation peaks and a very broad reduction peaks for 10^{-2}M, 10^{-3}M and 10^{-4}M. In the voltammogram of 10^{-4}M splitting of the reduction peak into two is observed. Perhaps first oxidation peaks are very

close to resolve. Similar explanation can be made for the rest of the oxidation and reduction peaks. This is evident from the voltammogram of 10^{-4}M solution in which splitting of the reduction peak is observed.

SnPPIXDME also exhibits similar pattern. 10^{-2}M solution gives a voltammogram consisting of two oxidation peak and one reduction peak. The ΔE value is quite large for one electron transfer process. Like in the case of NiPPIXDME, this voltammogram is that of the dimer. 10^{-5}M solution gives rise to voltammogram showing two oxidation peaks and two reduction peaks. Obviously, this voltammogram is that of the monomer.

The voltammogram of 10^{-2}M solution of VOMPIXDME show three oxidation peaks and three reduction peaks. This voltammogram is from the dimer. 10^{-3}M solution seems to contain more monomeric species. It is evident from the voltammogram which consist of two oxidation peaks and two reduction peaks. The voltammogram of 10^{-5}M solution exhibit two redox couples representing first and second oxidation of the ligand and their corresponding reductions. This voltammogram points to monomer.

The voltammogram of 10^{-2}M solution of CuMPIXDME also exists as dimer. The oxidation and reduction peaks are quite broad due to overlap of more than one peak. The peak height around 0.432V is higher than the rest. On careful examination we observed the voltammogram pattern to be the same till 10^{-5}M solution. Perhaps, 10^{-5}M solution contains predominantly monomeric species but due to dilution the voltammogram is not well resolved.

Similar voltammograms are observed for NiMPIXDME and CoMPIXDME (table 6.2). ForCoMPIXDME, no metal atom oxidation is observed. The first oxidation

occurs around 0.663V and is broad. This potential is quite low for ligand oxidation. Perhaps the metal oxidation peak is overlapped along with the ligand oxidation giving rise to a broad peak.

In the voltammogram of 10^{-2}M VOMPIXdiHCl solution, the peaks are broad indicating that each peak comprises of more than one peak. The ΔE values are 0.271V and 0.481V which are quite large for single electron transfer process (table 6.2). The voltammogram of 10^{-3}M is also not uniform. The first oxidation peak is very broad and its corresponding reduction peak is also very broad. The second oxidation peak is also very broad and its corresponding reduction peak is also broad and the peak height is more. Both the peaks seem to contain more than one peak. The voltammogram of 10^{-5}M solution show more of monomeric form. The broadness of the peak is mainly due to dilution, otherwise the voltammogram is resolved. Broadening out and shifting of the potentials of the peaks on subsequent scanning is due to the film formation on the surface of the electrode.

For all metallohematoporphyrins no proper resolved voltammograms could be observed. May be due to strong aggregation and film formation on the surface of the electrode.

In general, proto, meso and hemato, all metalloporphyrins which we have studied show strong aggregation and fast film formation on the electrode surface. The film formation is very clearly recorded in almost all the voltammograms we have obtained. On continous scan we have observed a gradual decrease in the peak height and

ultimately flatten out. This is one of the reasons why we could not resolve the voltammograms clearly.

6.6. MEASUREMENT OF CONDUCTANCE

The conductance of metalloporphyrin may not be very strong specially in organic solvent. However, we observed some conductance in organic solvent such as CH_2Cl_2. The conductance is of the order of m mhos. We expect that the conductance due to monomer, dimer and oligomers will be different and if we plot the specific conductance vs concentration there may be deviation from the linearity.

6.7. RESULTS:

We observed linearity for almost all the metalloporphyrin we studied except for the NiPPIXDME, SnPPIXDME and VOMPIXDME. For VOMPIXDME linearity breaks at 10^{-4}M. It continues till 10^{-5}M (figure 6.20, table 6.4).

6.8. DISCUSSION:

We cannot explain why linearity is shown for all the concentration. May be the changes in the conductance is very small to be detected. This means no appreciable changes in conductance on dimerization and oligomerisation.On the contrary we could observe the changes in the conductance due to dimer and monomer for NiPPIXDME, SnPPIXDME and VOMPIXDME. The result tally with the result of the visible absorption spectra and also with the result of the cyclic voltammetric measurements.

6.9 CONCLUSION

From the cyclic voltammetric study we conclude the following:

(i) All metalloporphyrins we have studied show dimerization[10-12] between 10^{-2}M and 10^{-5}M. In case of metallomesoporphyrin in neutral solvent such as CH_2Cl_2 dimer dissociates to monomer from 10^{-5}M concentration and below;

(ii) Strong aggregation are observed even in the neutral organic solvent such as CH_2Cl_2

(iii) All metalloporphyrins we have studied show rapid film formation on the electrode surface[9]. It shows that metalloporphyrins of proto, meso and hemato have strong tendency to aggregate even at low concentrations on oxidation; and

(iv) From the conductance measurements we observed that VOMPIXDME exhibit dimer at higher concentration range while it exists as monomer below 10^{-5}M solutions.

Table 6.1 Redox potentials (in volt) for MPPIXDME, M=VO, Mn, Co, Ni, Cu, Zn and Sn using TBAP as supporting electrolyte at room temperature.

Metal	Con(M)	E_1^{ox}	E_2^{ox}	E_3^{ox}	E_1^{red}	E_2^{red}	E_3^{red}	ΔE_1	ΔE_2	ΔE_3	$E_{1/2}$(I)	$E_{1/2}$(II)	$E_{1/2}$(III)
	10^{-2}	0.919	1.320		1.186	0.413		0.506	0.134		0.666	1.253	
VO	10^{-3}	0.973	1.439		0.720	0.298		0.675	0.719		0.636	1.080	
	10^{-4}	0.652	1.000	1.389	0.273				0.727			0.637	
	10^{-5}	1.005	1.400		0.252				1.148			0.826	
	10^{-2}	0.45	1.2	1.516	0.892	0.483		-0.033	0.308		0.467	1.046	
Mn	10^{-3}	1.076	1.438		0.9	0.335		0.741	0.538		0.705	1.169	
	10^{-4}	0.933	1.426		1.026	0.306		0.627	0.40		0.620	1.226	
	10^{-5}	0.773	1.346		1.113	0.279		0.494	0.233		0.526	1.229	
	10^{-2}	0.546	1.013	1.459	0.306				0.707			0.660	
Co	10^{-3}	0.846	1.340		0.453				0.887			0.9	
	10^{-4}	0.8	1.348		0.459				0.889			0.904	
	10^{-5}	0.6	1.373		0.479				0.894			0.926	
	10^{-2}	1.027			0.719								
Ni	10^{-3}	0.352	0.894		0.847	0.505		-0.153	0.047		0.429	0.870	
	10^{-4}	0.341	0.741		0.647	0.447		-0.106	0.094		0.394	0.694	
	10^{-5}	0.257	0.694		0.621	0.368		-0.111	0.073		0.313	0.657	
	10^{-2}	0.736	0.821	1.421	1.074	0.521	0.305	0.431	0.3	0.347	0.520	0.671	1.248
Cu	10^{-3}	0.813	1.387		0.473	0.326		0.487	0.914		0.570	0.930	
	10^{-4}	0.763	1.47		0.526	0.357		0.406	0.944		0.560	0.998	
	10^{-5}	0.453	1.146		0.440	0.239		0.214	0.706		0.346	0.793	
	10^{-2}	0.566	1.273		0.400				0.873			0.837	
Zn	10^{-3}	0.552	1.258		0.329				0.929			0.794	
	10^{-4}	0.706	1.226		0.453				0.773			0.840	
	10^{-5}	0.626	1.246		0.386				0.860			0.816	
	10^{-2}	0.670	1.4		0.376				1.024			0.888	
Sn	10^{-3}	0.684	1.4		0.442				0.958			0.921	
	10^{-4}	0.736	1.536		0.474				1.062			1.005	
	10^{-5}	0.779	0.926		0.421	0.258		0.521	0.505		0.519	0.674	

Table 6.2 Redox potentials (in volt) for metallomesoporphyrin IX dimethyl ester using TBAP as supporting electrolyte at room temperature.

Metal	Con (M)	E_1^{ox}	E_2^{ox}	E_3^{ox}	E_1^{red}	E_2^{red}	E_3^{red}	ΔE_1	ΔE_2	ΔE_3	$E_{1/2}$(I)	$E_{1/2}$(II)	$E_{1/2}$(III)
	10-2	0.294	0.917	1.4	1.047	0.688	0.376	-0.082	0.229	0.353	0.336	0.803	1.224
VO	10-3	0.973	1.360		1.053	0.640		0.333	0.307		0.806	0.307	
	10-4	0.839	1.146		1.066	0.520		0.319	0.08		0.680	1.106	
	10-5	0.879			0.600	0.319		0.560			0.599		
	10-2	0.694	1.189		0.336				0.853			0.763	
Mn	10-3	0.705	1.260		0.347				0.913			0.804	
	10-4		1.480		0.546				0.934				
	10-5		1.426		0.546				0.880				
	10-2	0.663	1.363		0.726	0.363		0.300	0.637		0.513	1.044	
Co	10-3	0.663	1.389		0.789	0.431		0.232	0.600		0.547	1.089	
	10-4	0.776	1.400		0.800	0.4		0.376	0.600		0.588	1.100	
	10-5	0.788	1.411		0.805	0.505		0.283	0.606		0.646	1.108	
	10-2	1.046	1.538		0.800	0.253		0.793	0.738		1.169	1.292	
Ni	10-3	0.773	1.213		0.853	0.466		0.307	0.360		1.033	0.993	
	10-4	0.700	1.13		0.935	0.510		0.190	0.195		1.033	0.915	
	10-5	0.659	1.33		0.566				0.764			0.948	
	10-2	0.800	1.357		1.126	0.431		0.369	0.231		0.615	1.241	
Cu	10-3	0.880	1.439		0.920	0.333		0.547	0.519		0.607	1.179	
	10-4	0.940	1.70		0.946	0.346		0.594	0.754		0.643	1.323	
	10-5	0.866	1.606		0.960	0.413		0.453	0.646		0.640	1.283	
VOMP	10-2	0.541	1.210		0.729	0.270		0.271	0.481		0.405	0.969	
IX	10-3	0.422	0.900		0.654	0.354		0.068	0.246		0.388	0.777	
di	10-4	0.429	0.844		0.722	0.300		0.129	0.122		0.365	0.783	
HCl	10-5	0.946	1.610		1.033	0.520		0.426	0.568		0.733	1.317	

Table 6.3 Redox potentials (in volt) for metallohematoporphyrin IX dimethyl ester using TBAP as supporting electrolyte at room temperature.

Metal	Con (M)	E_1^{ox}	E_2^{ox}	E_1^{red}	E_2^{red}	ΔE_1	ΔE_2	ΔE_3	$E_{1/2}(I)$	$E_{1/2}(II)$
	10-2	1.386		0.693	0.493	0.893		0.353	0.940	
VO	10-3	0.955		0.533						
	10-4	0.942		0.457						
	10-5	0.715	1.430	0.178			1.252			
	10-2	0.421	1.188	0.365		0.823			0.777	
Mn	10-3	0.411		0.368						
	10-4	0.370		0.900	0.400	-0.03			0.385	
	10-5									
	10-2	0.820	1.587	0.300			1.287		0.944	
Ni	10-3	0.800	1.346	0.466			0.880		0.915	
	10-4	0.726	1.333	0.439			0.894		0.886	
	10-5	0.600	1.136	0.236			0.900		0.686	
	10-2	0.642	1.400	0.768	0.352	0.290	0.632		0.497	1.084
Cu	10-3	0.746	1.499	0.520	0.239	0.507	0.979		0.493	1.010
	10-4	0.506	1.600	0.813	0.279	0.227	0.787		0.393	1.207
	10-5	0.600	1.503	0.711	0.294	0.306	0.792		0.447	1.107

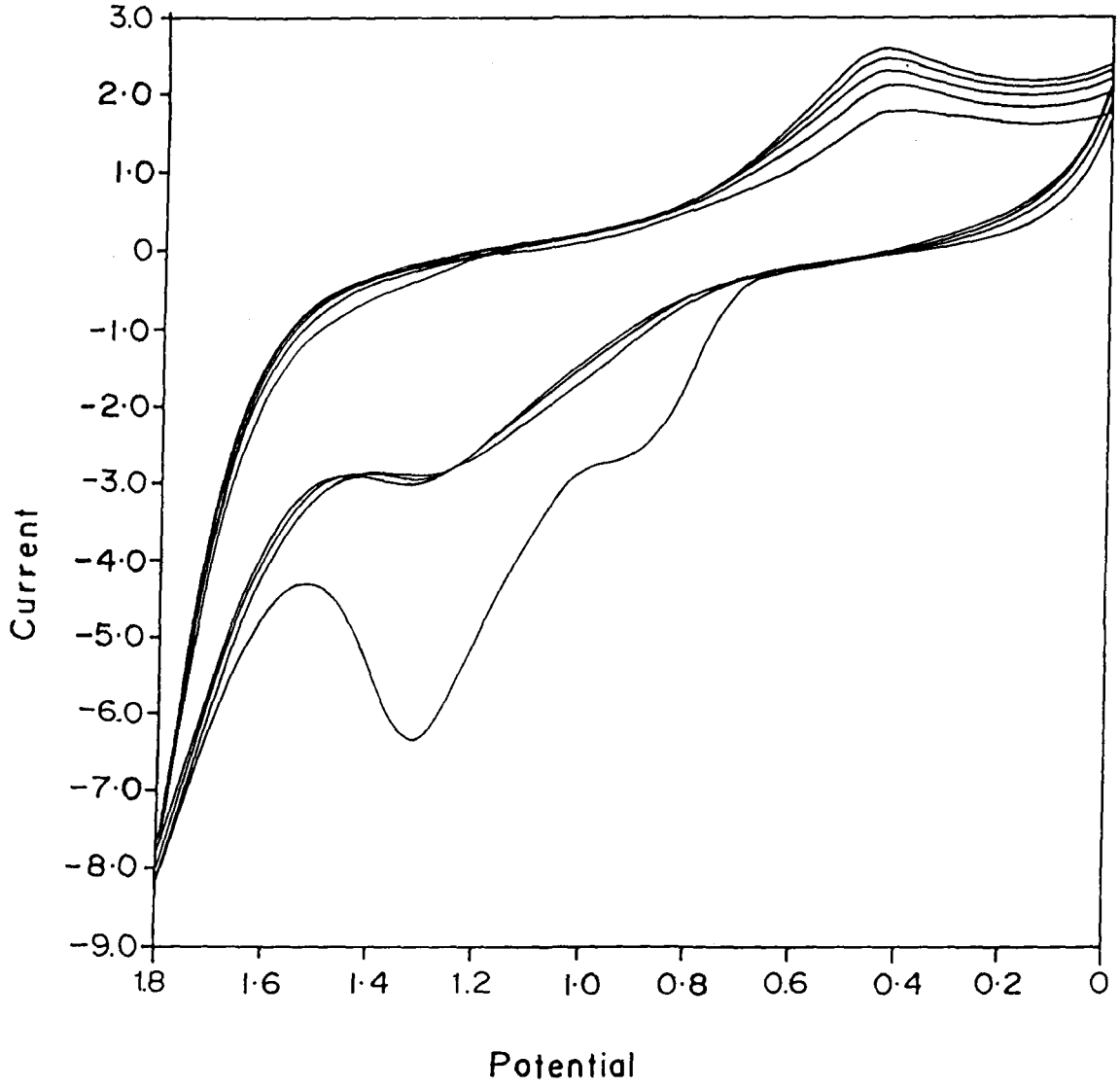

Figure 6.3(a) Cyclic Voltammogram of 10^{-2}M VOPPIXDME in CH_2Cl_2 containing 0.1M TBAP at room temperature. Scan rate =100mV/s

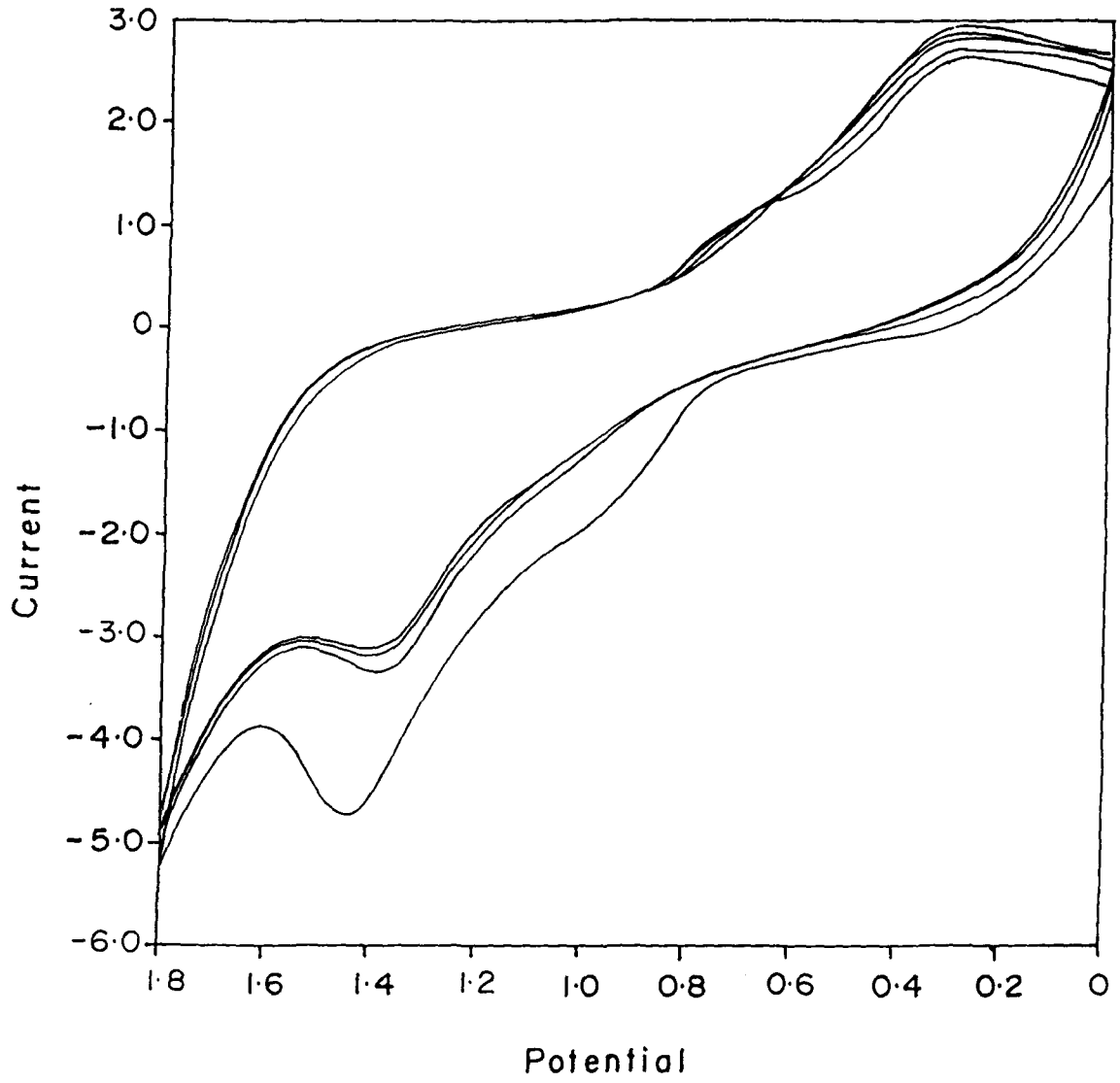

Figure 6.3(b) Cyclic Voltammogram of 10^{-3}M VOPPIXDME in CH_2Cl_2 containing 0.1M TBAP at room temperature. Scan rate =100mV/s

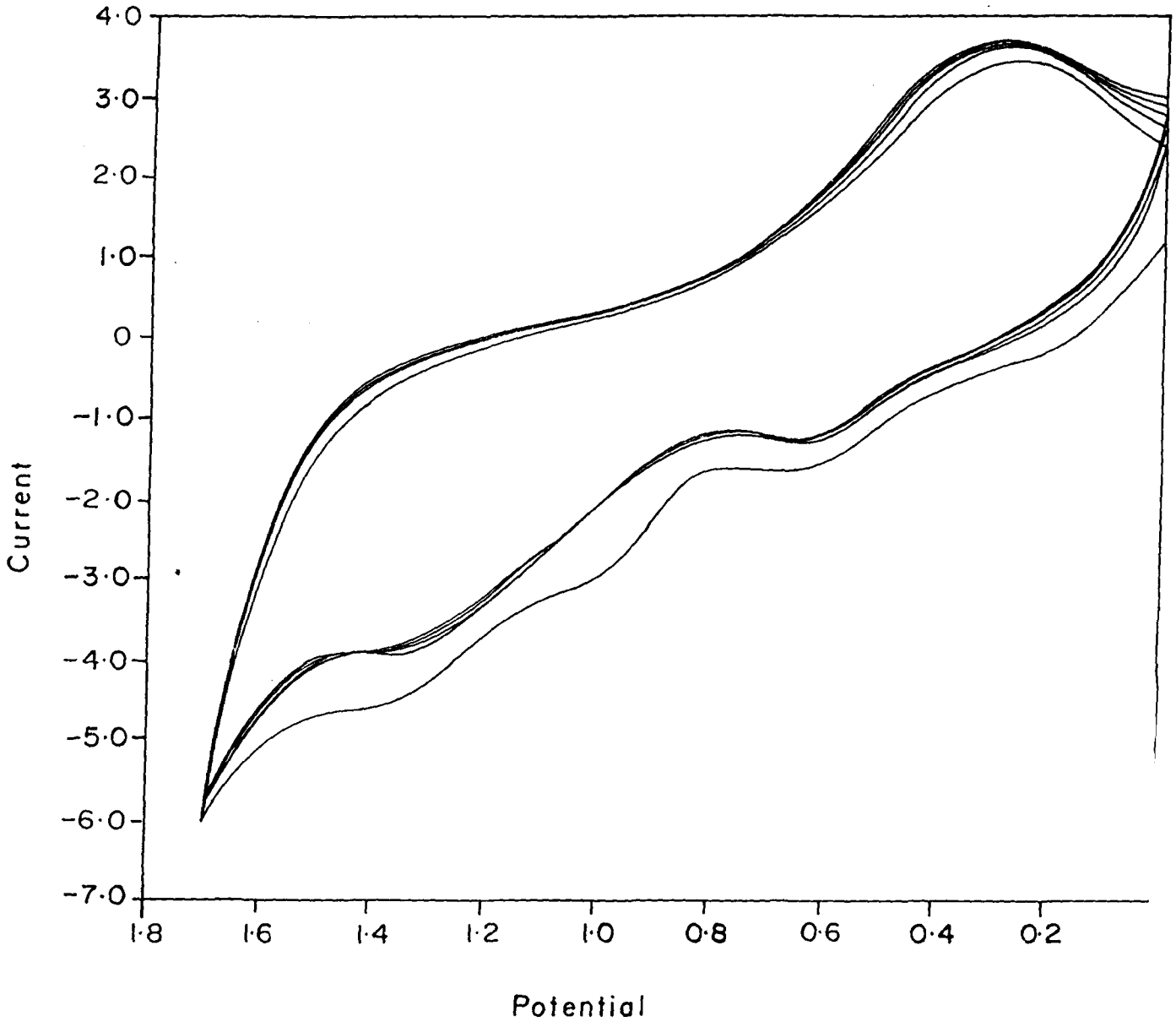

Figure 6.3(c) Cyclic Voltammogram of 10^{-4}M VOPPIXDME in CH_2Cl_2 containing 0.1M TBAP at room temperature. Scan rate =100mV/s

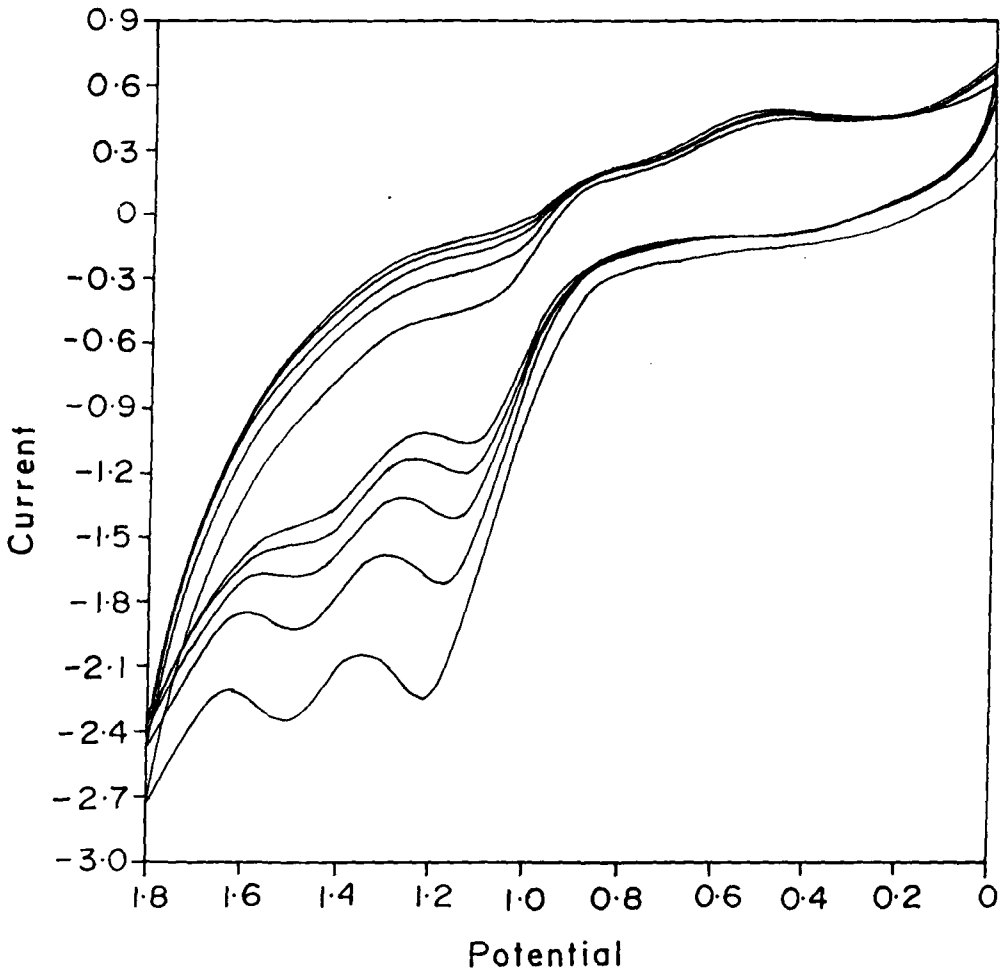

Figure 6.4(a) Cyclic Voltammogram of 10^{-2}M MnPPIXDME in CH_2Cl_2 containing 0.1M TBAP at room temperature. Scan rate =100mV/s

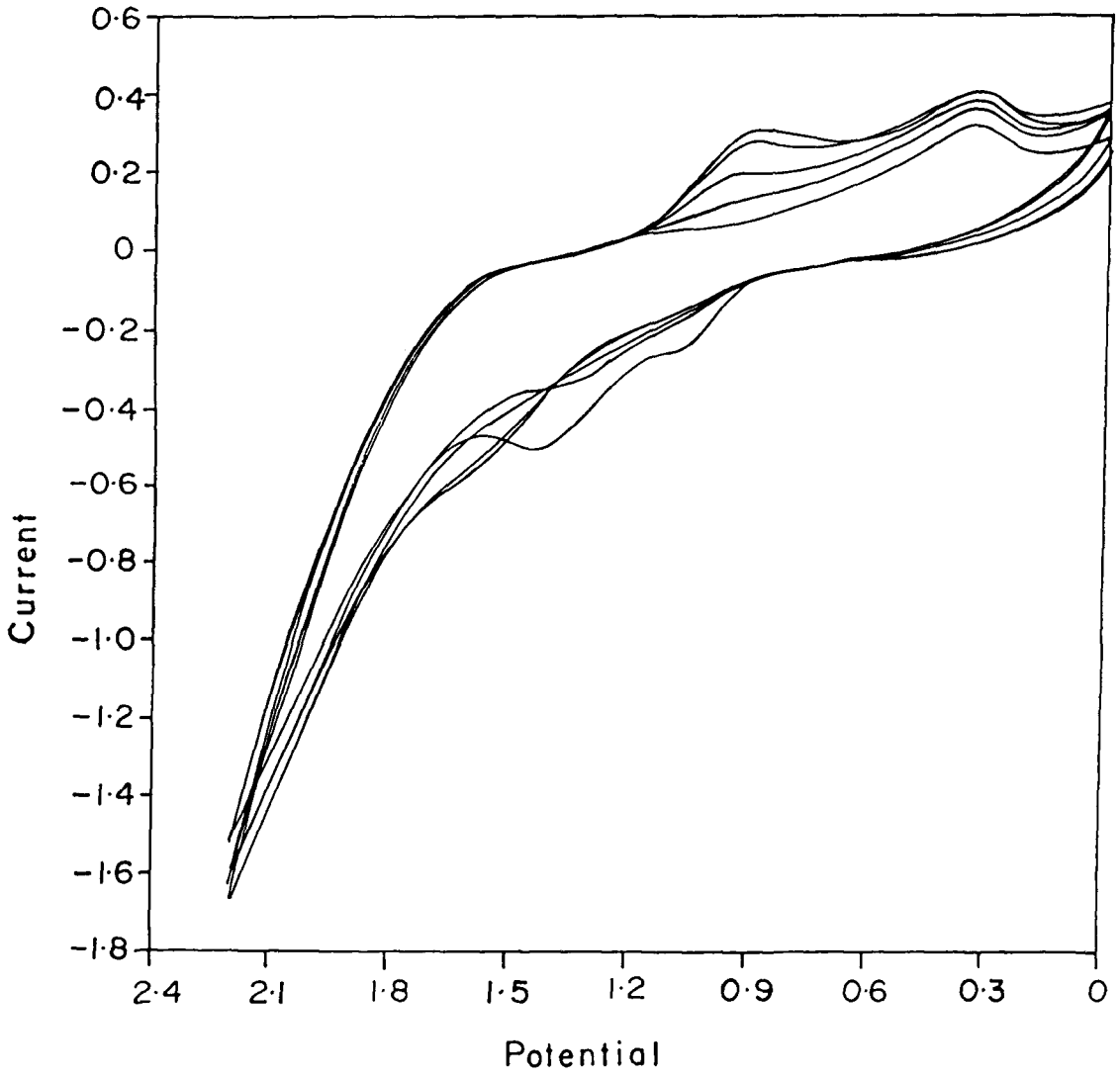

Figure 6.4(b) Cyclic Voltammogram of 10^{-3}M MnPPIXDME in CH_2Cl_2 containing 0.1M TBAP at room temperature. Scan rate =100mV/s

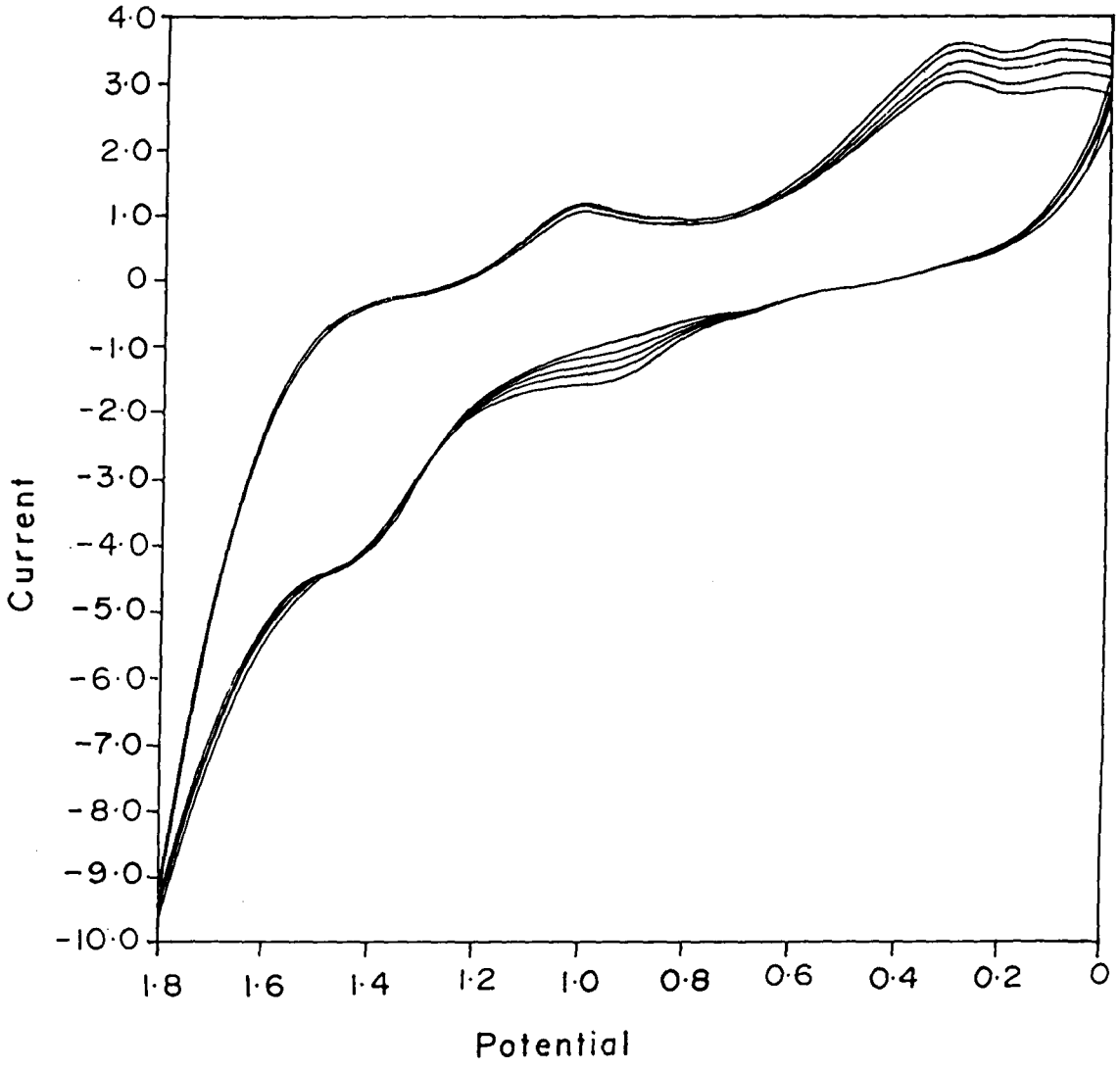

Figure 6.4(c) Cyclic Voltammogram of 10^{-4}M MnPPIXDME in CH_2Cl_2 containing 0.1M TBAP at room temperature. Scan rate =100mV/s

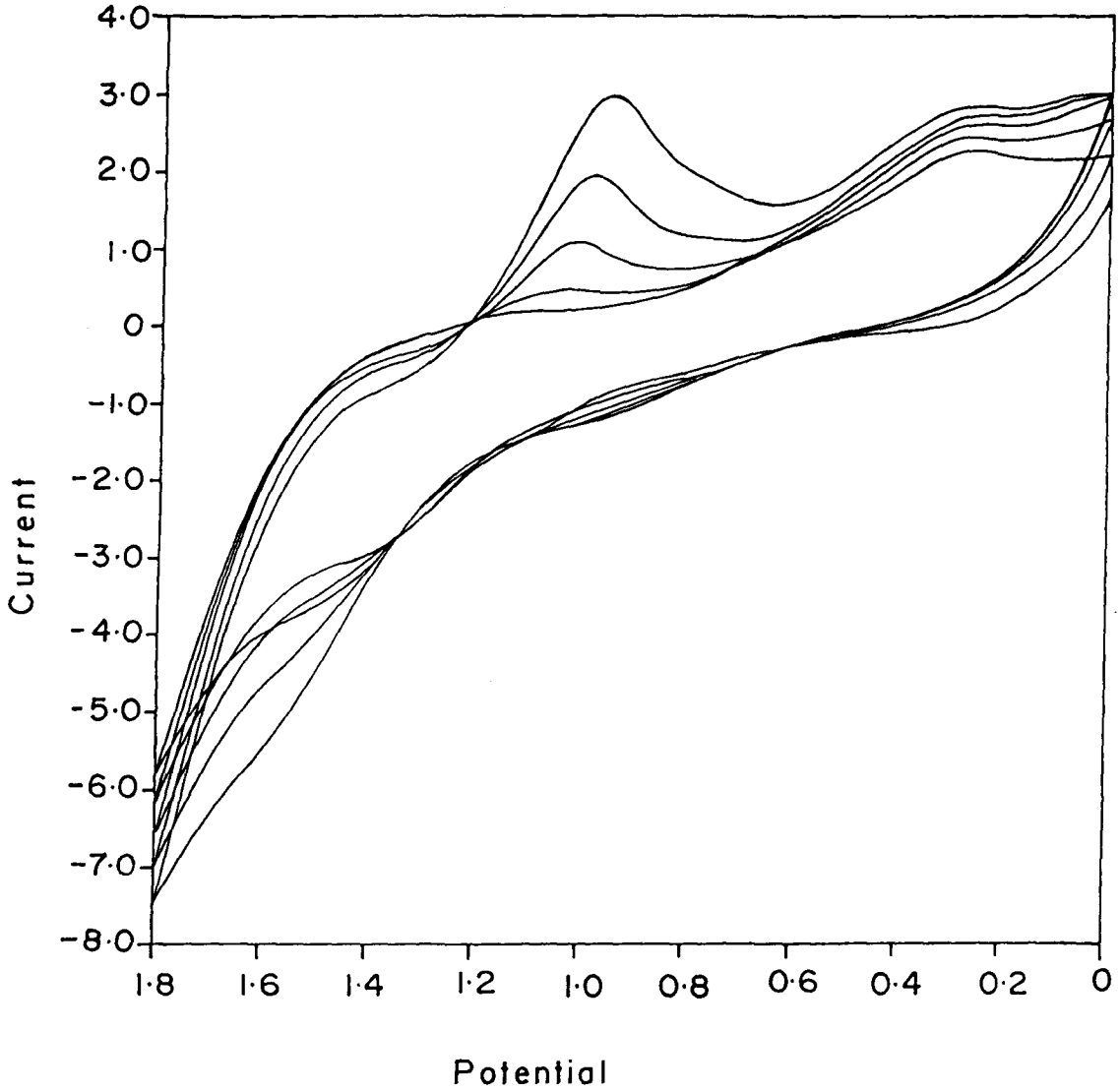

Figure 6.4(d) Cyclic Voltammogram of 10^{-5}M MnPPIXDME in CH_2Cl_2 containing 0.1M TBAP at room temperature. Scan rate =100mV/s

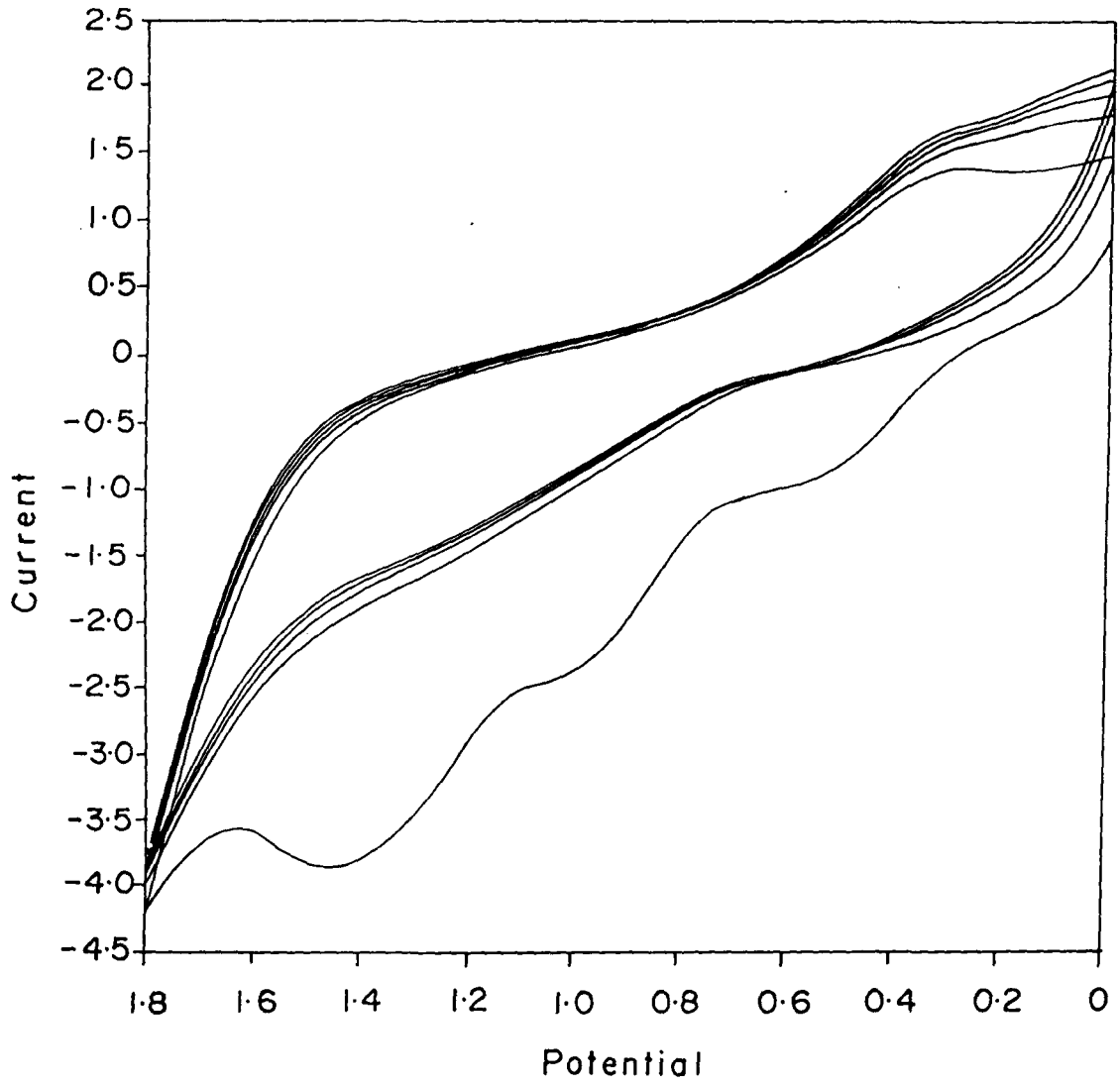

Figure 6.5(a) Cyclic Voltammogram of 10^{-2}M CoPPIXDME in CH_2Cl_2 containing 0.1M TBAP at room temperature. Scan rate =100mV/s

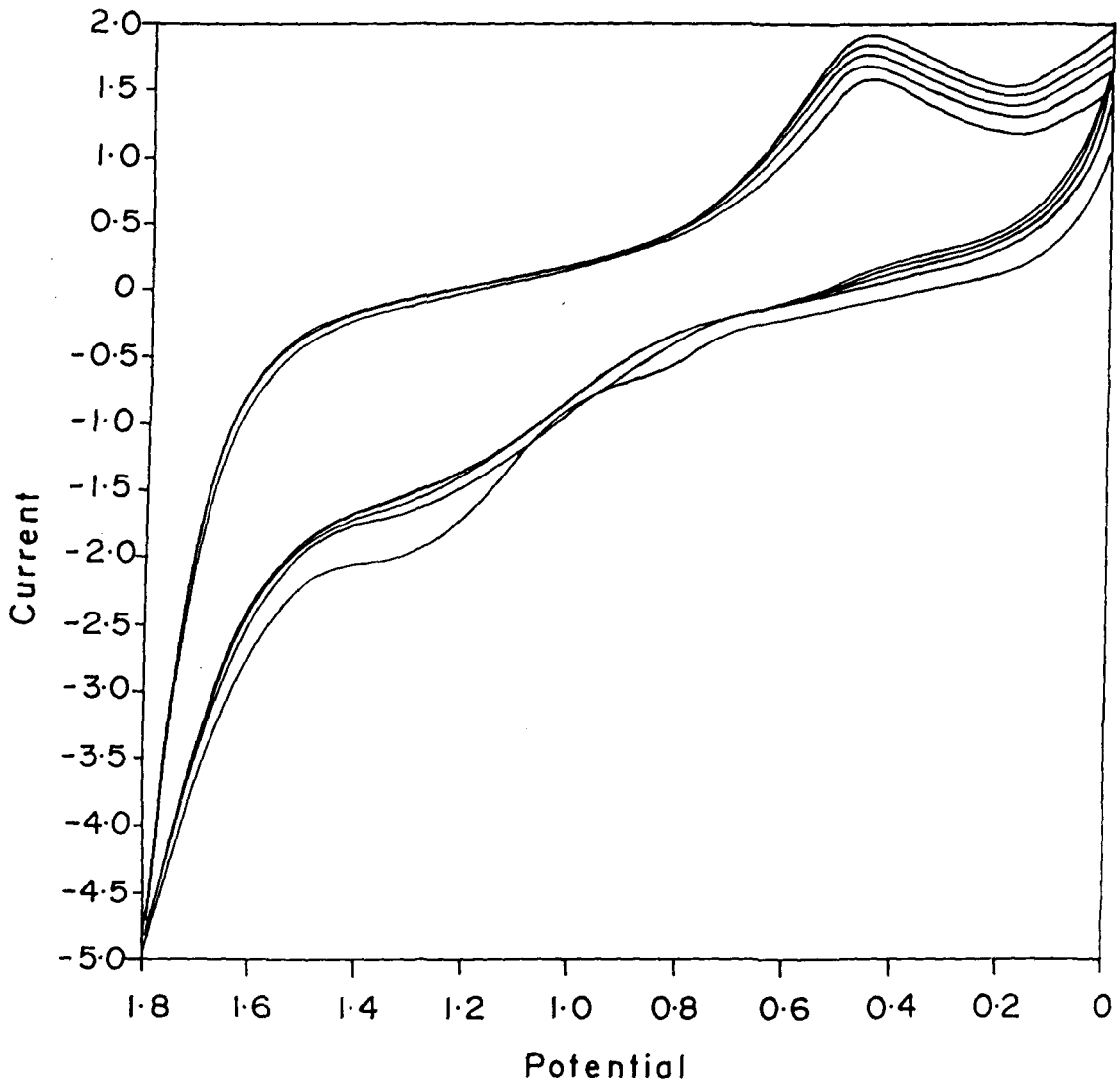

Figure 6.5(b) Cyclic Voltammogram of 10^{-3}M CoPPIXDME in CH_2Cl_2 containing 0.1M TBAP at room temperature. Scan rate =100mV/s

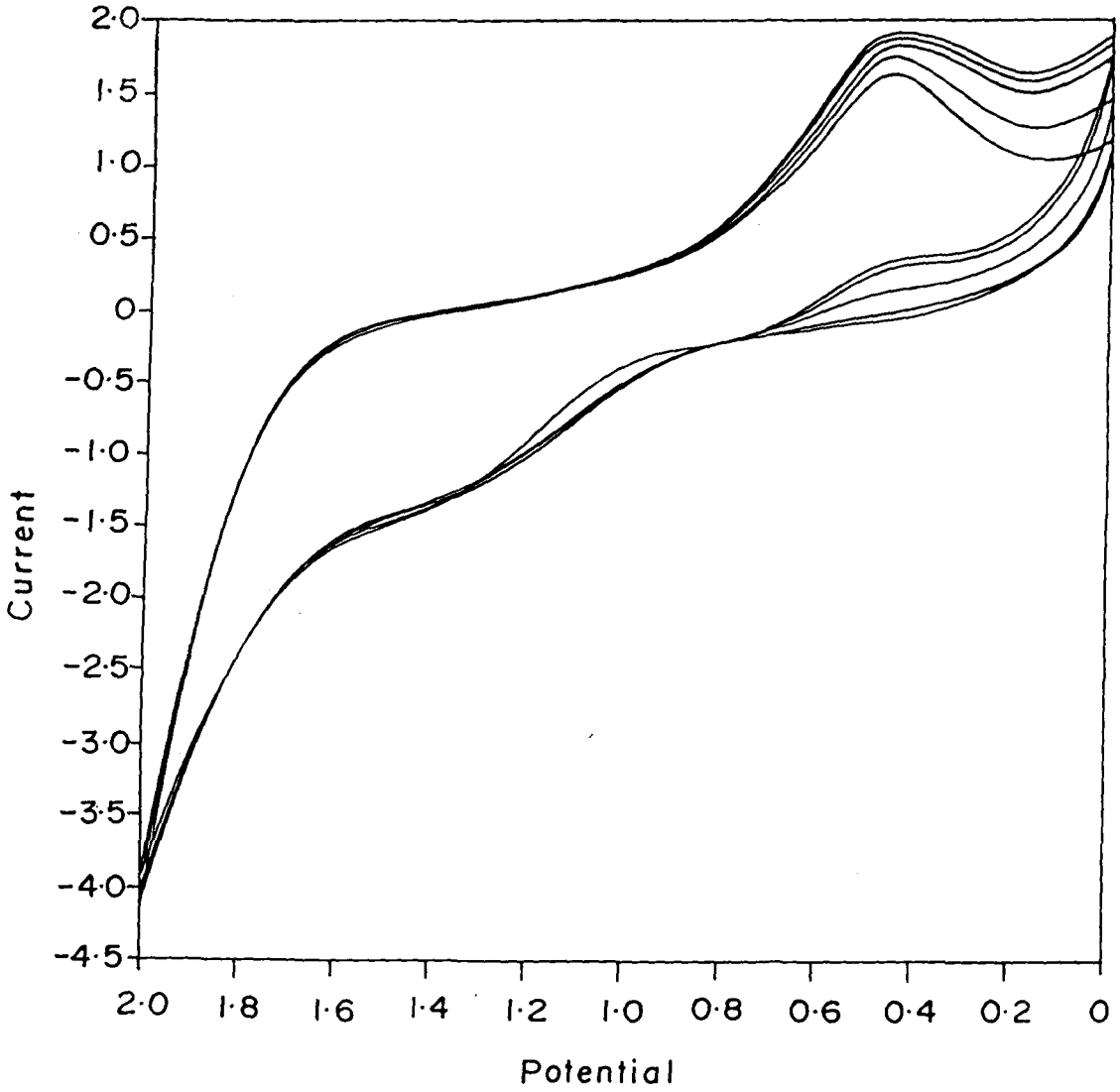

Figure 6.5(c) Cyclic Voltammogram of 10^{-4}M CoPPIXDME in CH_2Cl_2 containing 0.1M TBAP at room temperature. Scan rate =100mV/s

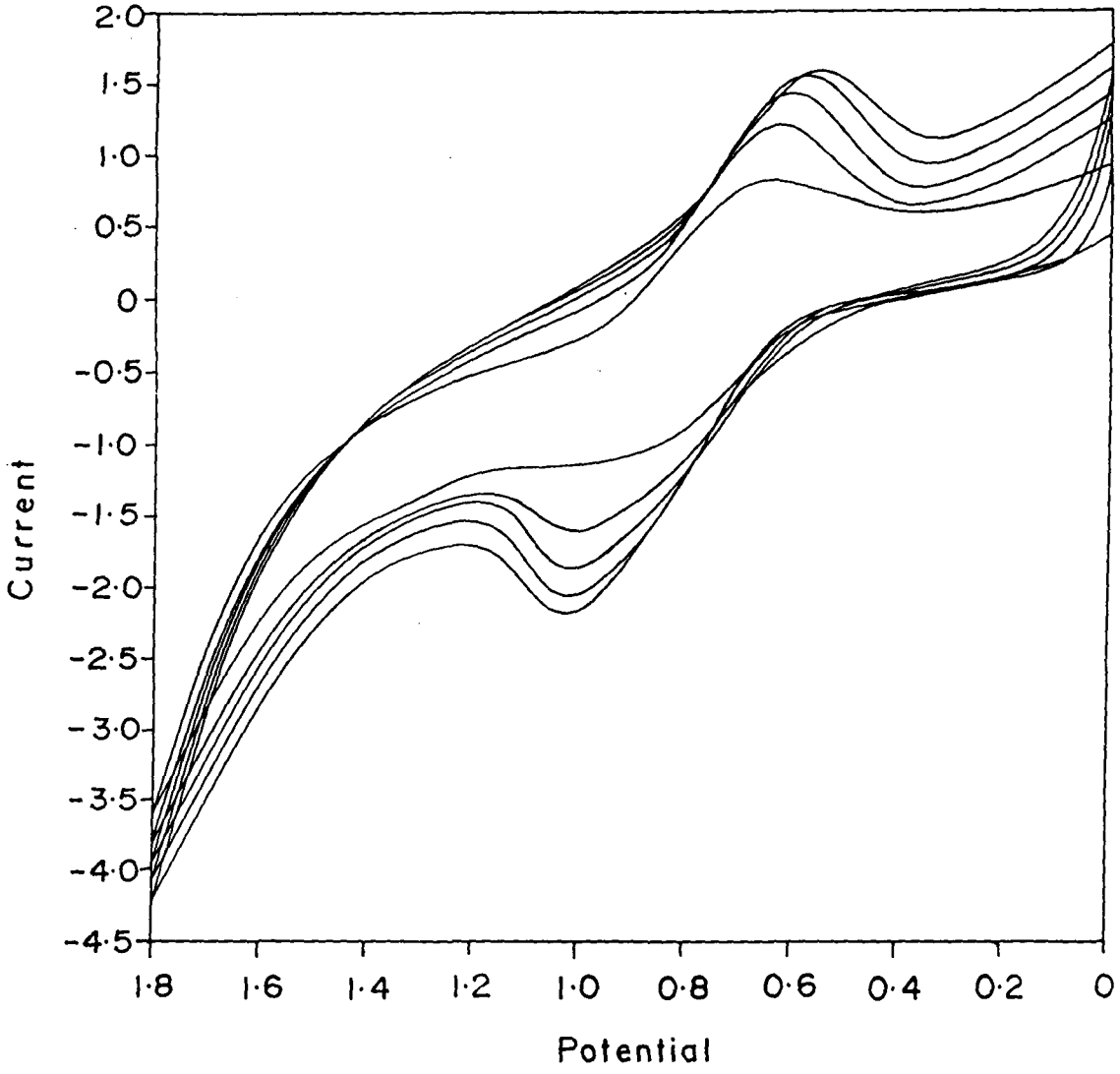

Figure 6.6(a) Cyclic Voltammogram of 10^{-2}M NiPPIXDME in CH_2Cl_2 containing 0 1M TBAP at room temperature. Scan rate =100mV/s

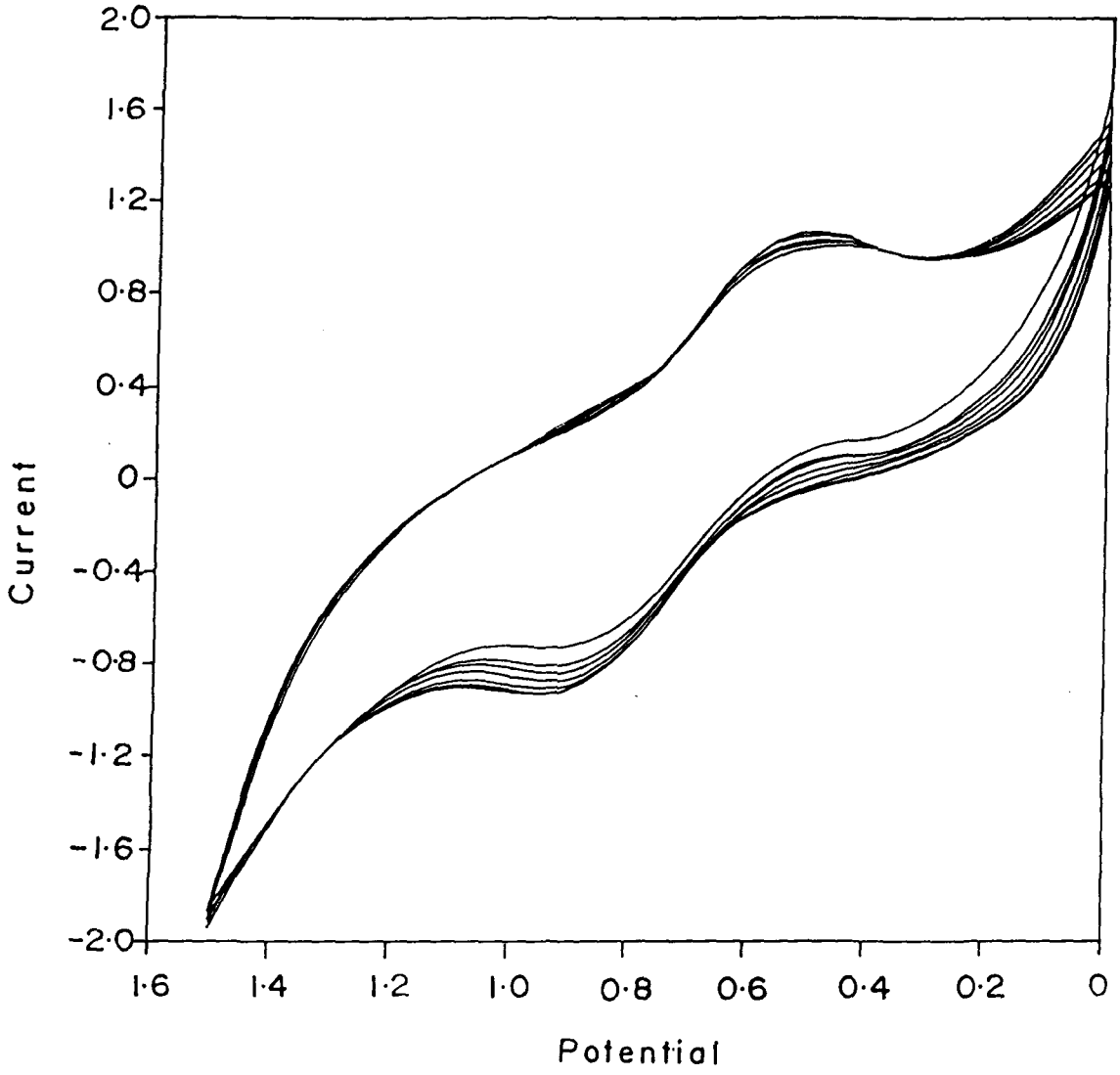

Figure 6.6(b) Cyclic Voltammogram of 10^{-3}M NiPPIXDME in CH_2Cl_2 containing 0.1M TBAP at room temperature. Scan rate =100mV/s

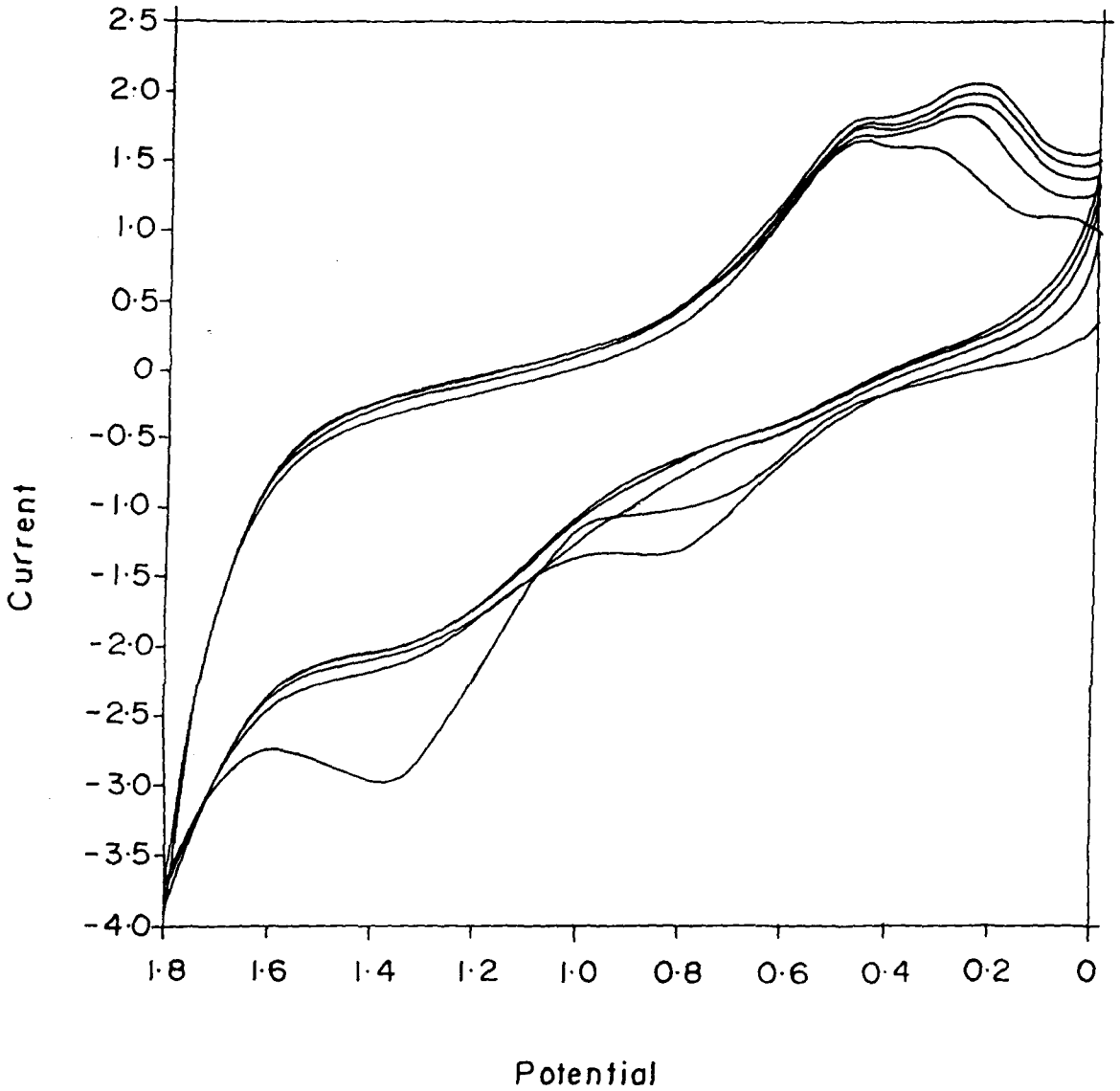

Figure 6.7 Cyclic Voltammogram of 10^{-3}M CuPPIXDME in CH_2Cl_2 containing 0.1M TBAP at room temperature. Scan rate =100mV/s

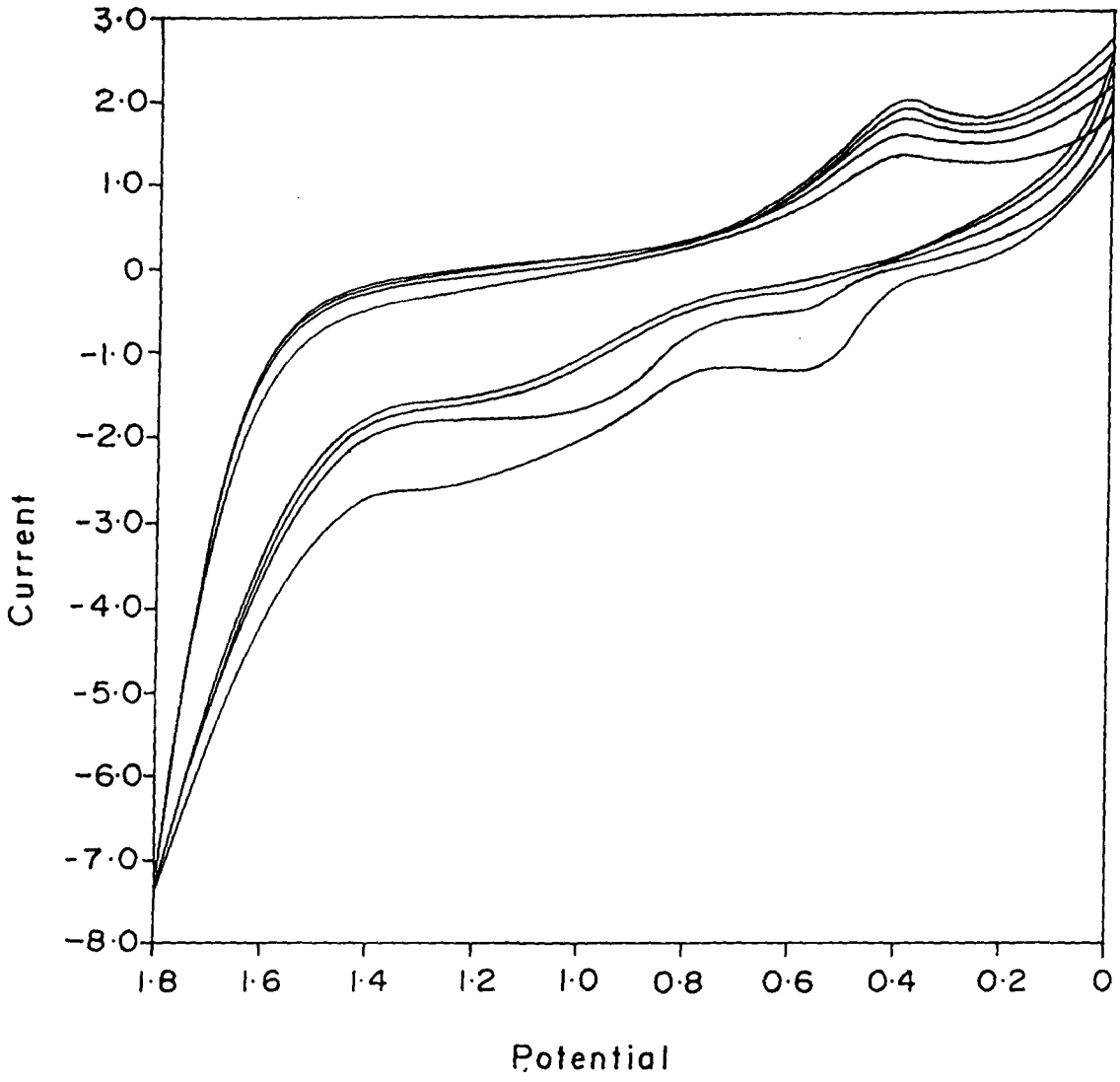

Figure 6.8(a) Cyclic Voltammogram of 10^{-2} M ZnPPIXDME in CH_2Cl_2 containing 0.1M TBAP at room temperature. Scan rate =100mV/s

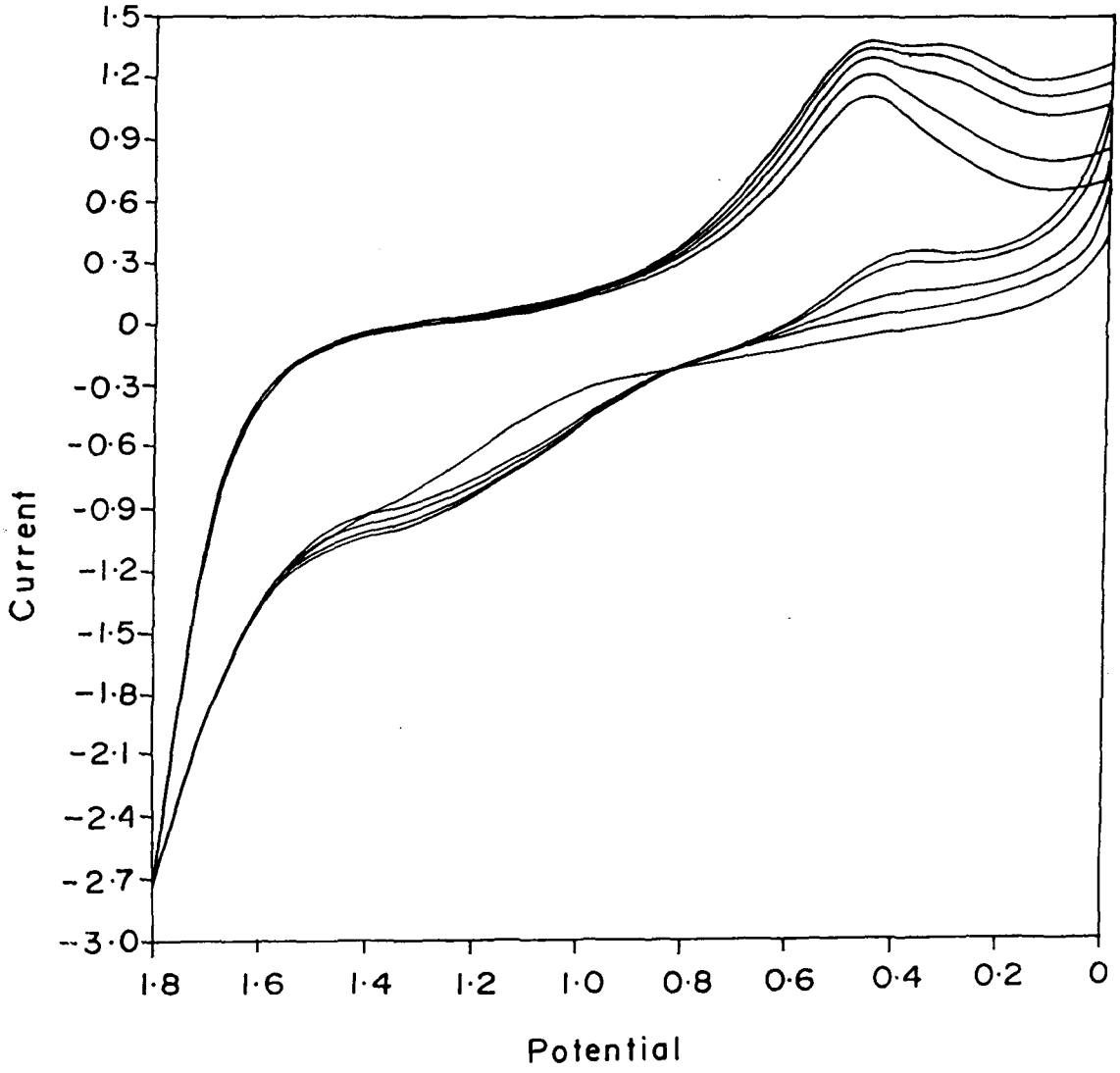

Figure 6.8(b) Cyclic Voltammogram of 10^{-4}M ZnPPIXDME in CH_2Cl_2 containing 0.1M TBAP at room temperature. Scan rate =100mV/s

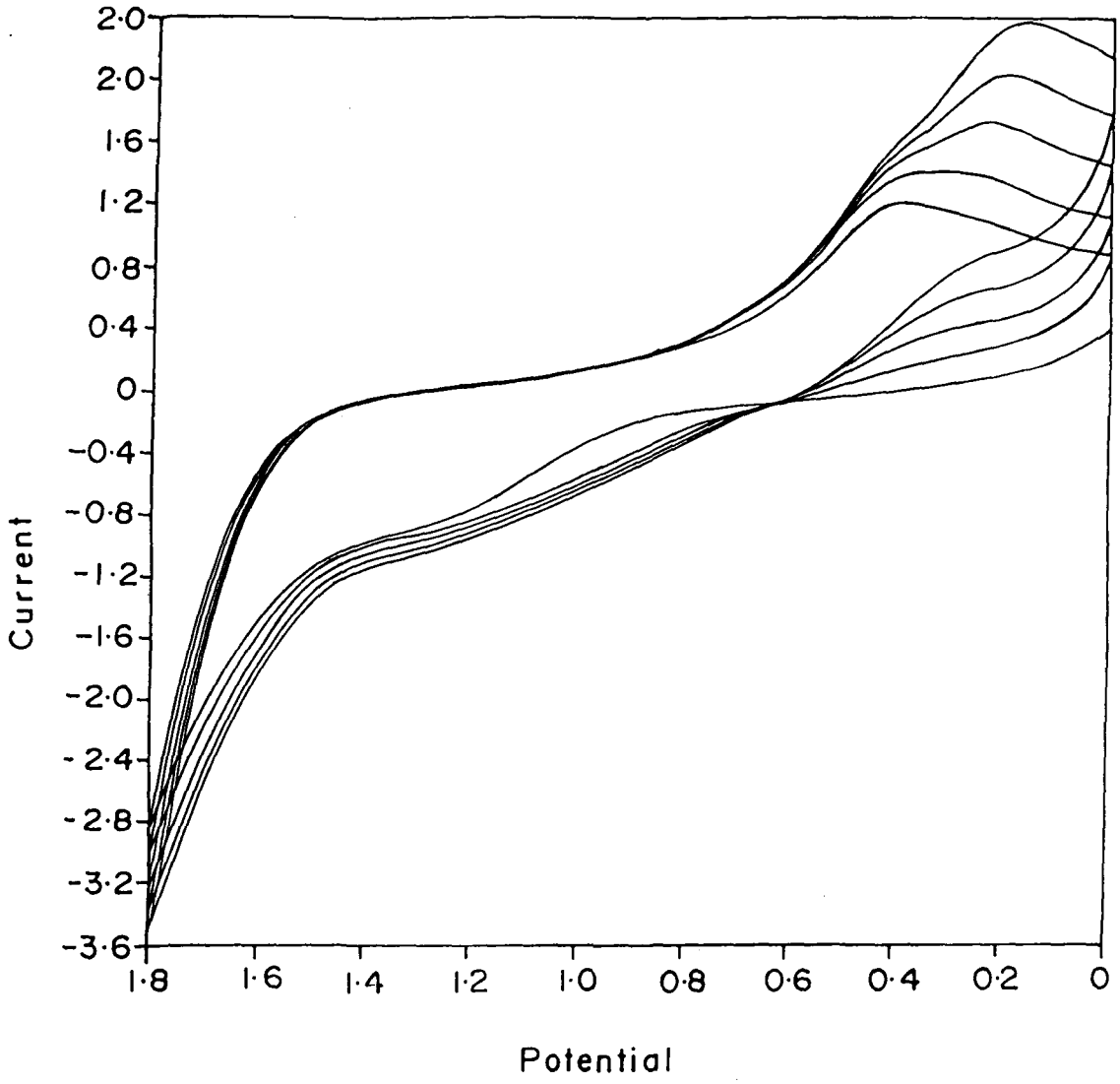

Figure 6.8(c) Cyclic Voltammogram of 10^{-5}M ZnPPIXDME in CH_2Cl_2 containing 0.1M TBAP at room temperature. Scan rate =100mV/s

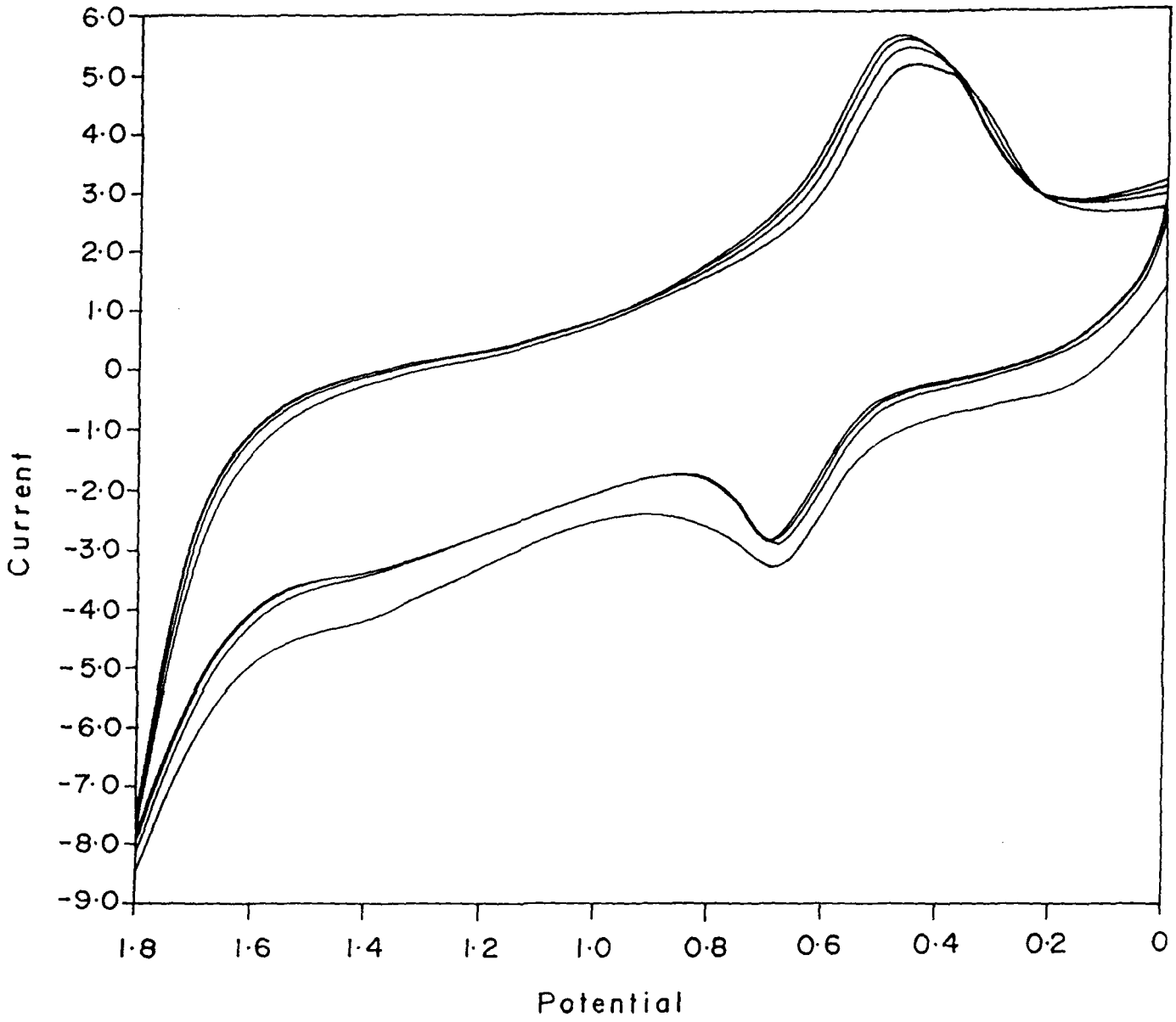

Figure 6.9a Cyclic Voltammogram of 10^{-3}M SnPPIXDME in CH_2Cl_2 containing 0.1M TBAP at room temperature. Scan rate =100mV/s

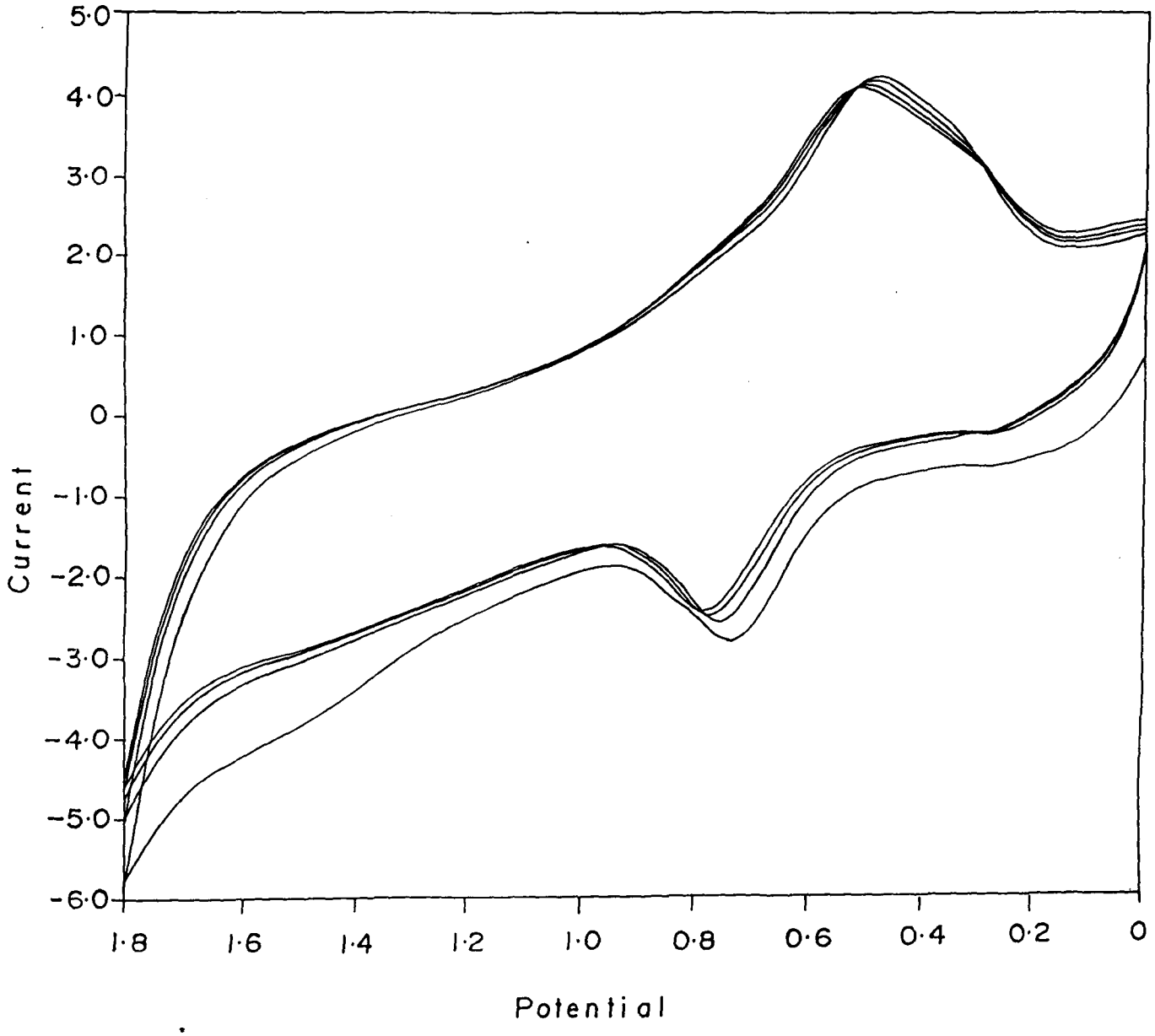

Figure 6.9b Cyclic Voltammogram of 10^{-4}M SnPPIXDME in CH_2Cl_2 containing 0.1M TBAP at room temperature. Scan rate =100mV/s

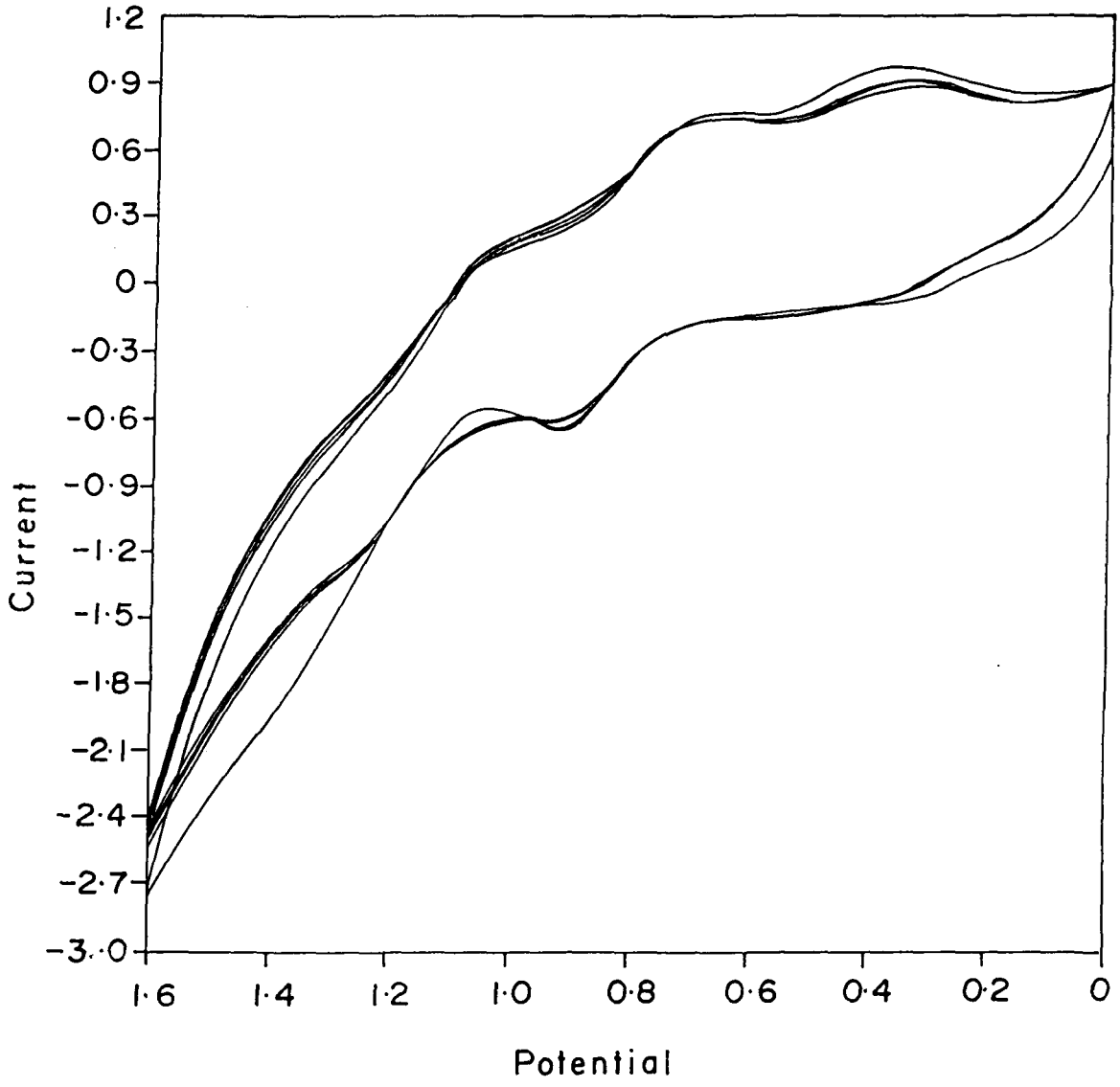

Figure 6.10a Cyclic Voltammogram of 10^{-2}M VOMPIXDME in CH_2Cl_2 containing 0.1M TBAP at room temperature. Scan rate =100mV/s

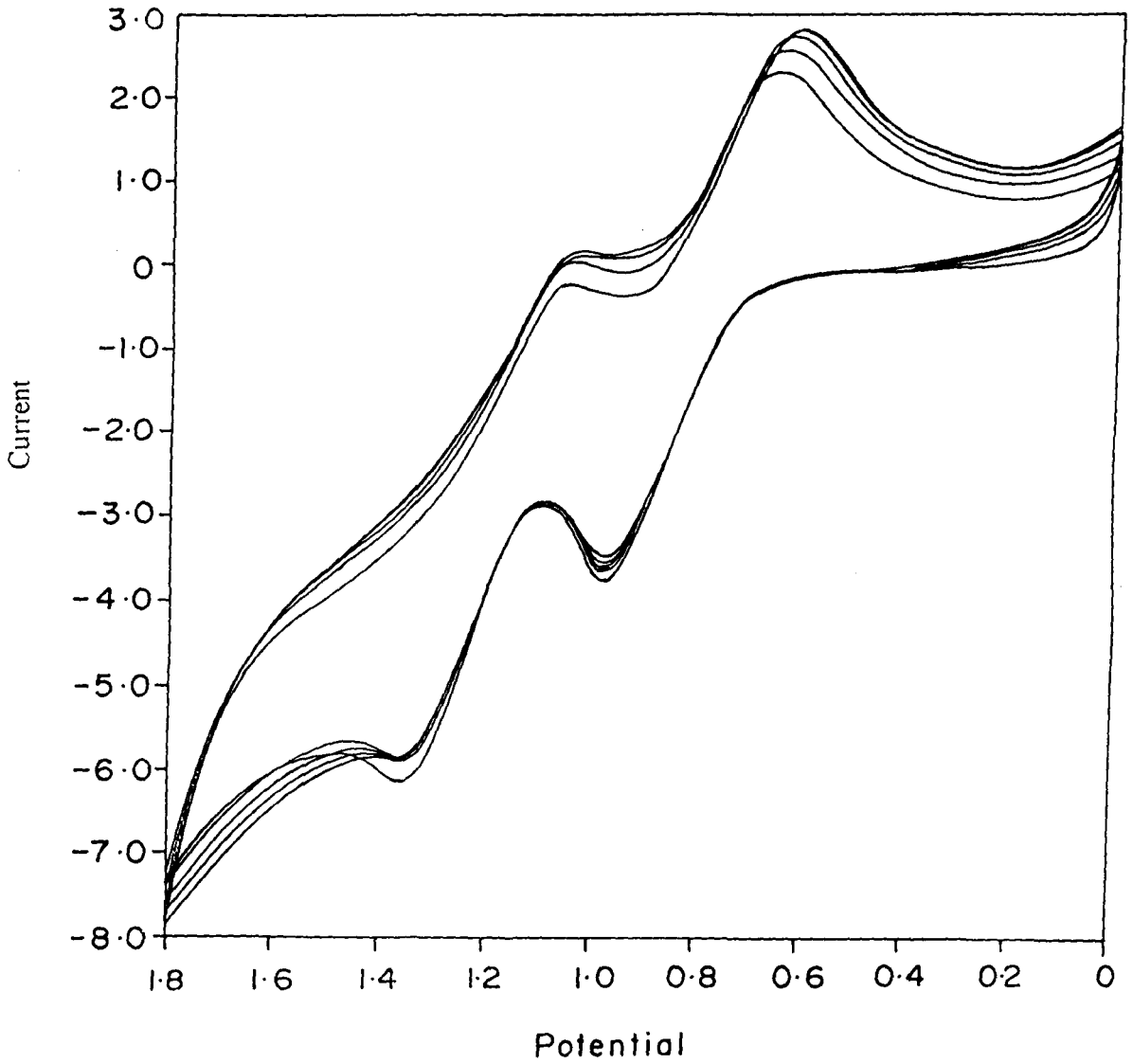

Figure 6.10b Cyclic Voltammogram of 10^{-3}M VOMPIXDME in CH_2Cl_2 containing 0.1M TBAP at room temperature. Scan rate =100mV/s

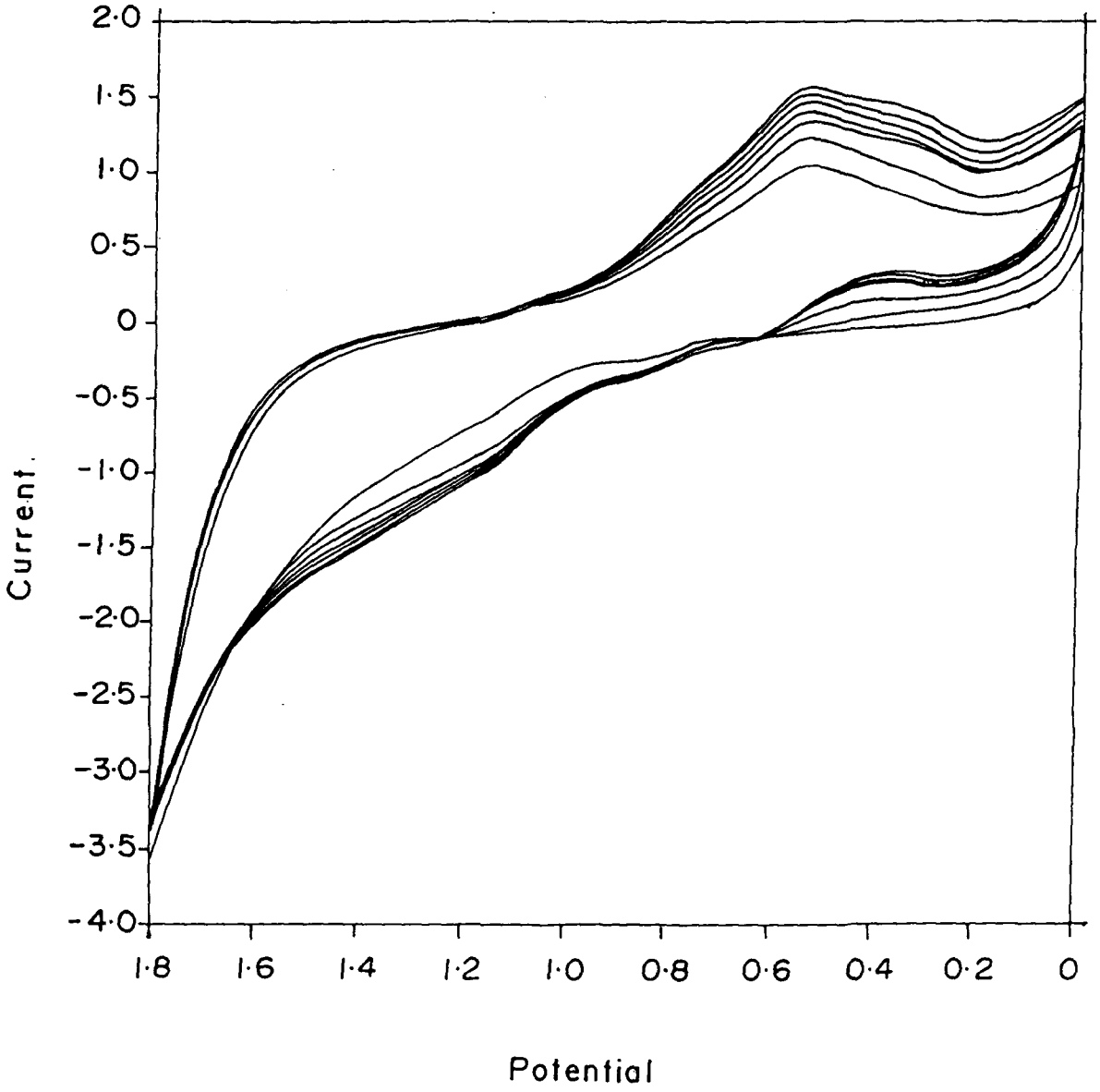

Figure 6.10c Cyclic Voltammogram of 10^{-4}M VOMPIXDME in CH_2Cl_2 containing 0.1M TBAP at room temperature. Scan rate =100mV/s

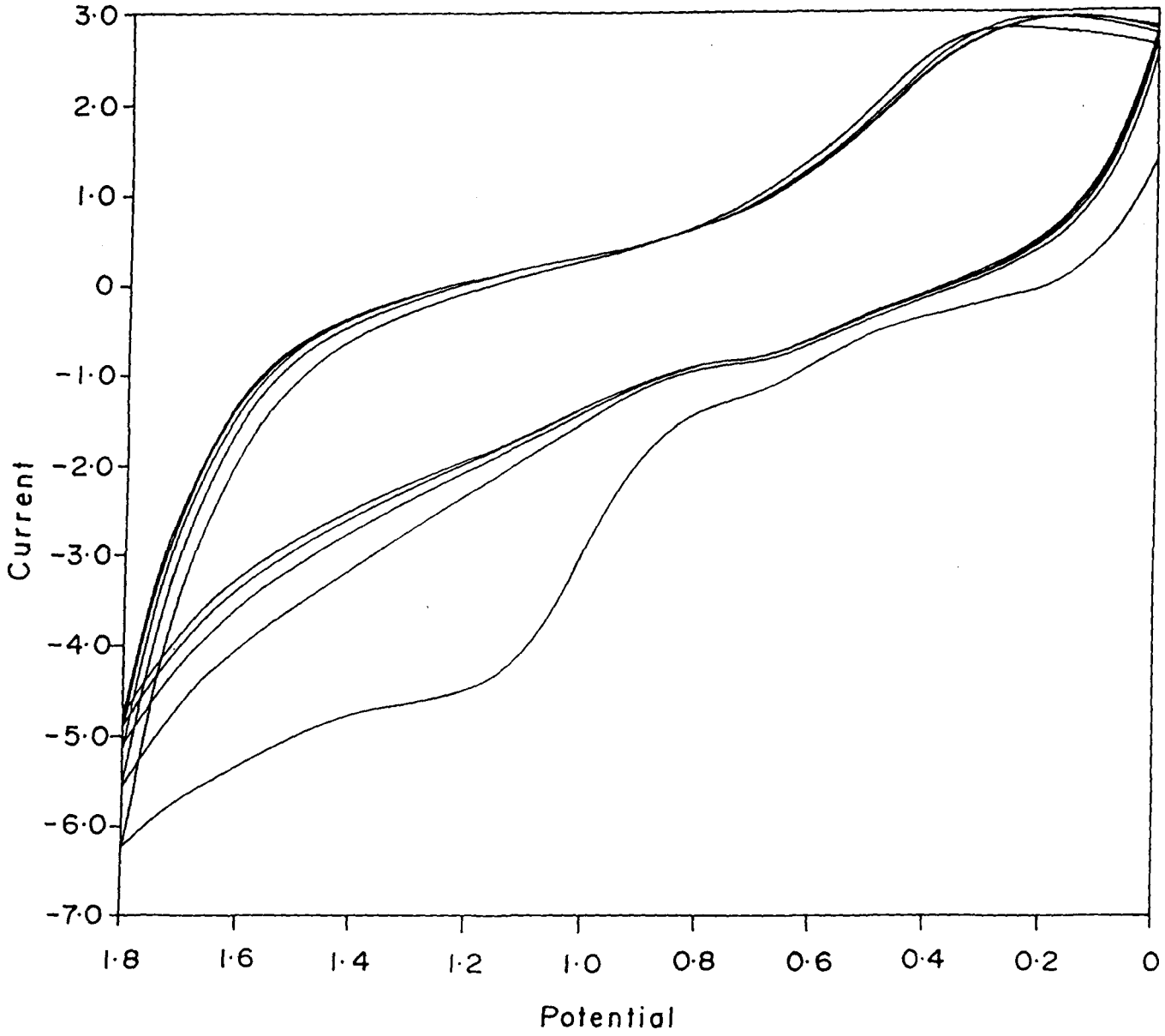

Figure 6.11 Cyclic Voltammogram of 10^{-2}M MnMPIXDME in CH_2Cl_2 containing 0.1M TBAP at room temperature. Scan rate =100mV/s

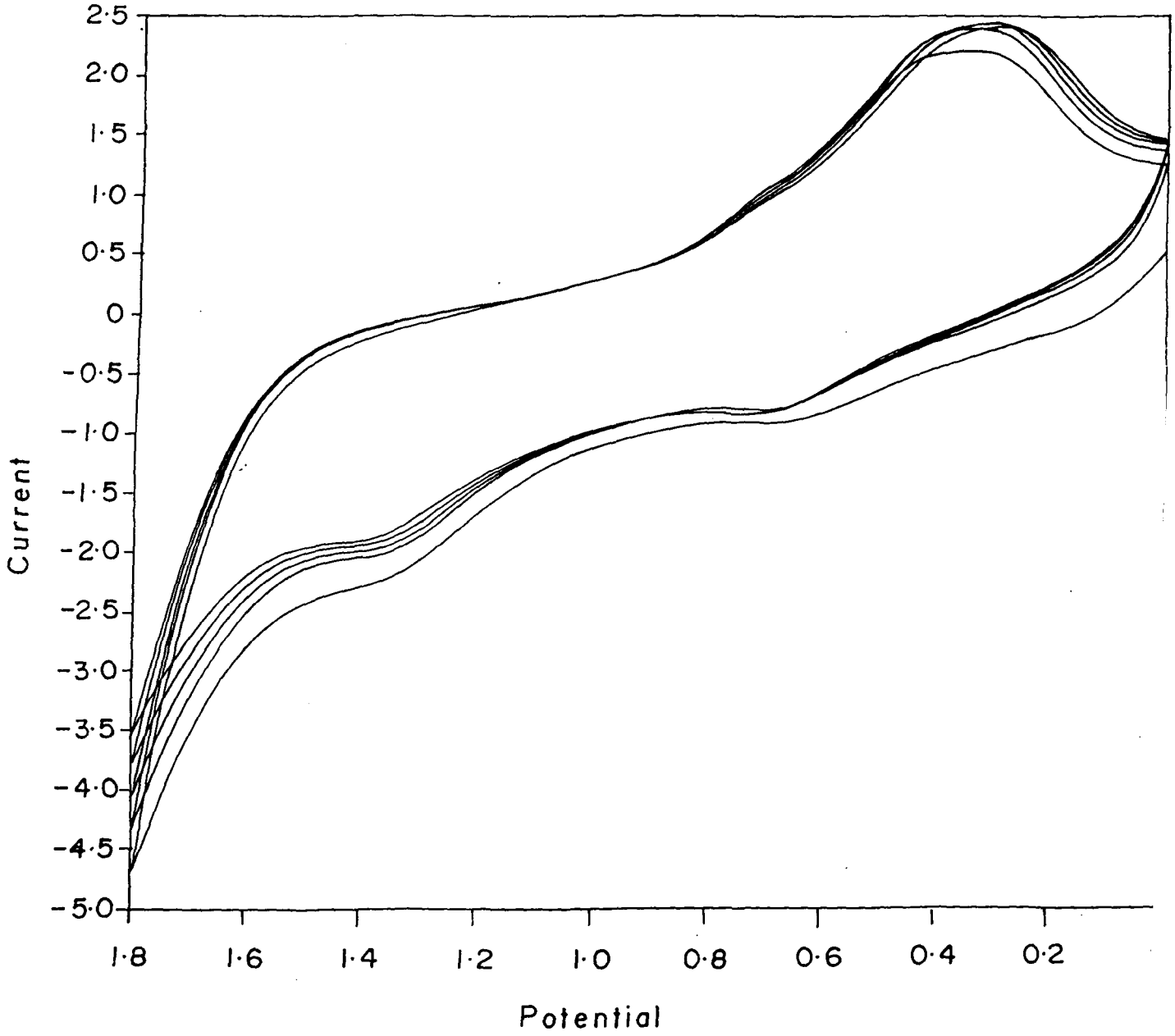

Figure 6.12a Cyclic Voltammogram of 10^{-2} M CoMPIXDME in CH_2Cl_2 containing 0.1M TBAP at room temperature. Scan rate =100mV/s

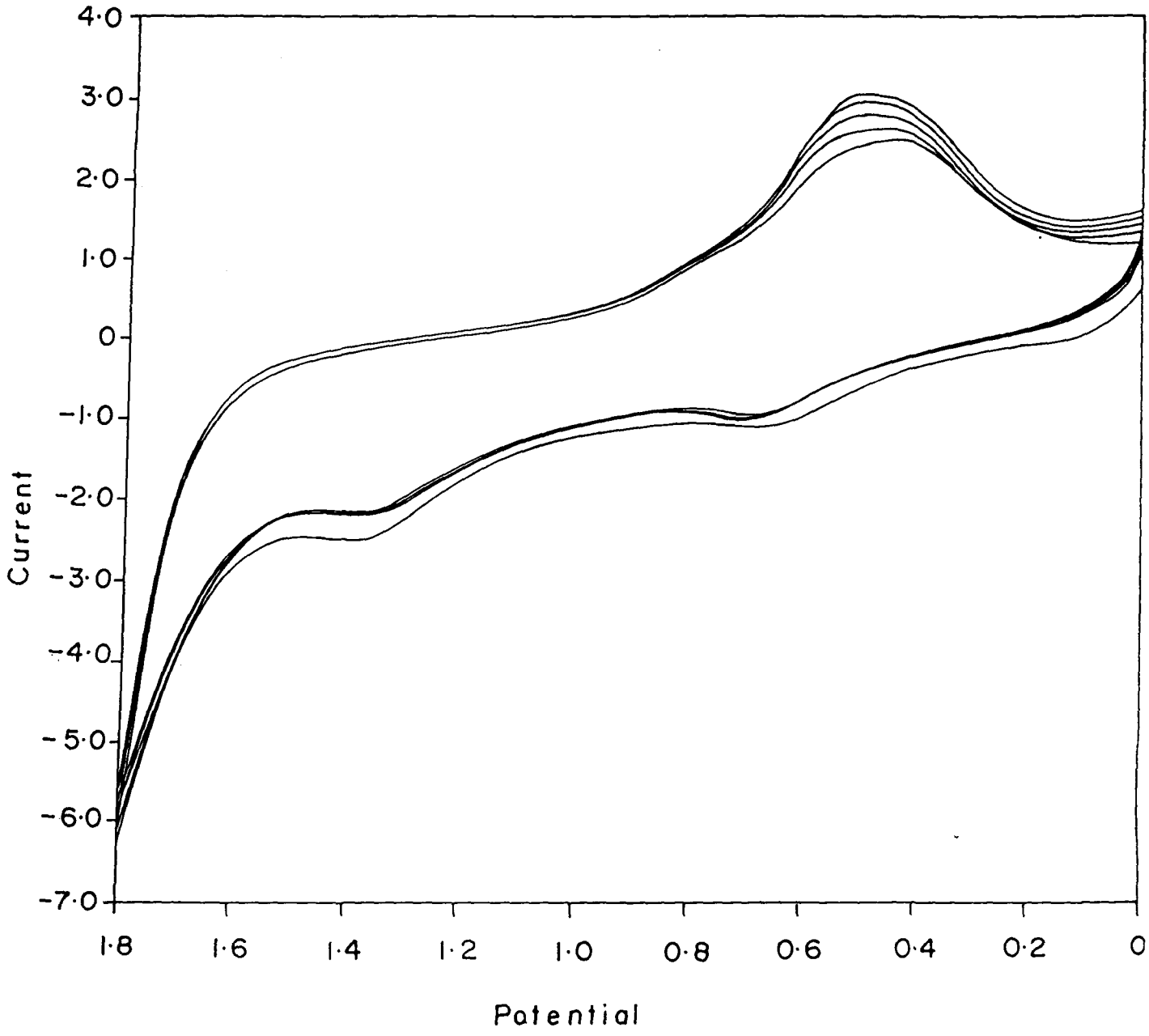

Figure 6.12b Cyclic Voltammogram of 10^{-3} M CoMPIXDME in CH_2Cl_2 containing 0.1M TBAP at room temperature. Scan rate =100mV/s

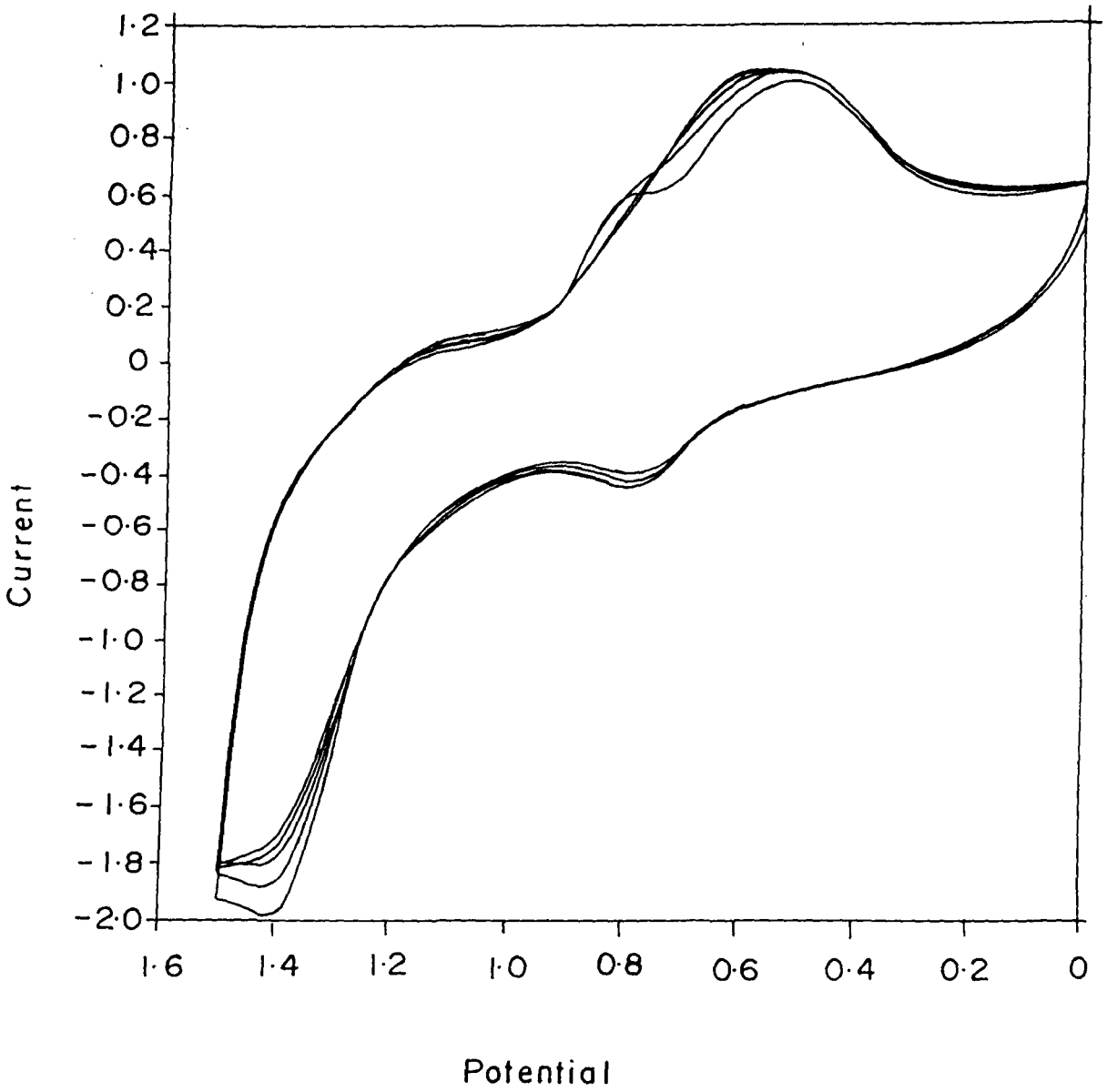

Figure 6.12c Cyclic Voltammogram of 10^{-5} M CoMPIXDME in CH_2Cl_2 containing 0.1M TBAP at room temperature. Scan rate =100mV/s

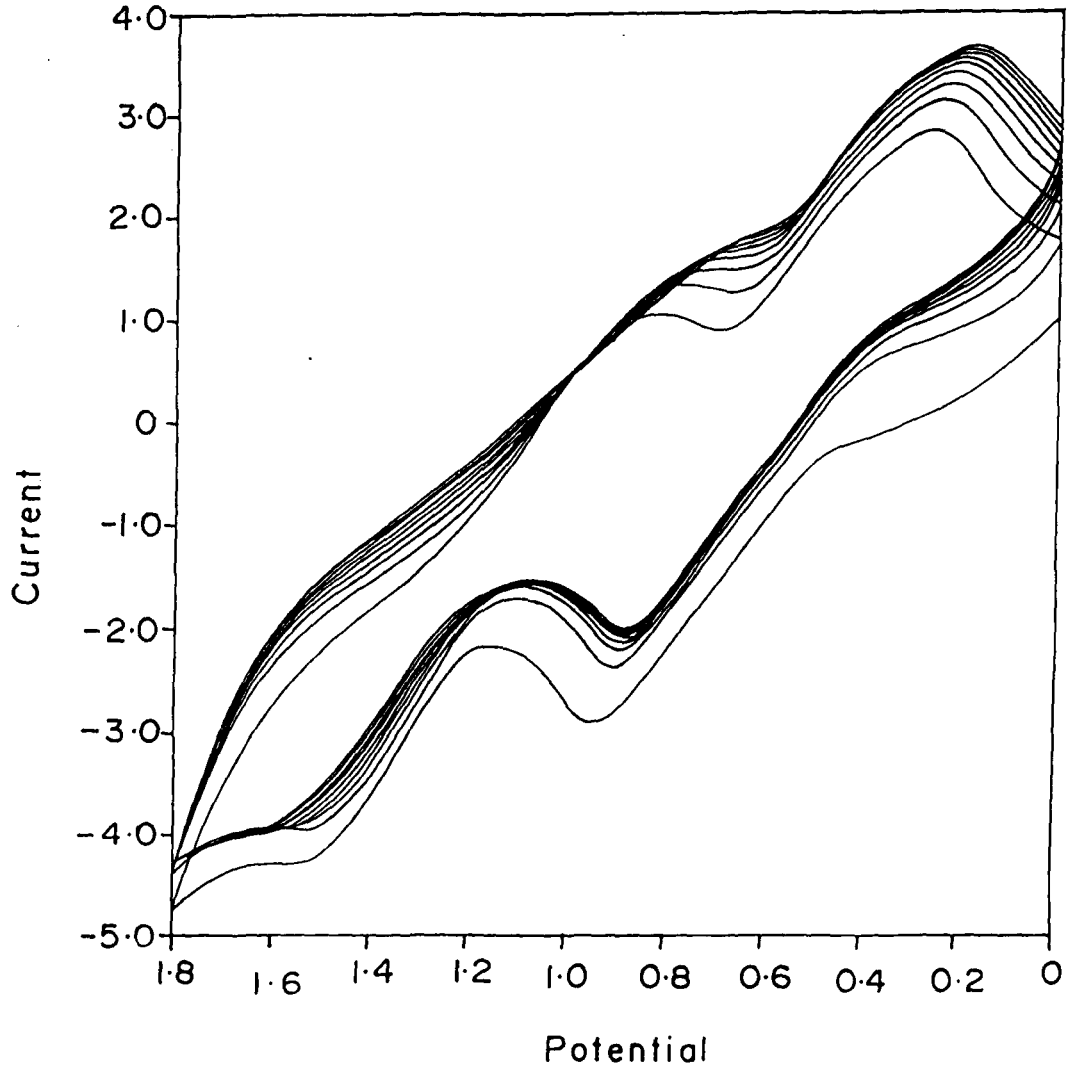

Figure 6.13a Cyclic Voltammogram of 10^{-2} M NiMPIXDME in CH_2Cl_2 containing 0.1M TBAP at room temperature. Scan rate =100mV/s

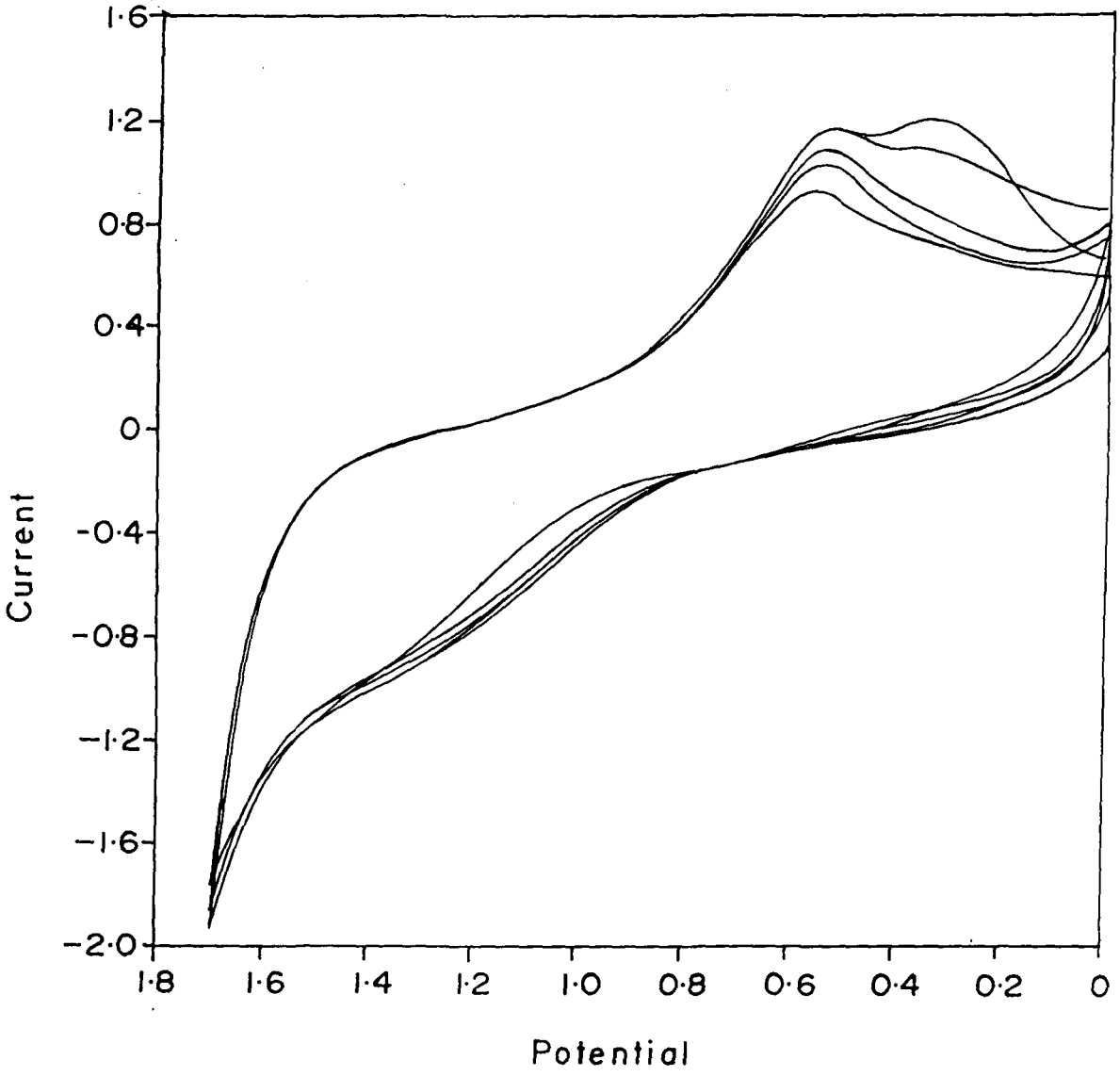

Figure 6.13b Cyclic Voltammogram of 10^{-5} M NiMPIXDME in CH_2Cl_2 containing 0.1M TBAP at room temperature. Scan rate =100mV/s

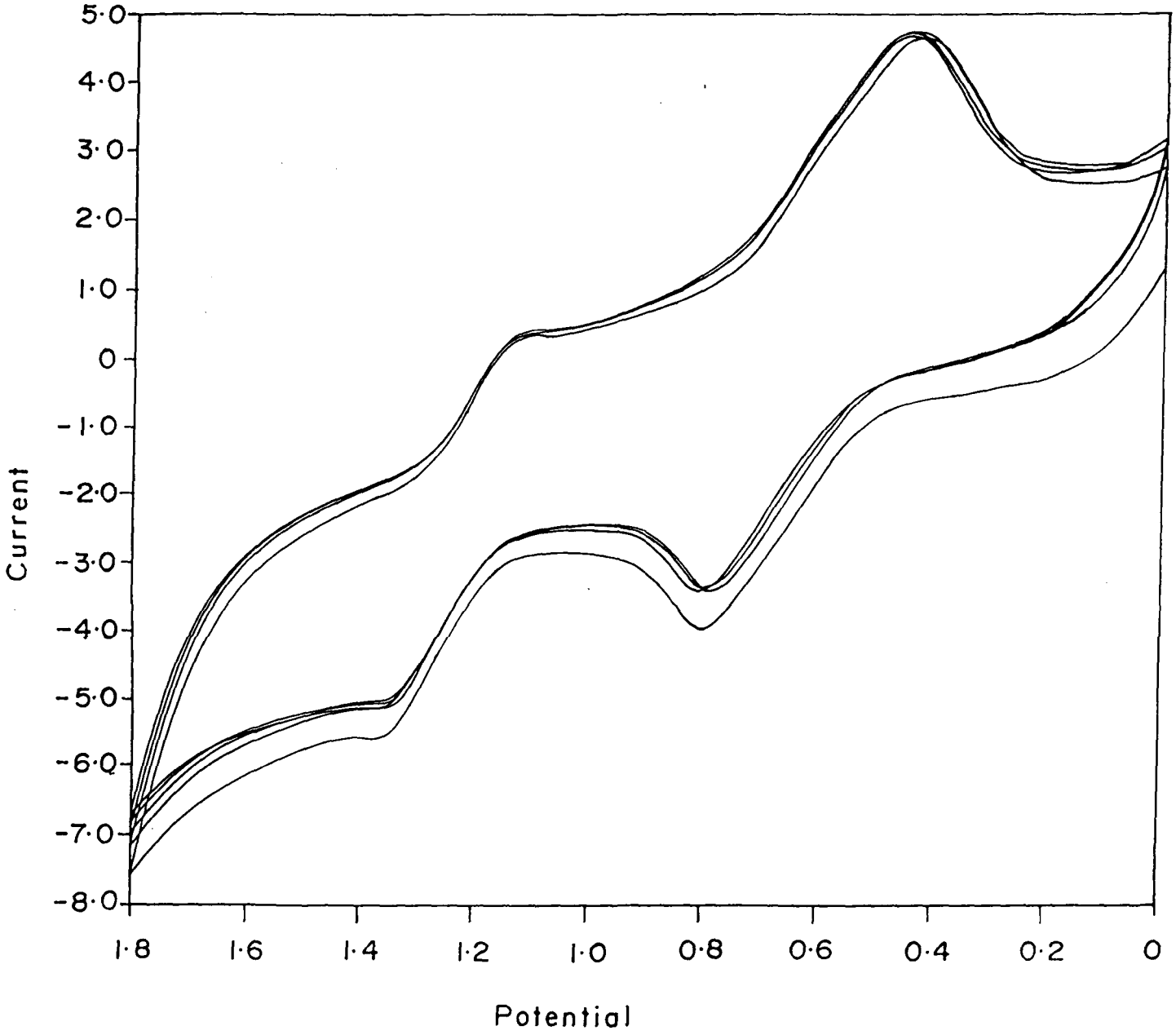

Figure 6.14a Cyclic Voltammogram of 10^{-2} M CuMPIXDME in CH_2Cl_2 containing 0.1M TBAP at room temperature. Scan rate =100mV/s

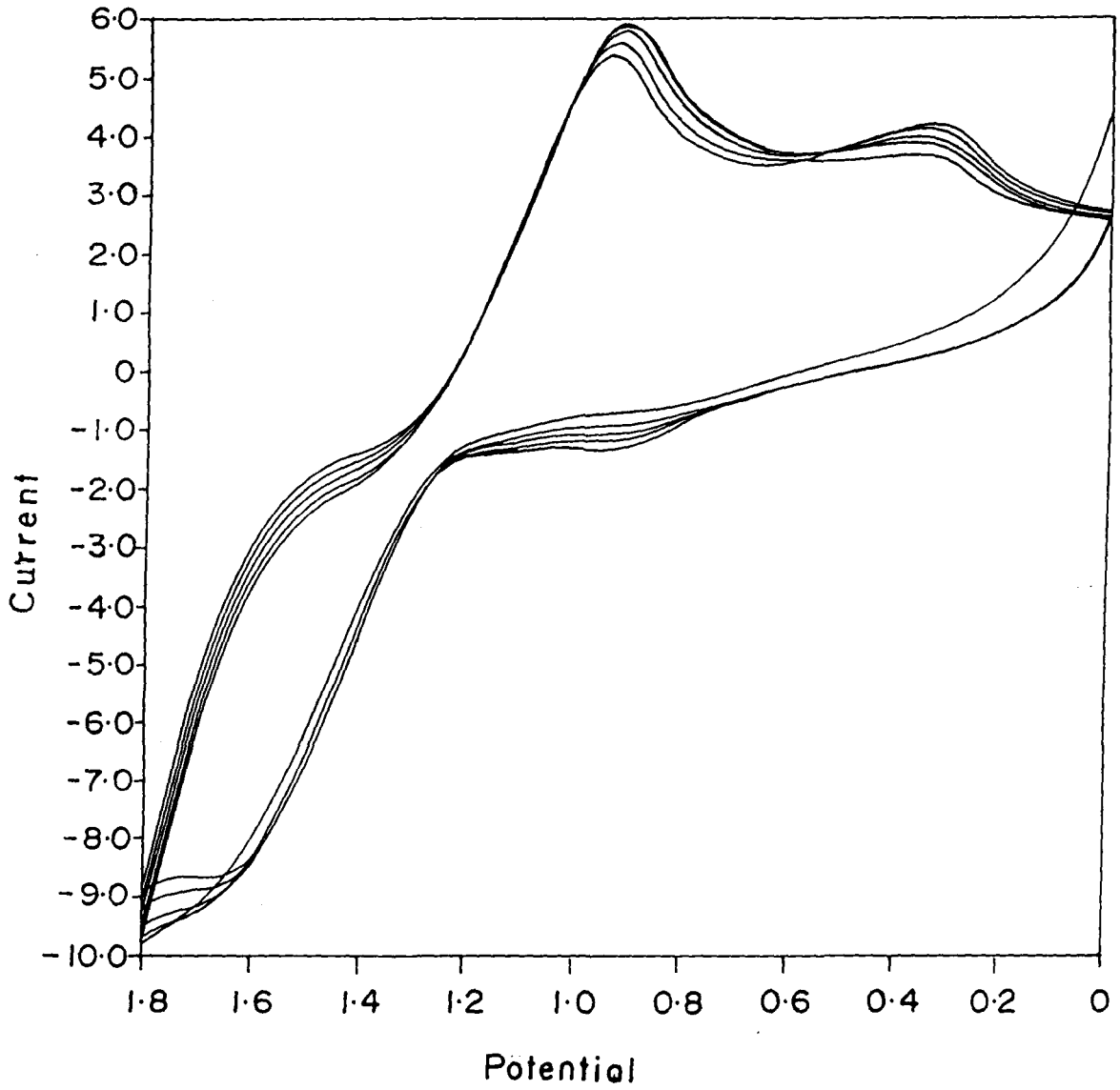

Figure 6.14b Cyclic Voltammogram of 10^{-4} M CuMPIXDME in CH_2Cl_2 containing 0.1M TBAP at room temperature. Scan rate =100mV/s

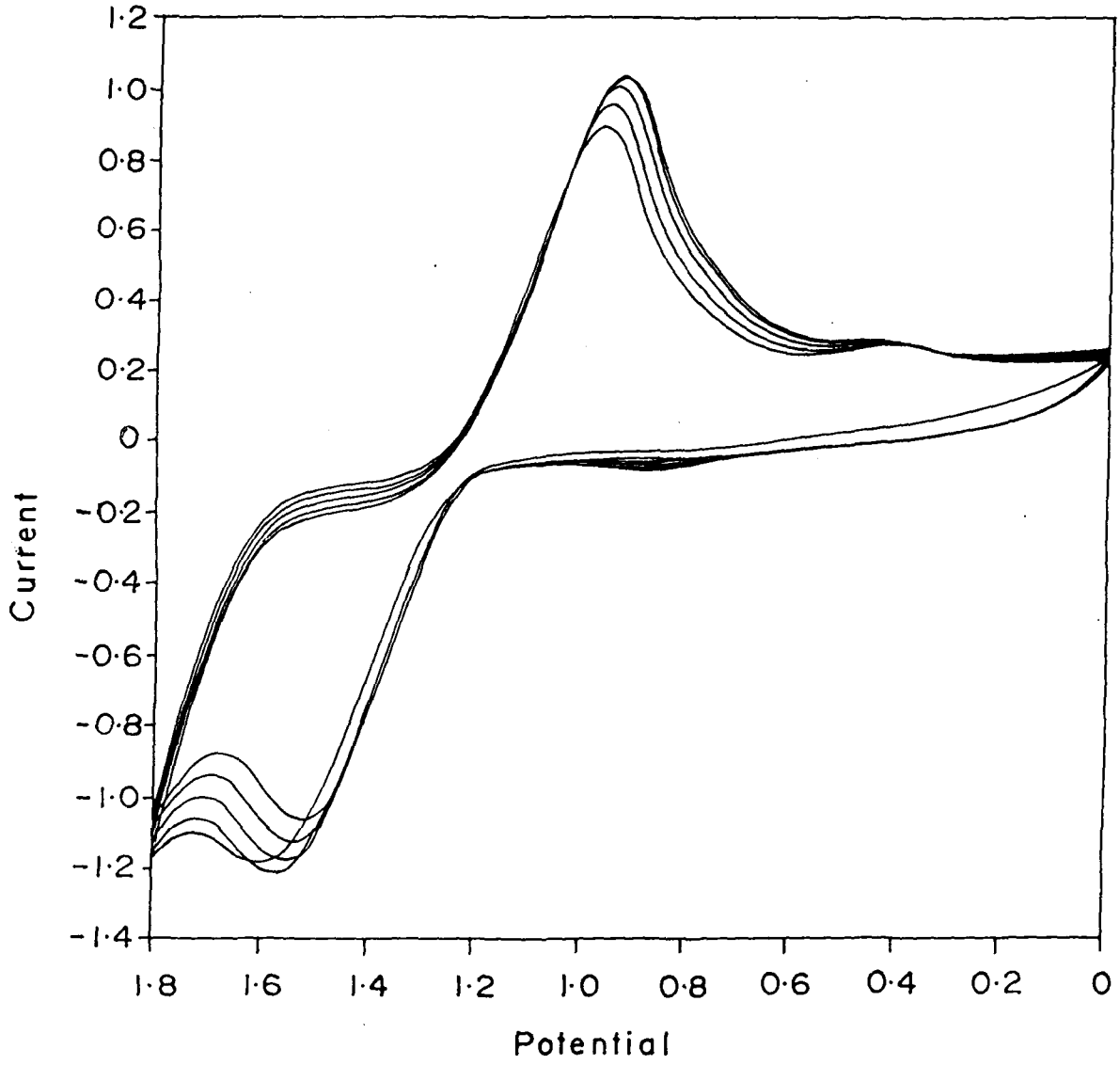

Figure 6.14c Cyclic Voltammogram of 10^{-5} M CuMPIXDME in CH_2Cl_2 containing 0.1M TBAP at room temperature. Scan rate =100mV/s

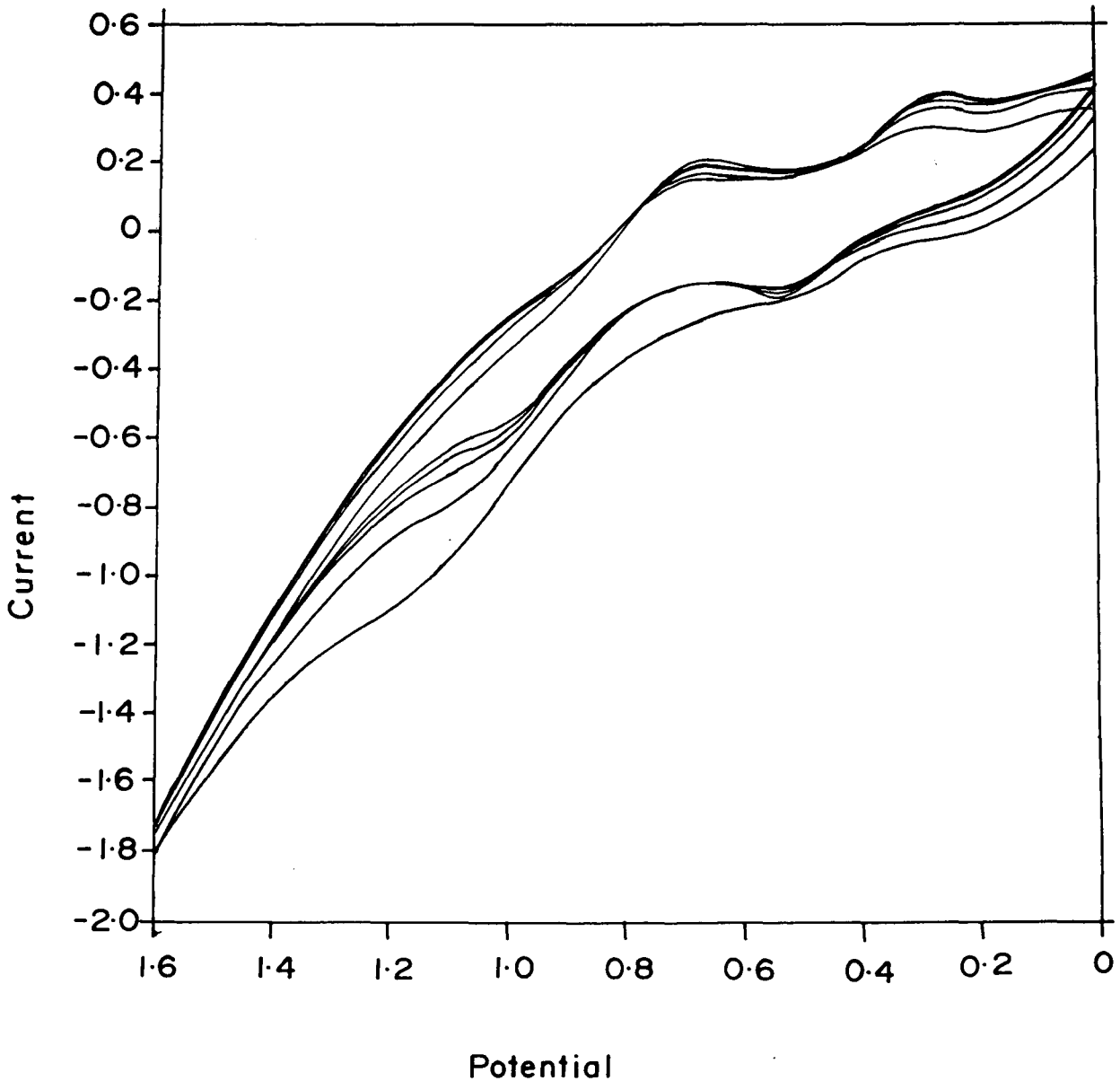

Figure 6.15a Cyclic Voltammogram of 10^{-2} M VOMPIXdiHCl in CH_2Cl_2 containing 0.1M TBAP at room temperature. Scan rate =100mV/s

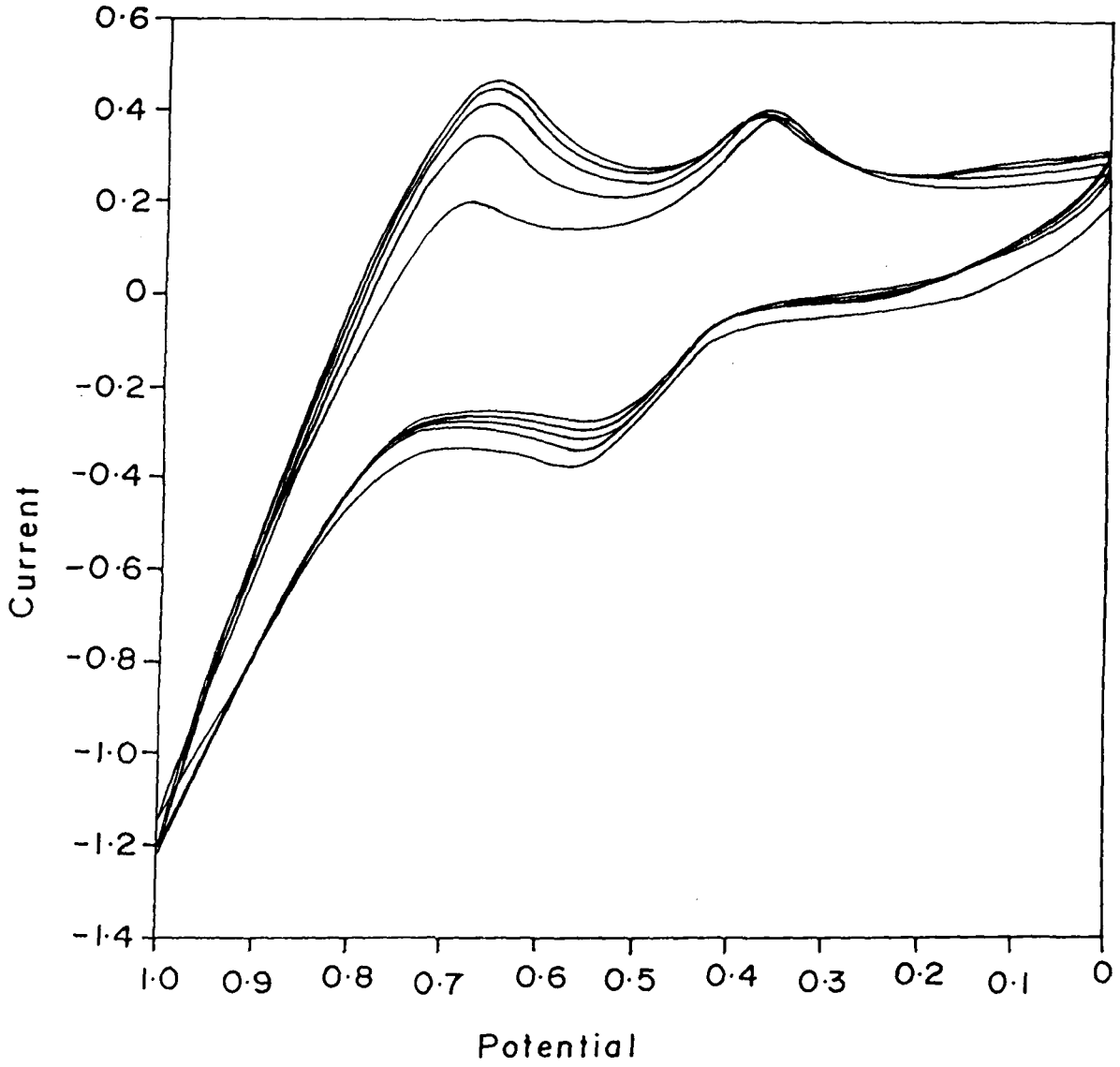

Figure 6.15b Cyclic Voltammogram of 10^{-3} M VOMPIXdiHCl in CH_2Cl_2 containing 0.1M TBAP at room temperature. Scan rate =100mV/s

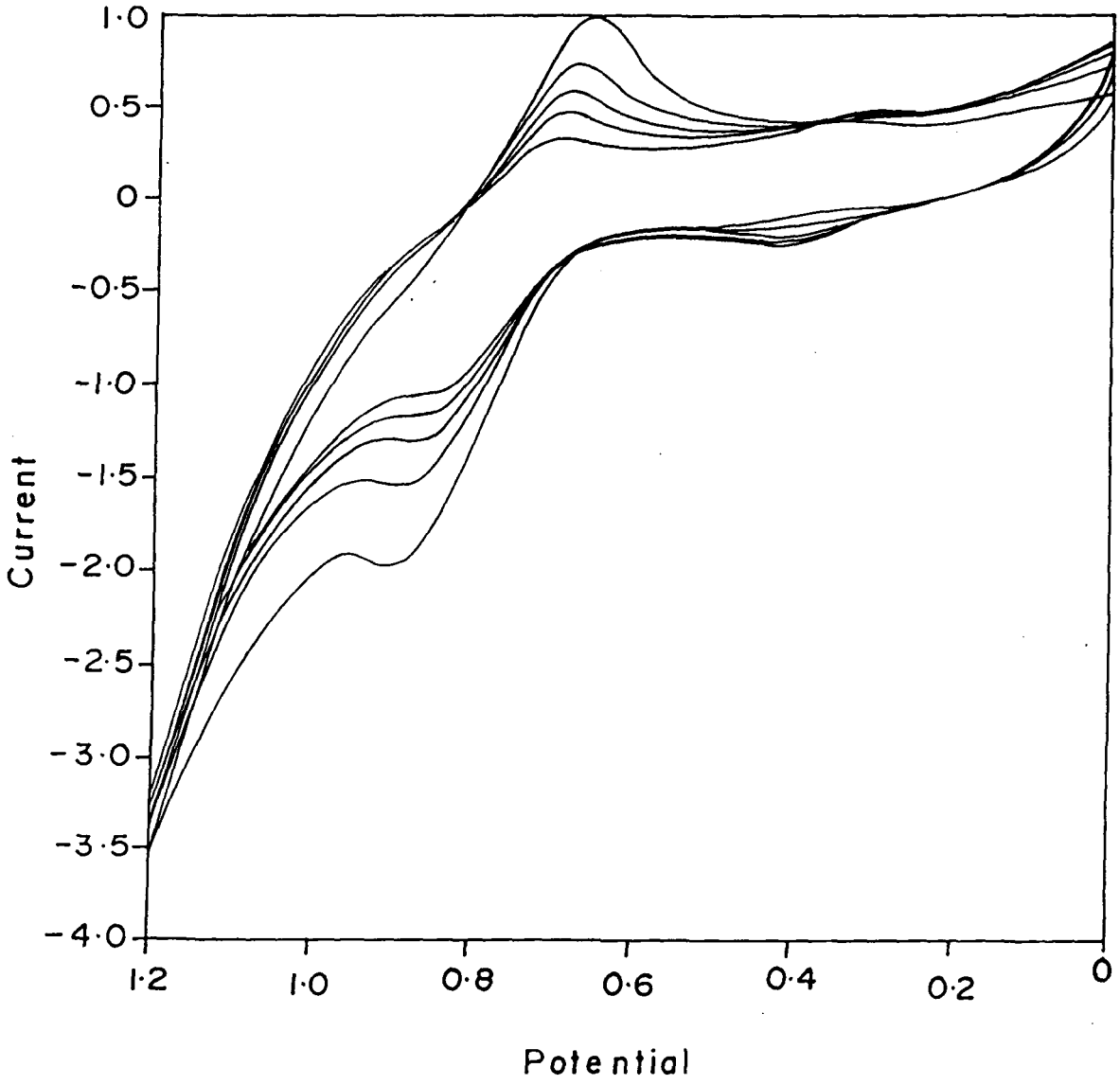

Figure 6.15c Cyclic Voltammogram of 10^{-4} M VOMPIXdiHCl in CH_2Cl_2 containing 0.1M TBAP at room temperature. Scan rate =100mV/s

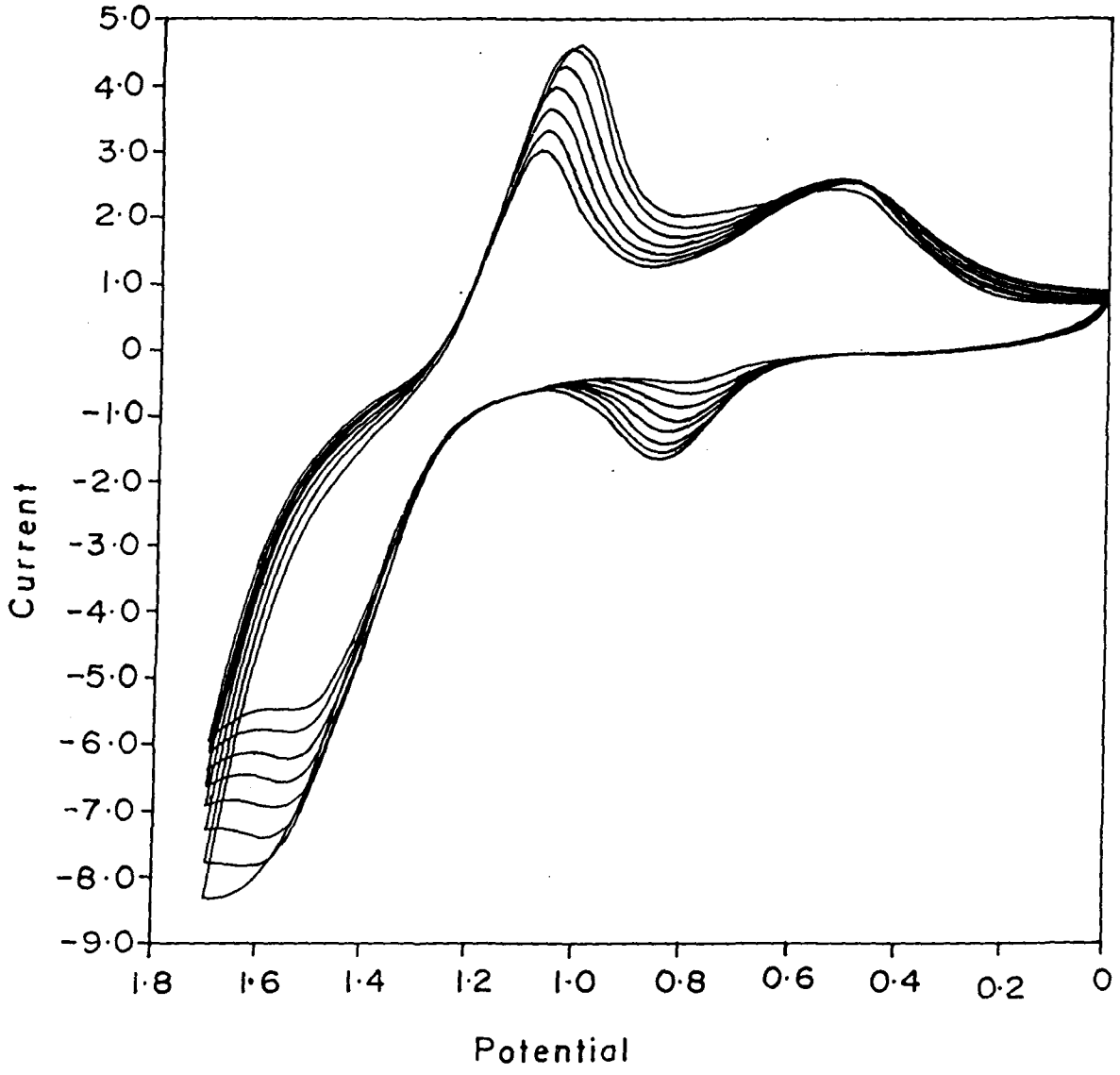

Figure 6.15d Cyclic Voltammogram of 10^{-5} M VOMPIXdiHCl in CH_2Cl_2 containing 0.1M TBAP at room temperature. Scan rate =100mV/s

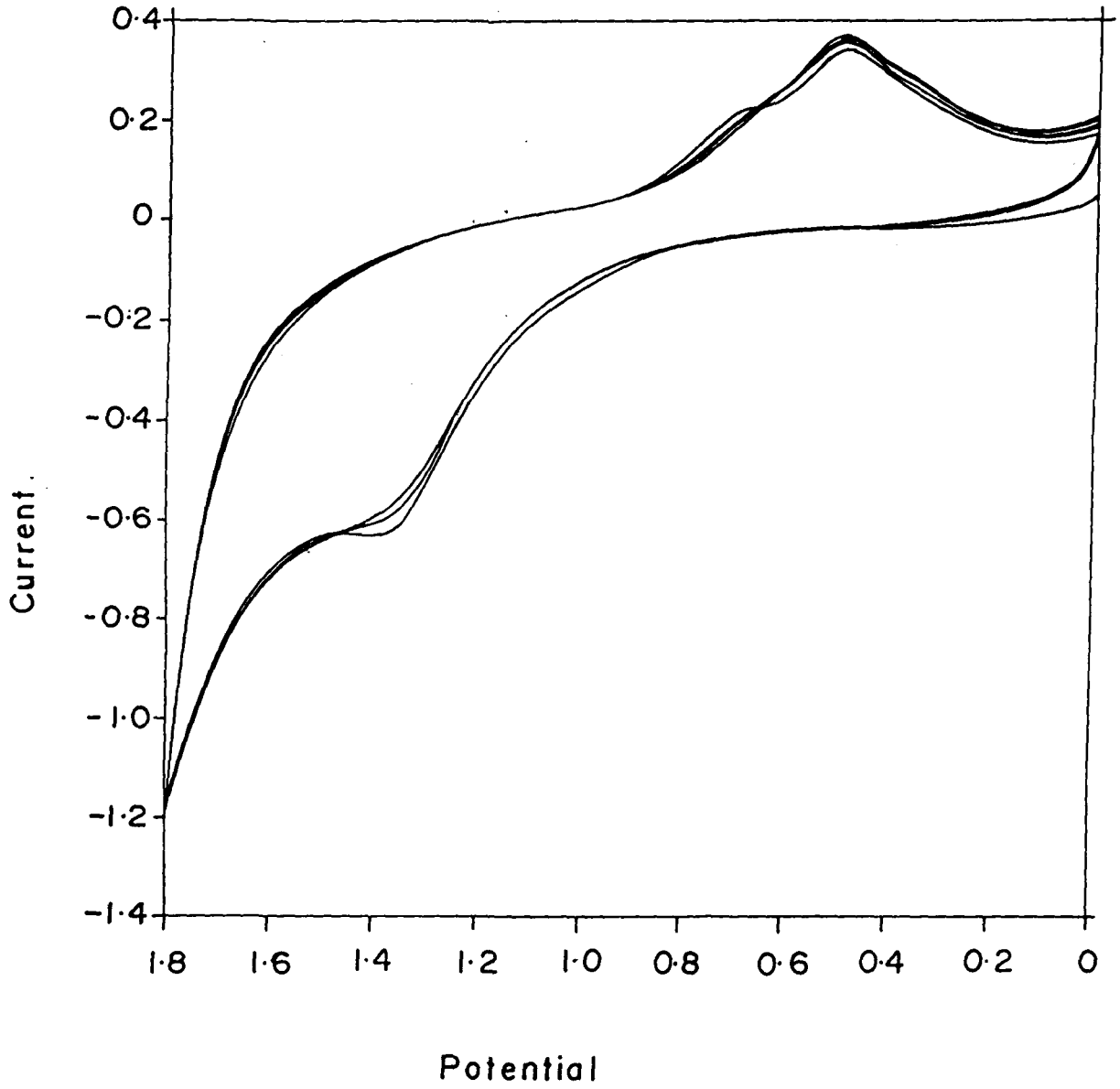

Figure 6.16 Cyclic Voltammogram of 10^{-2} M VOHPIXDME in CH_2Cl_2 containing 0.1M TBAP at room temperature. Scan rate =100mV/s

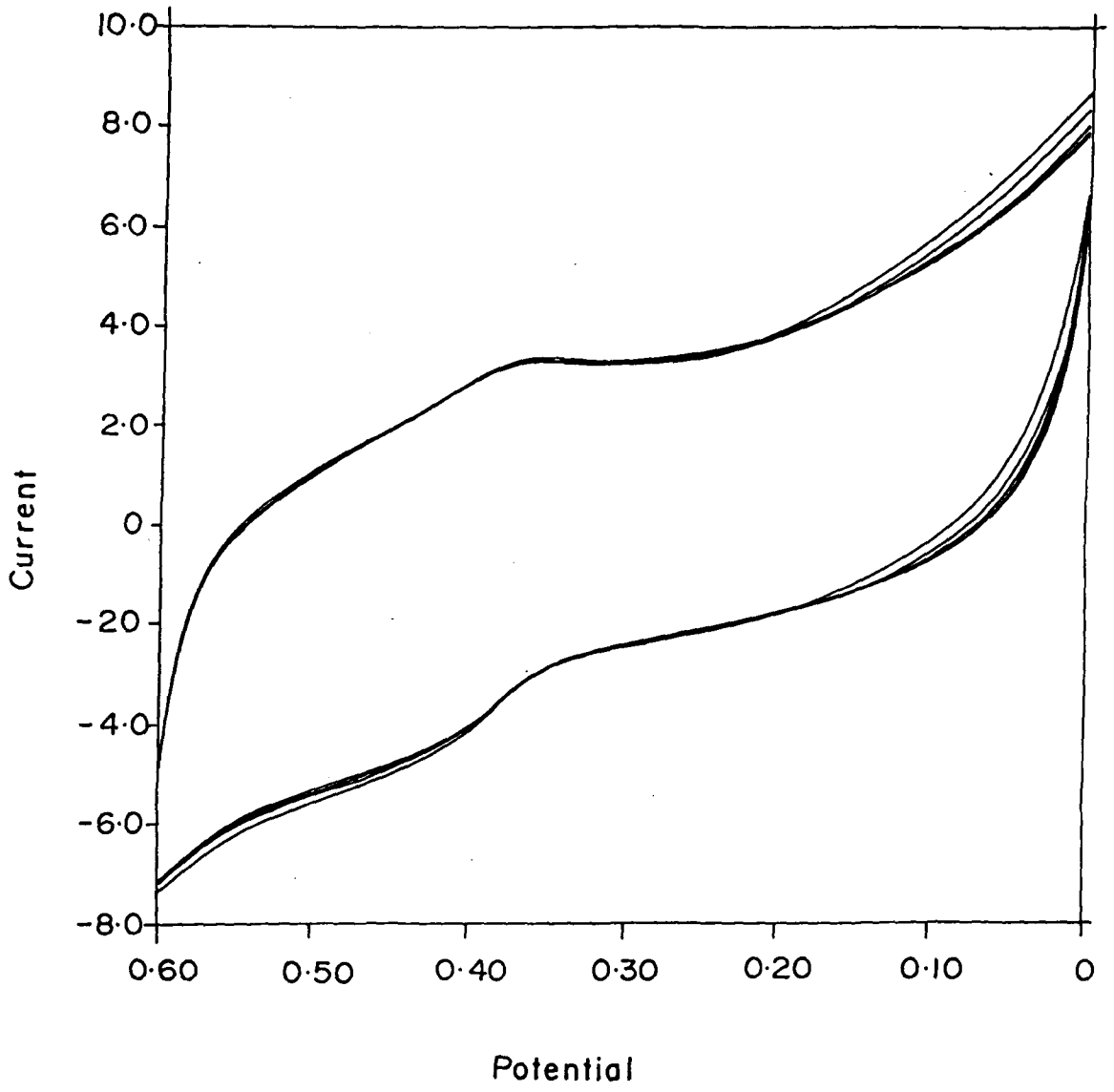

Figure 6.17 Cyclic Voltammogram of 10^{-3} M MnHPIXDME in CH_2Cl_2 containing 0.1M TBAP at room temperature. Scan rate =100mV/s

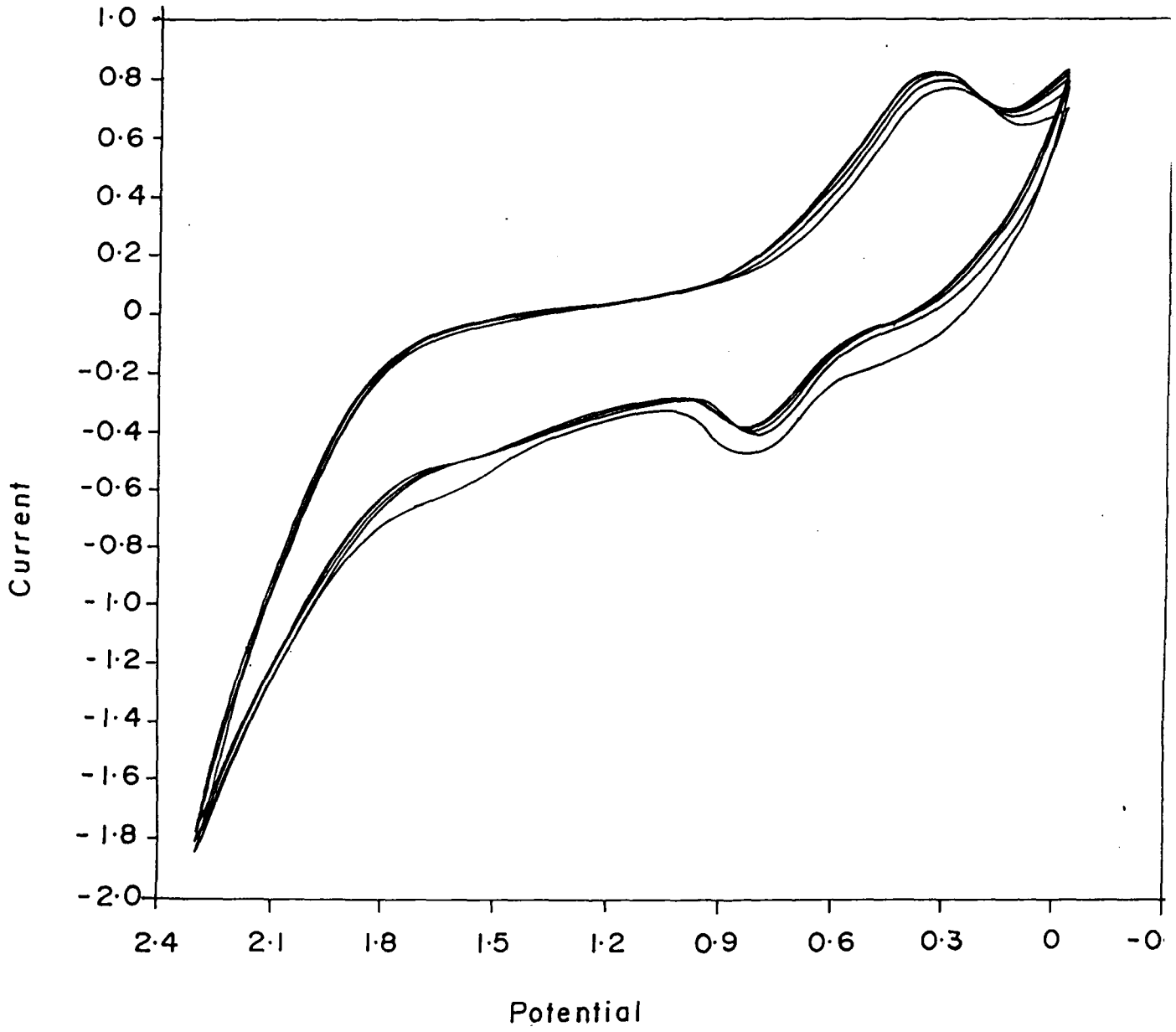

Figure 6.18 Cyclic Voltammogram of 10^{-2} M NiHPIXDME in CH_2Cl_2 containing 0.1M TBAP at room temperature. Scan rate =100mV/s

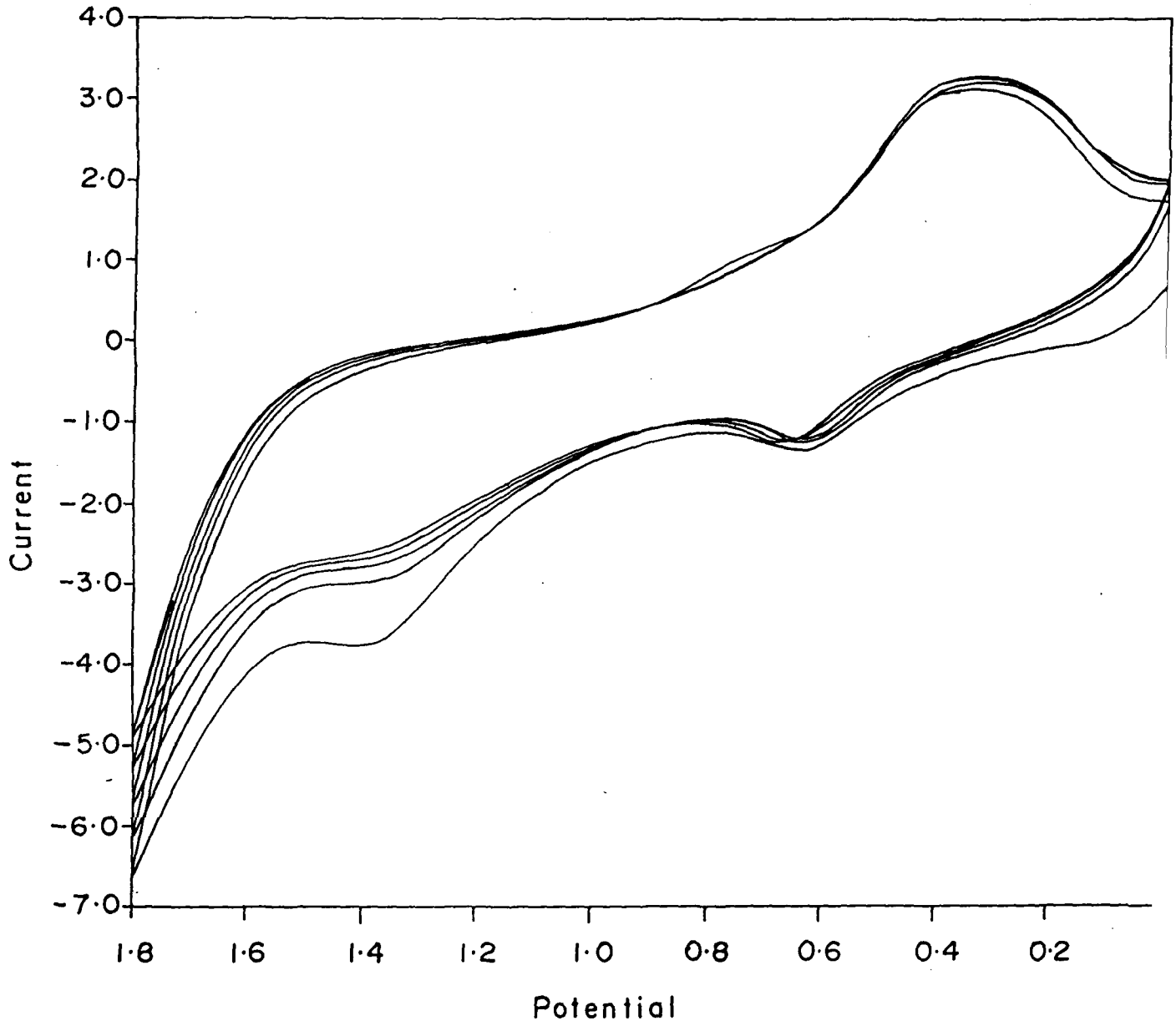

Figure 6.19 Cyclic Voltammogram of 10^{-2} M CuHPIXDME in CH_2Cl_2 containing 0.1M TBAP at room temperature. Scan rate =100mV/s

Table 6.4: Conductance measurements of Metalloporphyrins.
Cell constant= 0.9. Range=20mS

Compound	Conc.	Conductance	Compound	Conc.	Conductance	Compound	Conc.	Conductance
VOPPIX	10-2	4.9	VOMPIX	10-2	0.5	VOHPIX	10-2	4.6
DME	10-3	5.0	DME	10-3	0.9	DME	10-3	4.7
	10-4	5.1		10-4	1.1		10-4	4.8
	10-5	5.2		10-5	1.7		10-5	4.9
MnPPIX	10-2	1.3	MnMPIX	10-2	2.8	MnHPIX	10-2	9.6
DME	10-3	1.4	DME	10-3	2.9	DME	10-3	9.8
	10-4	1.5		10-4	3.0		10-4	10.0
	10-5	1.6		10-5	3.1		10-5	10.2
CoPPIX	10-2	4.9	CoMPIX	10-2	2.9	CoHPIX	10-2	12.0
DME	10-3	5.0	DME	10-3	3.0	DME	10-3	12.5
	10-4	5.1		10-4	3.1		10-4	13.0
	10-5	5.2		10-5	3.2		10-5	13.5
NiPPIX	10-2	0.1	NiMPIX	10-2	3.8	NiHPIX	10-2	3.0
DME	10-3	0.2	DME	10-3	3.9	DME	10-3	3.2
	10-4	0.3		10-4	4.0		10-4	3.4
	10-5	0.5		10-5	4.1		10-5	3.6
CuPPIX	10-2	3.1	CuMPIX	10-2	2.9	CuHPIX	10-2	4.0
DME	10-3	3.3	DME	10-3	3.0	DME	10-3	4.1
	10-4	3.5		10-4	3.1		10-4	4.2
	10-5	3.7		10-5	3.2		10-5	4.3
ZnPPIX	10-2	1.6	VOMPIX	10-2	2.2			
DME	10-3	1.7	diHCl	10-3	2.4			
	10-4	1.8		10-4	2.6			
	10-5	1.9		10-5	2.8			

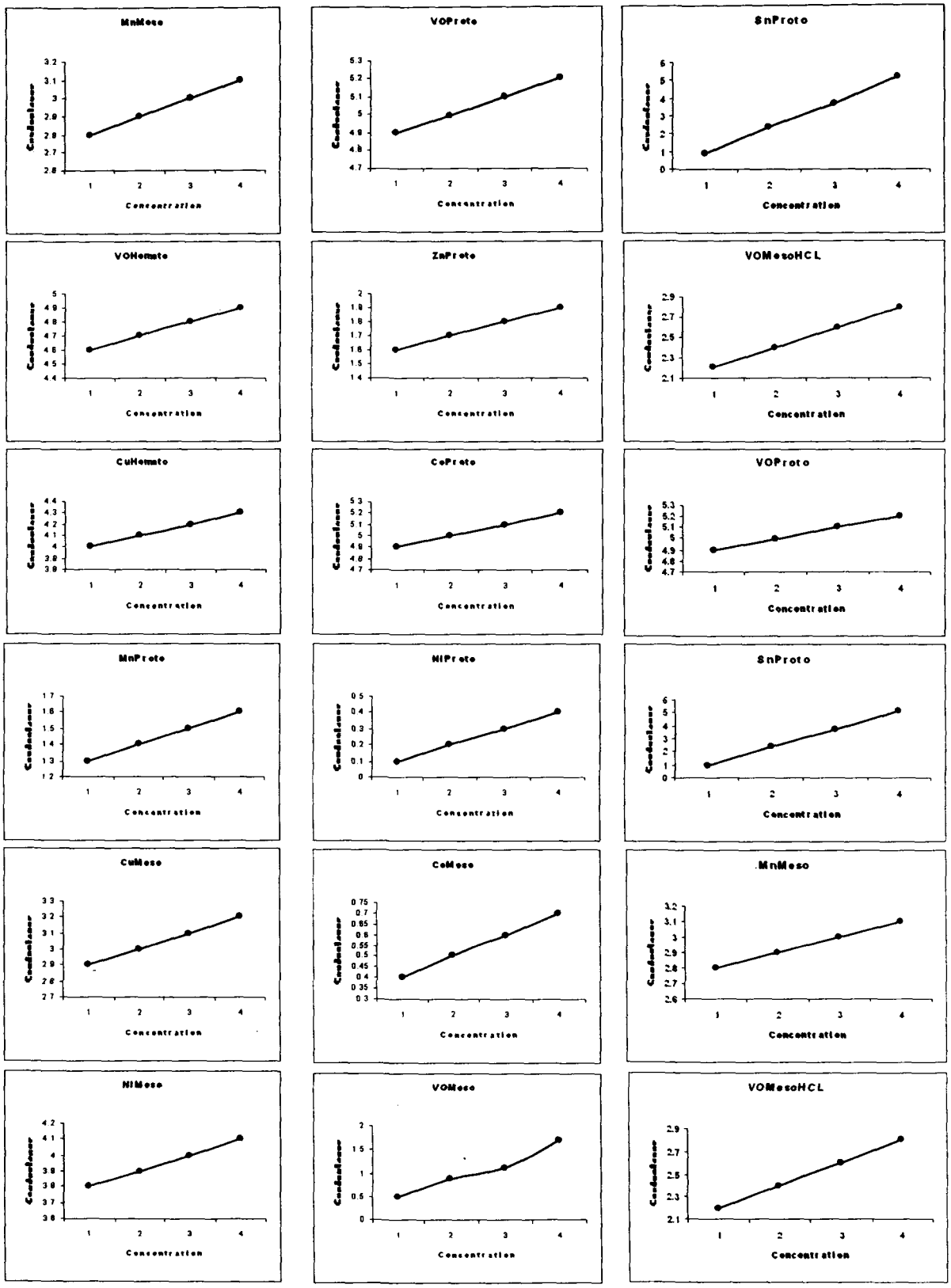

Figure 6.20 Plot of Conductance vs Concentration of Metallo –proto-,meso- and hemato-porphyrinIX DME

REFERENCES

1. R. H. Felton, in the porphyrin, Edited by D. Dolphin (Academic Press, New York, 1979) Vol V, p. 53 and the references therein.

2. D.G. Davis, in the porphyrins, Edited by D. Dolphin (Academic Press new York, 1979) vol V, p. 127 and references therein.

3. P. T. Kissinger and W. R. Heineman, J. Chem. Edu., 60, 702(1983) and references therein.

4. G. Canquis, V. D. Parker, in Organic Electrochemistry, Edited by M. M. Baiger (Marcel Dekar, New York, 1973) p. 93 and references therein.

5. J. A. Plambeck, Electro Analytical Chemistry(Wiley Interscience, New York, (1982) and references therein.

6. A. J. Bard and L.R. Faulkener, Electrochemical methods (Johnwiley, NY, 1980) and references therein.

7. G. A. Mabboti, J. Chem. Edu., 60, 697(1983).

8. J. H. Furhop, K. M. Kadish and D. G. Davis, J. Am. Chem. Soc., 95, 5140 (1973).

9. K.A. Macor and T. G. Spiro, J. Am. Chem. Soc., 105, 5601 (1983).

10. G. B. Maya and V. Krishanan, Inorg. Chem., 24, 3253 (1985).

11. A. Lemtur, B. Chakravorty, T. K. Dhar and J. Subramanian, J. Phys. Chem., 88, 5603 (1984).

12. J. Subramanian, V. P. Shedbalkar, A. Lemtur, R. Chakravorty and T.N. Saloi, J. Phys. Chem, 100, 4770 (1996).

SUMMARY

SUMMARY

This thesis entitled "**Physico-Chemical studies on the dimerisation of some Metalloporphyrins**" incorporates the information, results and discussion of our investigation on the dimerisation of some metalloporphyrins. It comprises of six chapters. We emphasize our investigation mainly to the visible absorption spectra and cyclic voltammetry. Our investigation is mainly on (metal = VO, Mn, Co, Ni, Cu, Zn and Sn) derivatives of protoporphyrin IX –dimethyl ester, mesoporphyrin IX-dimethyl ester and hematoporphyrin IX- dimethyl ester.

In the introduction, we have highlighted the reasons for carrying out this investigation.

Chapter-1 comprises a brief review on the dimerization of porphyrin, mainly H_2O soluble porphyrin. Different types of dimerization are also briefly reviewed.

Chapter-2 discusses the experimental details such as the synthesis of metalloprotoporphyrin IX-dimethyl ester, metallomesoporphyrin IX- dimethyl ester, vanadyl mesoporphyrin IX-dihydrochloride and metallohematoporphyrin IX-dimethyl ester; purification of solvents and reagents.. Besides the experimental parameters such as Cyclic Voltammetry, UV-Visible Spectroscopy and Conductance measurements also described briefly.

Chapter-3 discusses the dimerization of metalloprotoporphyrin IX-dimethyl ester by means of UV-Visible absorption spectroscopy. Visible absorption spectra of unoxidised species obtain at different concentrations; changes of the different visible band are studied. Dimerization is observed at the concentration range 10^{-4}M and above while monomers are observed at concentration range 10^{-5}M and below. Deviation from the Beer's Law is also indicative of the dimerization. Different plots of Beer's Law have shown the deviation for all the system we have studied.

Further, we carried out the oxidation of the metalloporphyrin with $SbCl_5$ and studied the effect on dimerization. In most cases we observed a blue shift of the soret band accompanied by splitting indicating dimerization. The presence of isosbestic points in the Q bands also indicates the presence of two species i.e. monomer and dimer. From the visible absorption studies we conclude the following.

(i) Un-oxidized MPPIXDME systems exist as dimers above the concentration range 10^{-5}M in the neutral solvents such as Dichloromethane.

(ii) Below 10^{-6}M it exists as monomer and

(iii) On oxidation with $SbCl_5$, dimerization occurs even below 10^{-5}M.

Chapter-4 discusses the dimerisation of some metallomesoporphyrin IX-dimethyl ester and vanadyl mesoporphyrin IX- dihydrochloride at different concentration range (10^{-4}M and 10^{-5}M) by using UV-visible Spectroscopy at room temperature. The dimerisation is observed within the concentration range of 10^{-4}M and 10^{-5}M. The dimer dissociate into monomer below 10^{-5}M solution. The soret bands shift towards the shorter wavelength and the Q bands shift towards the longer wavelength

when the dimer dissociate into monomer. The oxidation of the metallomesoporphyrin IX-dimethyl ester with $SbCl_5$ was carried out and observed the changes in the soret and Q bands on dimerisation. The isosbestic points and splitting of the soret bands also indicate that the system is dimer or oligomer. From these studies we conclude the following points

i) For unoxidised metallomesoporphyrin IX-dimethyl ester, the blue shift of the soret band on dilution cannot be explained by the exciton theory. Therefore, we qualitatively attribute it to the dissociation of the dimer to monomer at around 10^{-5}M concentration and

(ii) Even at concentration 10^{-5}M due to the presence of $SbCl_5$, metallomesoporphyrins IX- dimethyl ester and Vanadyl mesoporphyrin IX-dihydrochlode dimerises and show shifts as predicted by exciton theory.

Chapter-5 discusses the dimerisation of some metallohematoporphyrin IX-dimethyl ester as above and concluded the following points

(i) Most of the MHPIXDME exists as dimer at the concentration around 10^{-5}M. Below this concentration the dimer dissociate to monomers and

(ii) On oxidation almost all MHPIXDME, we have studied show dimerization.

Chapter-6 discusses the cyclic voltammetric and conductance measurements of some metalloprotoporphyrin-IX-dimethyl ester, metallomesoporphyrin IX-dimethyl ester, vanadyl mesoporphyrin IX-dihydrochloride and metallohematoporphyrin IX-dimethyl ester. Almost all metalloporphyrin studied at different concentrations (10^{-2} M,10^{-3}M, 10^{-4}M and 10^{-5}M) exhibits broad redox peaks. The broad peaks indicate to be an overlap of two waves. Their ΔE and i_a/i_c values deviate from one-electron transfer processes because ΔE values are not equal to 59mV and i_a/i_c are also not equal to one. Almost all

the voltammograms on repeated scan show reduce peak heights and shifted their peak positions. This may be due to the thin film formation on the electrode surface.

From the cyclic voltammetric study we conclude the following:

(i) All metalloporphyrins we have studied show dimerization between 10^{-2}M and 10^{-5}M. In case of metallomesoporphyrin in neutral solvent such as CH_2Cl_2 dimer dissociates to monomer from 10^{-5}M concentration and below

(ii) Strong aggregation is observed even in the neutral organic solvent such as CH_2Cl_2

(iii) All metalloporphyrins we have studied show rapid film formation on the electrode surface. It shows that metalloporphyrins of proto, meso and hemato have strong tendency to aggregate even at low concentrations on oxidation and

(iv) From the conductance measurements we observed that VOMPIXDME exhibit dimer at higher concentration range while it exists as monomer below 10^{-5}M solutions.